DESIGN AND ANALYSIS REPORT FOR THE RL10-IIB BREADBOARD LOW THRUST ENGINE

FINAL REPORT

CONTRACT NAS3-24238

UNITED TECHNOLOGIES PRATT&WHITNEY

FOREWORD

This report presents the design and analysis of the RL10-IIB breadboard low thrust engine which was initiated by Contract NAS3-22902 and is submitted in compliance with the requirements of Contract NAS3-24238.

This project was initiated in October 1982 and the final report was delivered in December 1984. The effort was headed by Joseph S. Henderson, Project Engineer.

The following individuals have provided significant contributions in the preparation of this report.

James R. Brown
Robert R. Foust
Donald E. Galler
Paul G. Kanic
Thomas D. Kmiec
Charles D. Limerick
Richard J. Peckham
Thomas Swartwout

SUMMARY

The breadboard low thrust RL10-IIB engine is shown in Figures 1 through 4. The steady-state cycle analysis data and schematics shown in Figures 5 and 6. The breadboard engine utilizes a three stage oxygen heat exchanger (OHE) and four open-loop, hydraulically-actuated breadboard control valves, which were adapted from earlier throttling engine programs. The steady state and transient RL10-IIB engine cycle analyses shown in Section III were based on anticipated flight propellant inlet pressures of 20 psia for both fuel and oxidizer in order to provide data for the "flight representative" valves and OHE designs. The first engine test series using the breadboard design will be performed at fuel and oxidizer inlet pressures of 25 psia and 33 psia respectively, because the Pratt & Whitney (P&W) E-6 test stand cannot currently provide the flight-representative inlet conditions. Sections IV and V provide the design/analyses of the OHE and the breadboard valves, respectively.
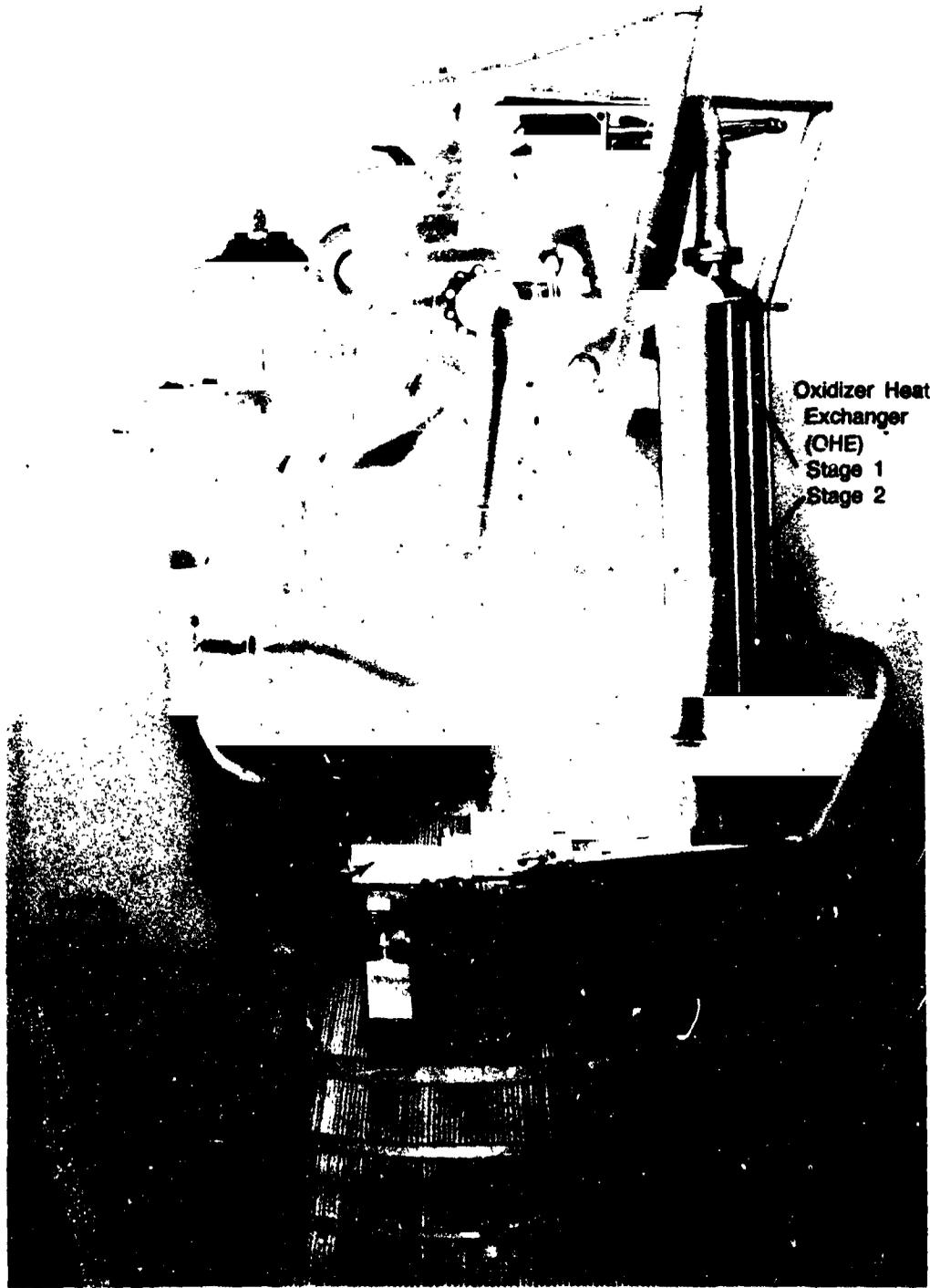
ORIGINAL PAGE IS
OF POOR QUALITY

Oxidizer
Control
Valve (OCV)

Cavitating
Venturi
Valve (CVV)

urbine
ypass
alve (TBV)
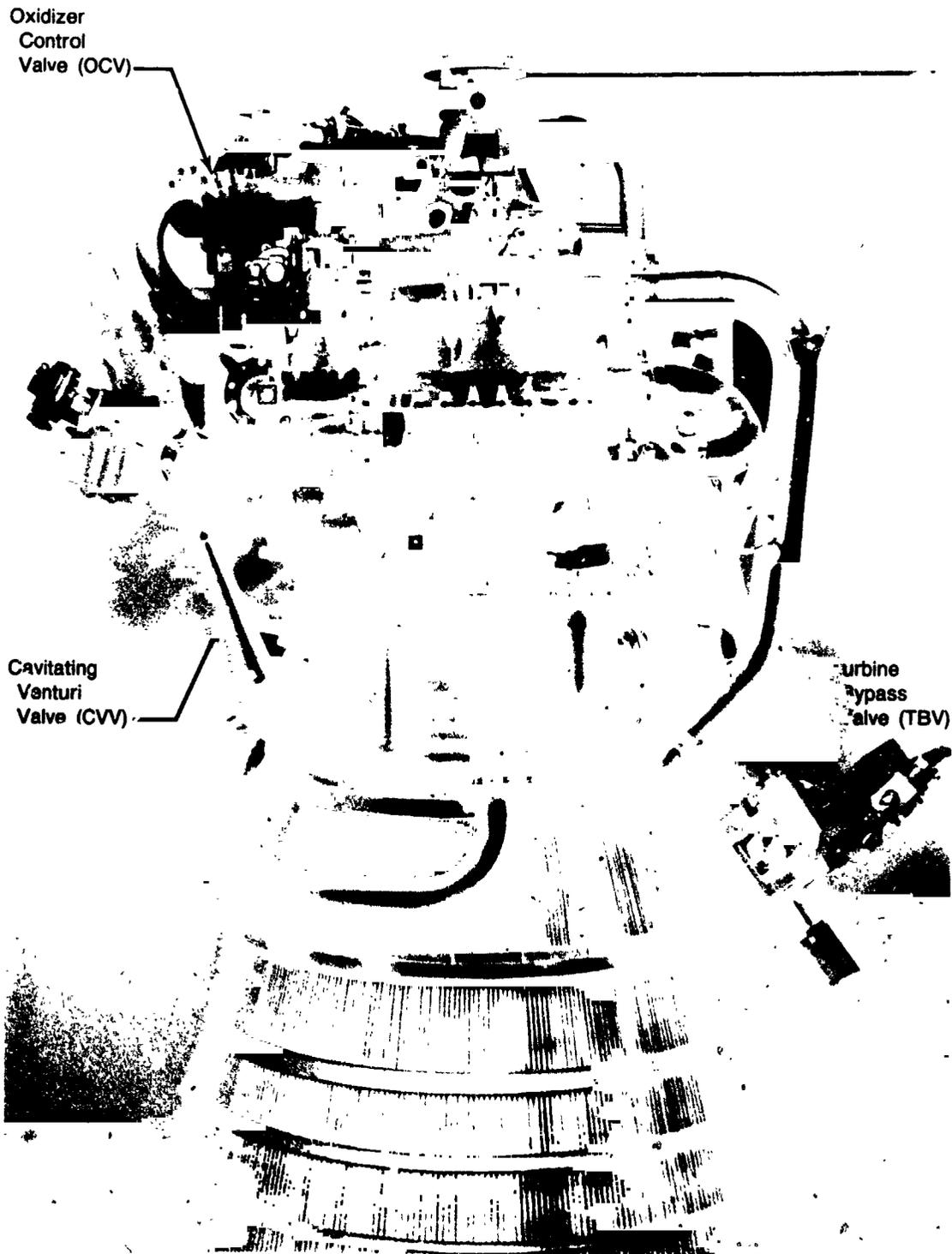
FE 225029

Figure 1.   Breadboard Low-Thrust RL10-IIB Engine (View 1)

Oxidizer Heat
Exchanger
(OHE)
Stage 1
Stage 2

FE 225032

Figure 2.   Breadboard Low-Thrust RL10-IIB Engine (View 2)

FE 225030
84C-12
9992B
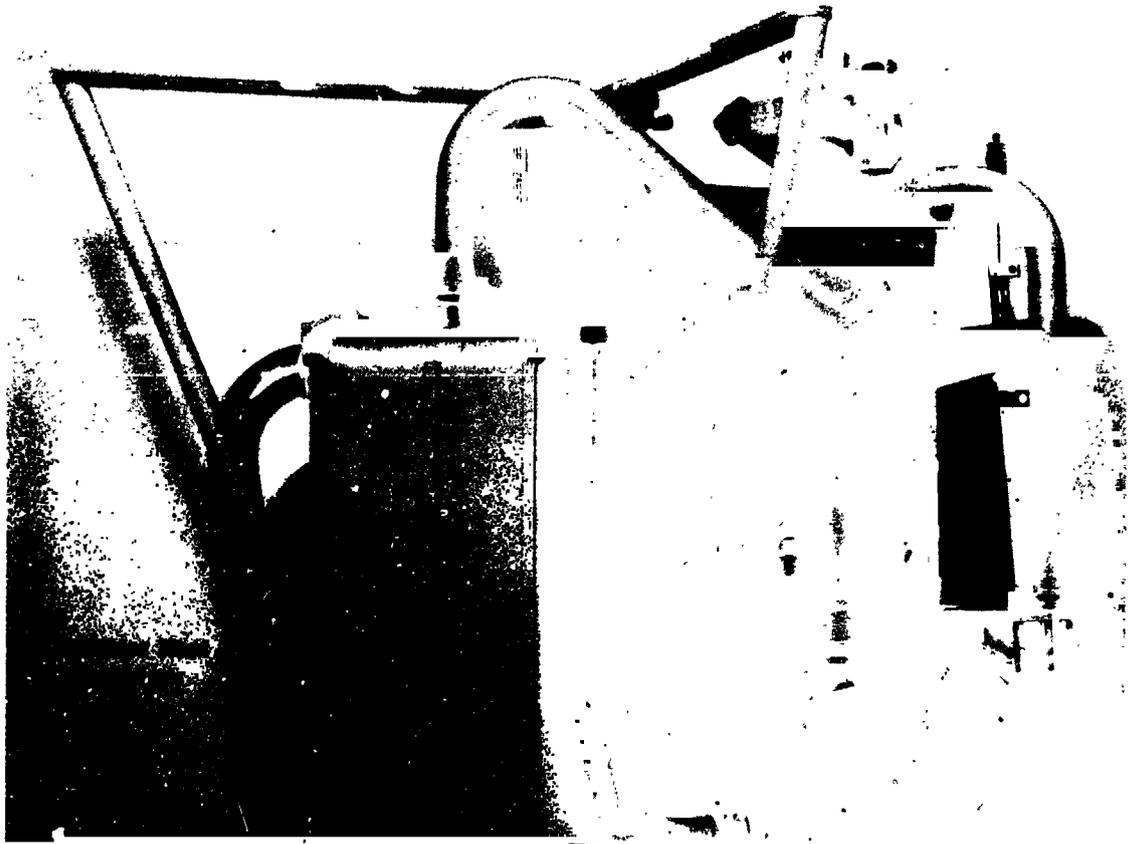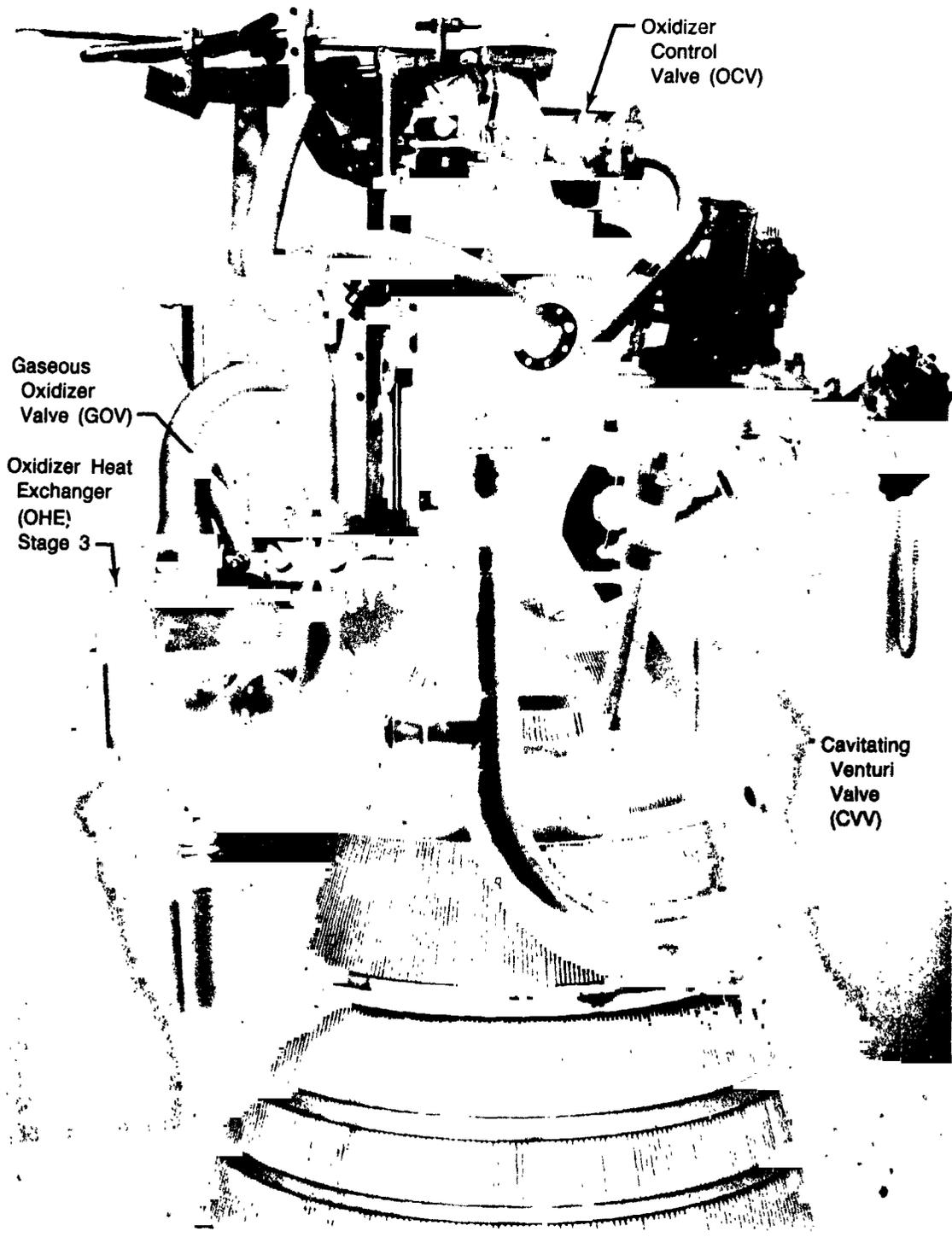
Figure 3. Breadboard Low-Thrust RL10-IIB Engine (View 3)

Figure 4. Breadboard Low-Thrust RL10-IIB Engine (View 4)

FE 225031
840412
9992B
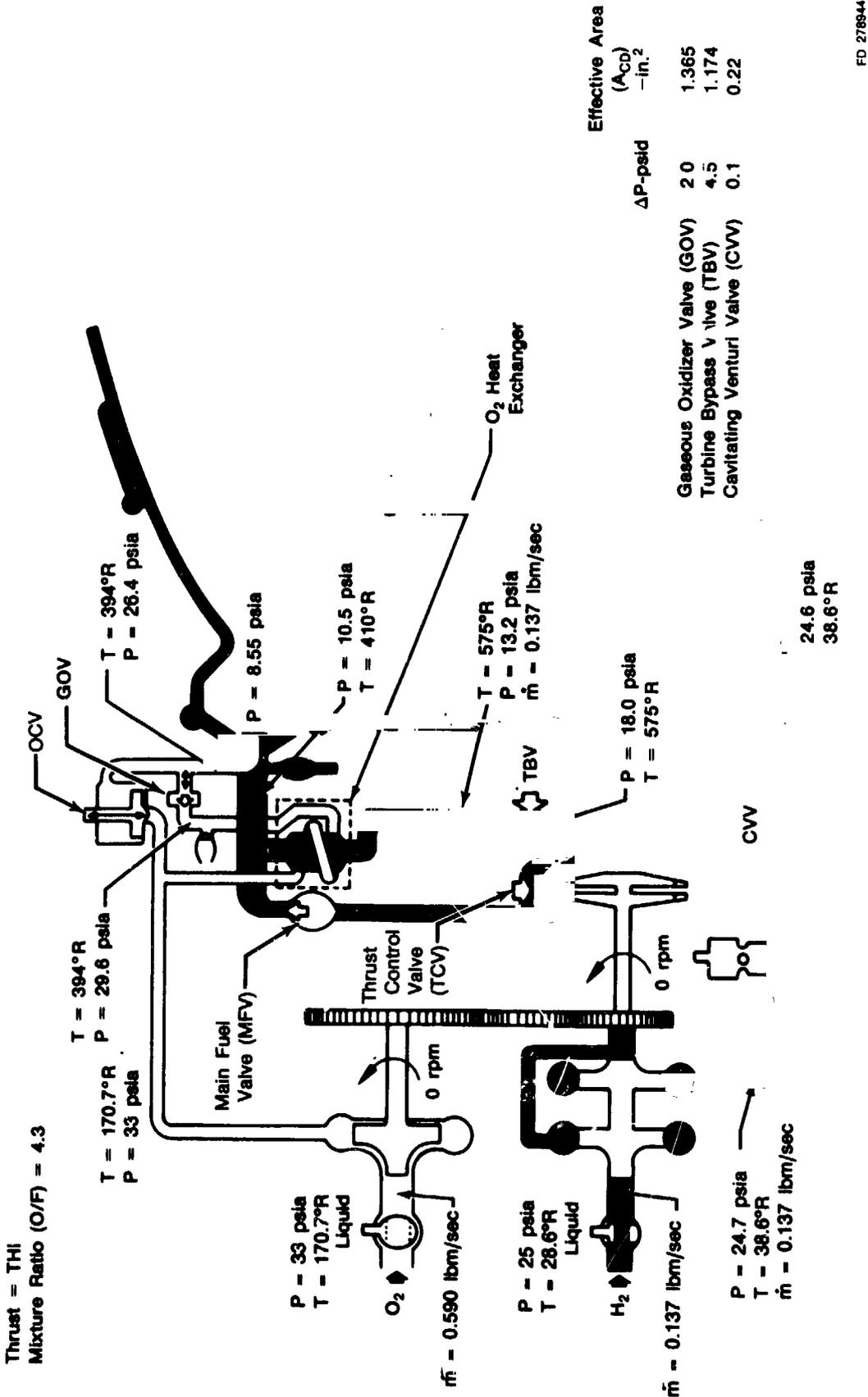
Figure 5. RL10-IIB Breadboard Engine — Tank Head Idle (THI) Operating Mode

Thrust Level = PI
Mixture Ratio (O/F) = 6.0

Gaseous Oxidizer Valve (GOV)
Turbine Bypass Valve (TBV)
Cavitating Venturi Valve (CVV)

	ΔP-psid	Effective Area (A_{CD}) –in.^{2}
Gaseous Oxidizer Valve (GOV)	2.0	1.365
Turbine Bypass Valve (TBV)	6.9	1.365
Cavitating Venturi Valve (CVV)	8.3	0.965

FO 278945

T = 205°R
P = 97.3 psia

P = 40 psia

– 46.0 psia
438°R

T = 609°R
P = 47.7 psia
ṁ – 0.224 lbm/sec

O₂ Heat
Exchanger

T = 207.8°R
P = 109.3 psia

OCV
GOV

T = 172.6°R
P = 115.8 psia

P = 56.1 psia
T = 609°R

TBV

T = 591°R
P = 46.8 psia
ṁ – 0.276 lbm/sec

MFV

P = 83.6 psia
T = 47.6°R

CVV

TCV

10,272
rpm

4850
rpm

P = 33 psia
T = 170.7°R
Liquid

O₂

ṁ – 3.125 lbm/sec

P = 25 psia
T = 38.6°R
Liquid

H₂

ṁ – 0.521 lbm/sec

P – 135 psia
T – 47.6°R
ṁ – 0.5 lbm/sec

Figure 6. RL10-IIB Breadboard Engine — Pumped Idle (PI) Operating Mode

CONTENTS

PRECEDING PAGE BLANK NOT FILMED

1073C

ILLUSTRATIONS

ILLUSTRATIONS (Continued)

ILLUSTRATIONS (Continued)

1079C

ILLUSTRATIONS (Continued)

ILLUSTRATIONS (Continued)

ILLUSTRATIONS (Continued)

1073C

TABLES

SECTION I
INTRODUCTION

This report describes the breadboard low thrust RL10-IIB engine which is scheduled for testing in early 1984. A summary is also provided of the analysis and design effort which has been completed to define the multimode thrust concept applicable to the anticipated requirements for upper stage vehicles in the late 1980s. Baseline requirements were established early in the current program for operation of the RL10-IIB engine at the following conditions: 1) Tank Head Idle (THI) at low propellant tank pressures, without vehicle propellant conditioning or settling thrust, 2) Pumped Idle (PI) at a 10% thrust level for low "G" deployment and/or vehicle tank pressurization, and 3) full thrust (FT) (15,000 lb). Several variations of the engine configuration were investigated and results of the analyses are also included in this report.

0892C

SECTION II
DEFINITION AND REQUIREMENTS

The RL10-IIB engine (Figure 7) is derived from the basic RL10A-3-3 but has increased performance and operating flexibility for use in the Orbit Transfer Vehicle (OTV). With a nominal full thrust level of 15,000 lb (in vacuum) at a mixture ratio of 6.0:1, and multi-mode operational capability as shown in Figure 8, the IIB engine is defined as an RL10A-3-3 with the following changes:

1. Two-position extendible nozzle with recontoured primary section to give a large increase in specific impulse with an engine installed length of 55 inches.

2. Injector reoptimized for operation at a full thrust level mixture ratio of 6.0:1.

3. Tank head idle (THI) capabilities, where the engine is run without its turbopump rotating but pressure-fed on propellants supplied from the vehicle tanks at saturation pressure. Propellant conditions at the engine inlets can vary from superheated vapor, through mixed phase, to liquid. The objectives are to supply low thrust to settle vehicle propellants and also to obtain useful impulse from the propellants used to condition the engine and vehicle feed system.

4. Operation at low thrust in pumped mode (maneuver thrust) to provide low ΔV and autogenous tank pressurization capability.

5. Capability for both H_2 and O_2 autogenous tank pressurization.

Thrust	: 15,000 lb
Chamber Pressure	: 400 psia
Area Ratio:	: 205
I_{sp}	: 459.8 sec at 6.0 MR
Operation	: Full Thrust
	(Saturated Propellants)
	Maneuver Thrust
	(Saturated Propellants)
Conditioning	: Tank Head Idle

55 in.
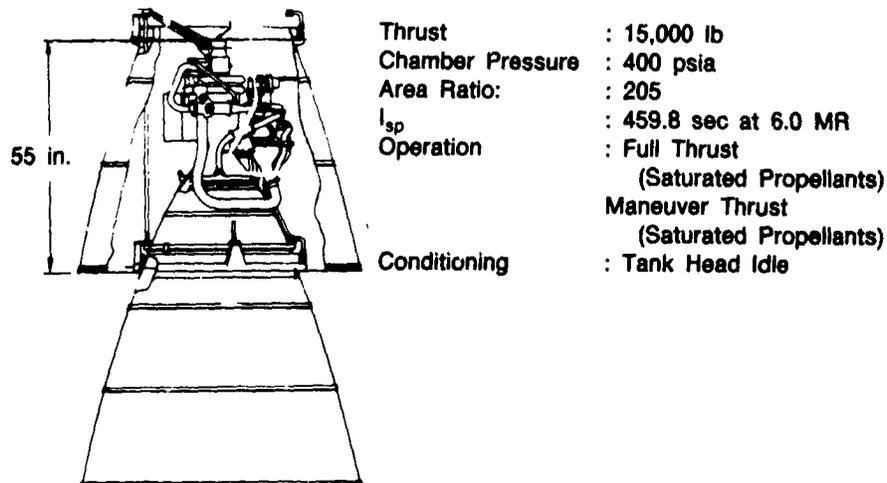
PRECEDING PAGE BLANK NOT FILMED

FD 280478

Figure 7. RL10-IIB Engine Configuration

Thrust = 100%

Propellant
Setting
and Engine
Thrust ≈ 0.8% to 3.5%

↓
Thrust

Tank
Pre-Pressurization
Thrust ≈ 10%

|←— Tank Head —→| |←————————→| |←— Rated Thrust —→|
Idle (THI)   Pumped
                    Idle (PI)

Time →
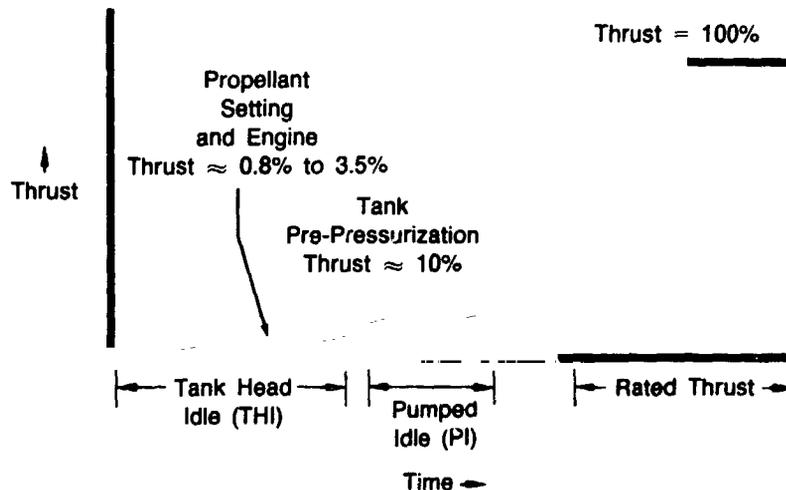
FD 280485

Figure 8. RL10-IIB Engine Multimode Operation Capability

A. DESCRIPTION

Figure 9 shows an engine flow schematic for the current RL10A-3-3A engine, and Figure 10 for the IIB engine. The fuel pump interstage cooldown valve is deleted, since the engine is conditioned by running in THI mode. A GO_2 heat exchanger, GO_2 control valve, turbine bypass valve and cavitating venturi valve are added to enable the engine to run in THI and PI. Fuel and oxidizer tank pressurization valves are added to give autogenous tank pressurization capability. Additional solenoid valves and modifications to the oxidizer control valve and thrust control valve give the engine its capability to operate in three modes. A dual exciter gives improved ignition reliability in THI. The primary nozzle is recontoured and a jackscrew-operated, two-position, dump-cooled extendible nozzle is added. The primary nozzle exit diameter is fixed at 40 in., since this is the limiting diameter for the extendible nozzle to be retracted over the engine's power head, and is also the largest size which allows installation with a truncated extendible nozzle in P&W/GPD E-6 test stand. The injector is reoptimized to give improved performance at a mixture ratio of 6.0.

B. OPERATION

1. Tank Head Idle (THI)

The engine is started in THI mode, with propellants supplied in vapor, mixed, or liquid phases.

4

0892C
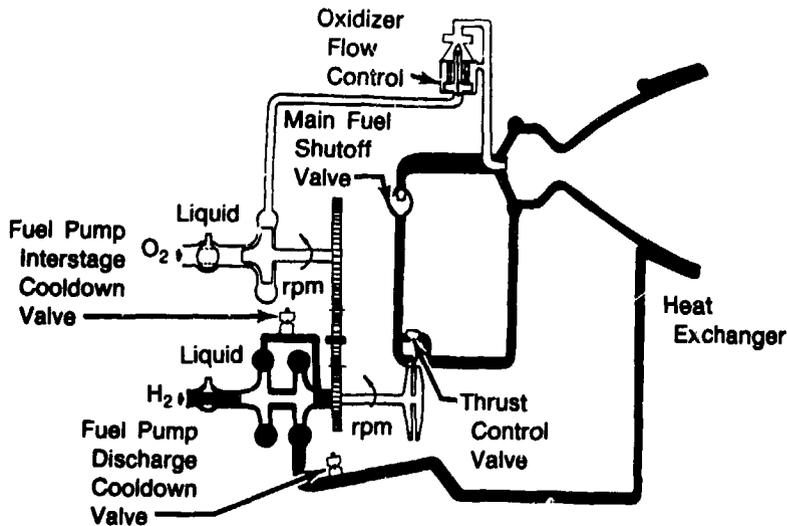
FD 280486

Figure 9. RL10-3-3A Engine Flow Schematic — Current Design Provi'es Single Thrust Level
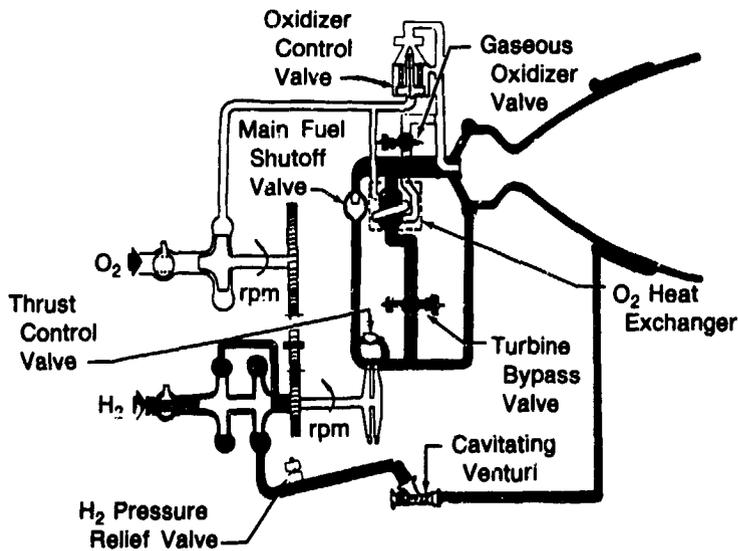
FD 280487

Figure 10. RL10-IIB Engine — GOX Heat Exchanger and Throughflow Control Valves are Primary Changes

With the inlet shutoff valves open, fuel flows through the pump, the thrust chamber cooling jacket, around the turbine, through the GO_2 heat exchanger, and into the main injector. Similarly, the oxidizer flows through the pump, and with the oxidizer control valve shut, all the flow goes through the heat exchanger to the injector.

2. Pumped Idle (PI)

After pump conditioning has been completed in THI mode, the engine is ready to be operated its pumped idle thrust level for low ΔV maneuvers or as a step on its acceleration to full thrust. To start the turbopumps, the main fuel shutoff valve is opened, and the turbine bypass valve is closed momentarily to give a high initial turbine torque and is then reopened to the maneuver-thrust position. The cavitating venturi is decreased in area to isolate the fuel pump from jacket boiling instabilities.

3. Full Thrust (FT)

The engine is accelerated to full thrust by closing the turbine bypass valve, opening the liquid oxidizer valve, closing the gaseous oxygen valve, and opening the cavitating venturi valve. At about 90% of full thrust, the thrust control valve opens to reduce thrust overshoot.

SECTION III
ENGINE CYCLE ANALYSIS

The RL10-IIB rocket engine multi-mode operation analysis and design addressed in this report was preceded by extensive analysis and testing, at low thrust levels, of earlier RL10 engine models. Testing on the RL10A-3-2, RL10A-4, and RL10A-3-7 throttling engine models between 1963 and 1967 resulted in over 800 engine firings and 70,000 seconds of runtime at tank head idle (THI) and pumped idle (PI) modes of operation. These RL10 engine models required active controls to obtain moderately stable low thrust operation. The 55 inch long, RL10 Derivative IIB engine concept, defined in the early 1970s, was required to be capable of stable operation at THI, 25% PI and full thrust (FT) using an oxidizer heat exchanger (OHE) and simple, solenoid-actuated engine valves instead of active controls. These analyses of RL10 Derivative II engines, conducted during the 1970-1973 period, included Derivative IIB thrust chamber heat transfer predictions, thermal skin OHE performance requirements, definition for stable PI operation at 10% thrust with fixed position valves. Both steady state and transient cycle simulations were included in these Derivative Engine Study results as reported in P&W Report No. FR-6011, dated 15 December 1973, under contract NAS8-28989. Later analyses were reported in the P&W Space Tug Engine Report, P&W Report No. FR-7498, dated 21 May 1976 under contract NAS8-31151, and an Orbital Transfer Vehicle (OTV) engine study P&W Report No. FR-14615, dated 15 March 1981, under contract NAS8-33637. All of the background data from these studies were reviewed for applicability and documentation to prevent duplication of effort during this RL10-IIB design and analysis program under NASA contract NAS3-22902.

The evolution of the RL10-IIB engine cycle during this design/analysis program, under the Product Improvement Program (PIP), is shown on Table 1. The engine was derived from the RL10A-3-3 engine, and modifications were made as required to satisfy the particular goals and operating conditions for the RL10-IIB engine. The initial configuration shown, which had been carried forward to this program from earlier analyses, had a pumped idle thrust level of 25% of FT. Table 1 also presents characteristics of the Preliminary Engine Design, an Alternative Design, the Baseline Design (which was used for Flight Representative controls and OHE performance predictions), and the Breadboard Design intended to be used for the 1st Test Series. These analyses were required primarily because of the 10% PI thrust-level selected for the RL10-IIB engine and changes identified by the series of hardware design/analyses.

A. PRELIMINARY CONFIGURATION

Preliminary RL10-IIB engine steady state cycle analyses defined the operating characteristics, engine configuration requirements, and control valve requirements at low thrust using estimated performance for an oxygen heat exchanger at the 10% thrust PI design point identified at the start of this effort. The RL10 Derivative Engine steady-state cycle deck ME7277 described in Appendix A was modified to provide the 10% thrust PI simulation with estimated heat exchanger characteristics. Incorporation of a reduced effective flow area (0.9 in.^{2}) turbine stator configuration, tested extensively during the 1960s, matched the turbine power to the required 10% PI flow rates. Engine operation was investigated using propellant inlet conditions achievable on the E-6 test stand (Fuel Pump Inlet Pressure (FPIP) = 25 psia, Oxidizer Pump Inlet Pressure (OPIP) = 33 psia) for the scheduled breadboard low thrust test series, as well as with the lower propellant inlet conditions (FPIP = 20 psia, OPIP = 20 psia) that will be available for subsequent low thrust test series. The later propellant inlet conditions are more representative of the expected flight vehicle propellant conditions and will be used for the "flight representative" (FR) component designs and the second engine test series.

Table 1. Breadboard RL10-IIB Design/Analysis Iteration Summary

Item No.	Configuration	O_2 Injector Area (in.^{2})	H_2 Injector Area (in.^{2})	Chamber/ Nozzle Heat Transfer	OHE Heat Transfer	Turbine Nozzle Area (in.^{2})	H_2/O_2 Gear Ratio	Inlet Conditions	Applicable Figures
1	RL10 A-3-3	0.8	2.25	RL10A-3-3 (70 in.)	NA	1.1	2.5	NA	NA
2	Initial PIP RL10-IIB	0.8	2.25	RL10A-3-3	Estimated (25% PI)	1.1	2.5	Flight Representative	None
3	Preliminary RL10-IIB	1.0	2.25	RL10A-3-3	Estimated (10% PI)	0.9	2.5	Flight Representative	11 to 32
4	Preliminary Update RL10-IIB	1.0	2.25	RL10-IIB (55 inch)	Estimated	0.9	2.5	Flight Representative	33 to 37
5	Alternate Gas/Gas RL10-IIB	3.0	1.7	RL10-IIB	Estimated	0.9	2.1	Flight Representative	38 to 44
6	Baseline RL10-IIB	0.8	2.25	RL10-IIB	Estimated	0.9	2.1	Flight Representative	45 to 47
7	Baseline RL10-IIB Update	0.8	2.25	RL10-IIB Update	3 Stage OHE	0.9	2.1	Flight Representative	48 to 64
8	Final Baseline	0.8	2.25	RL10-IIB Update	3 Stage OHE Update "reversed flow	0.9	2.1	Flight Representative	65 to 68
9	Breadboard RL10-IIB	0.8	2.25	Final Baseline	Final Baseline	0.9	2.1	Breadboard	69 and 70

NA — Not Applicable

Parametric analyses of requirements for the PI Gaseous Oxidizer Valve (GOV) area and oxidizer injector temperatures as functions of venturi pressure loss and mixture ratio are shown in Figure 11 for the breadboard test series inlet conditions. As indicated, marginally acceptable valve differential pressures (ΔP's) and oxidizer injector conditions could be obtained with the 0.8 in.^{2} RL10A-3-3 Bill-of-Material (BOM) oxidizer injector flow area and 2.5 gear ratio. However, increased GOV ΔP would be available with the oxidizer injector flow area increased to 1.0 in.^{2}

Using the flight-representative inlet conditions showed that PI operation with the 0.8 in.^{2} oxidizer injector area would require a gear ratio change to 2.1 to provide acceptable GOV ΔP (Figure 12). The 2.1 ratio gears had previously been tested on the RL1OA-4 engine. Increasing the oxidizer injector flow area to 1.0 in.^{2} not only increased the control margin, it also provided satisfactory oxidizer injector conditions and control valve ΔP with the 2.5 gear ratio at the flight representative inlet conditions as shown in Figure 13. Incorporating the 2.1 gears would increase GOV ΔP margin further as indicated. However, the 2.1 gear parts were long-lead items and none were available, so continued analysis was concentrated on the 2.5 gears and 1.0 in.^{2} injector configuration. The 10% thrust operating points at mixture ratios of 4.0, 5.0, and 6.0 were compared on RL10 pump operating maps with test data points (development engine FX141-45)

obtained during low thrust testing in 1966 and .... As shown in Figures 14 and 15, the test data indicate that there should be no problem with main ump stability.

Steady-state THI operation with the flight representative fuel pump inlet conditions and preliminary valve areas indicated that the system would require undesirable throttling to provide a target mixture ratio of 4.0 with 90 psia oxidizer pump inlet pressure. With valve areas (A_FT set to the planned wide open position ... 3V A_CD = 2.0 in.² and GOV A_CD = 1.273 in.²), mixture ratio stabilized at 3.3 (Figure 18)

The RL10-IIB engine configuration at completion of the preliminary analysis is summarized as item 3 in Table 1. Valve area and flow schematics for engine conditions corresponding to the three required operating levels (THI, PI, and FT) are shown in Figures 16 through 18. A comparison of configurations studied during the preliminary analysis is presented in Table 2.

Transient analyses were conducted with the computer programs defined in Appendix B using this preliminary engine configuration to provide data for the flight-representative control valve designs. The transients from start to THI, from THI to PI, and from PI to FT were each examined separately. The start-to-THI transients were evaluated with flight representative inlet pressures and a combination of both saturated liquid and saturated vapor propellants. Preliminary THI transient engine characteristics with saturated liquid propellants are shown in Figures 19 through 22. As indicated, steady-state THI operation is achieved in less than 45 seconds after start. Preliminary engine characteristics for transient operation from THI to PI mode were also generated and critical engine parameters are shown in Figures 23 through 25. Steady-state PI operation is achieved in less than 1 second after initiation of the transient, as shown.

Preliminary RL10-IIB engine transient characteristics from PI (10% thrust) to FT were also defined. Initial engine transient valve scheduling required that the simulated RL10 thrust control valve (TCV) stay closed up to 300 psia chamber pressure, which is normal operation. This required the turbine bypass valve to be ramped closed very slowly (~ 800 msec — an unreasonable requirement) to increase duration of the transient and prevent pump overspeed. Transient characteristics with a more reasonable TBV ramp time (~ 200 msec) produced an acceleration with unacceptable pump overspeed and thrust overshoot (denoted as squares on Figures 26 through 29). Opening the TCV at a chamber pressure of 100 psia produced a more acceptable transient (denoted as circles on the figures). The complete transient characteristics were not defined during this preliminary analysis and the simulation was arbitrarily terminated when chamber pressure reached 300 psia. The selected valve sequencing and flow rates for these transients are presented in Figures 30 through 32.

B. PRELIMINARY UPDATE CONFIGURATION

An update of the preliminary RL10-IIB engine cycle analysis incorporated results of the thermal analysis of the recontoured and shortened RL10-IIB thrust chamber/primary nozzle assembly. The new heat transfer characteristics were incorporated into the cycle deck and new design points at THI, PI, and FT were generated. Flow schematics are shown in Figures 33 through 35. Pumped idle (10% thrust) operation at a mixture ratio of 6.0 required a reduction in cavitating venturi pressure loss (Figure 36) to provide the desired conditions at the oxidizer injector. Control capability on the oxidizer side was diminished because the GOV pressure loss was decreased by 30%. Control capability would have been reduced further at lower mixture ratios as it would have been necessary to further decrease the venturi pressure loss to maintain gaseous conditions at the oxidizer injector.
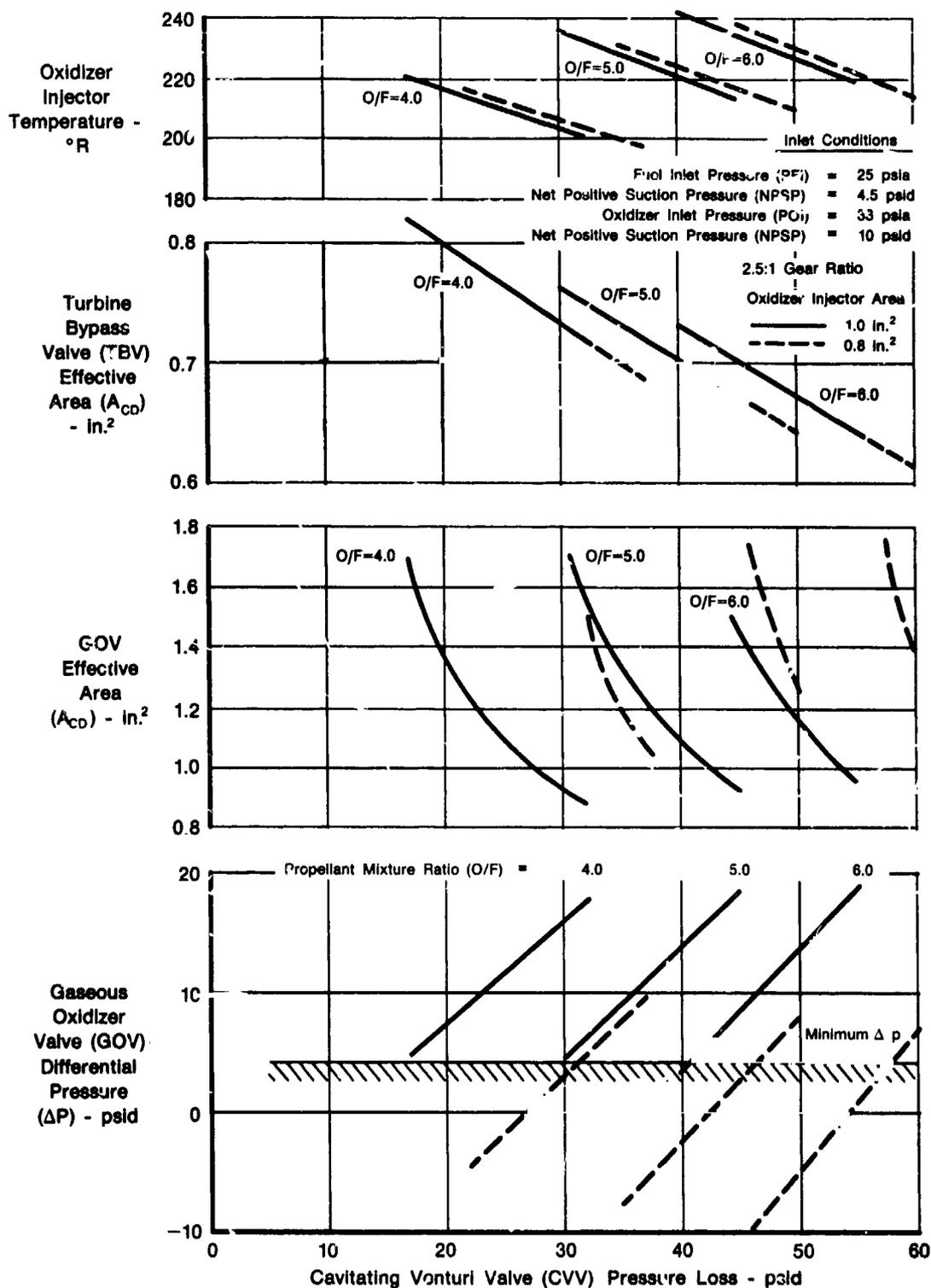
Figure 11. RLiv-IIB Engine Operation at Pumped Idle (Breadboard Test Series Inlet Conditions)

FD 278887

10
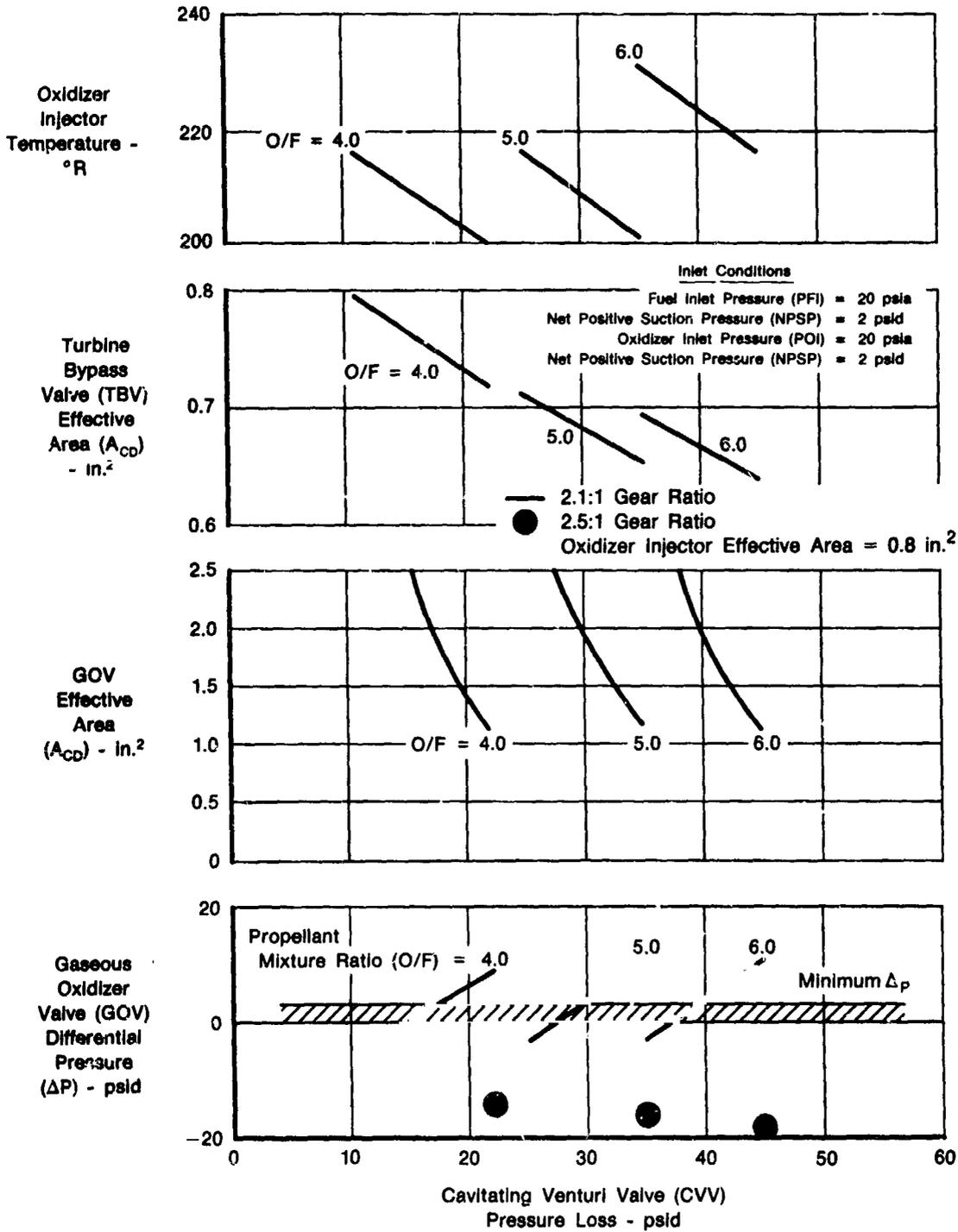
Figure 12. *RL10-IIB Engine Operation at Pumped Idle (Flight-Representative Inlet Conditions)*

FD 278888

11
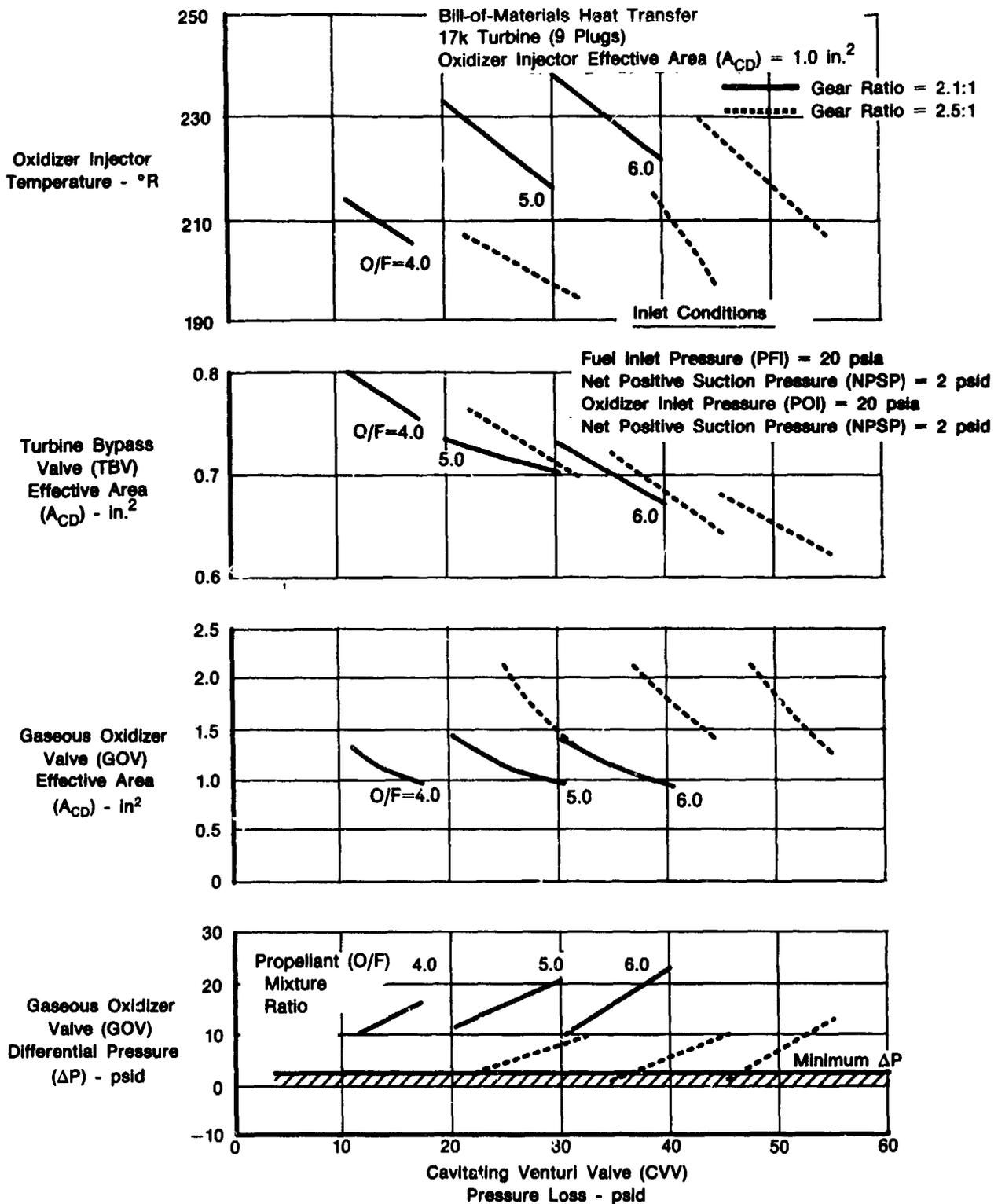
Figure 13. RL10-IIB Engine Operation at Pumped Idle (Flight Representative Inlet Conditions, Increased Injector Area)
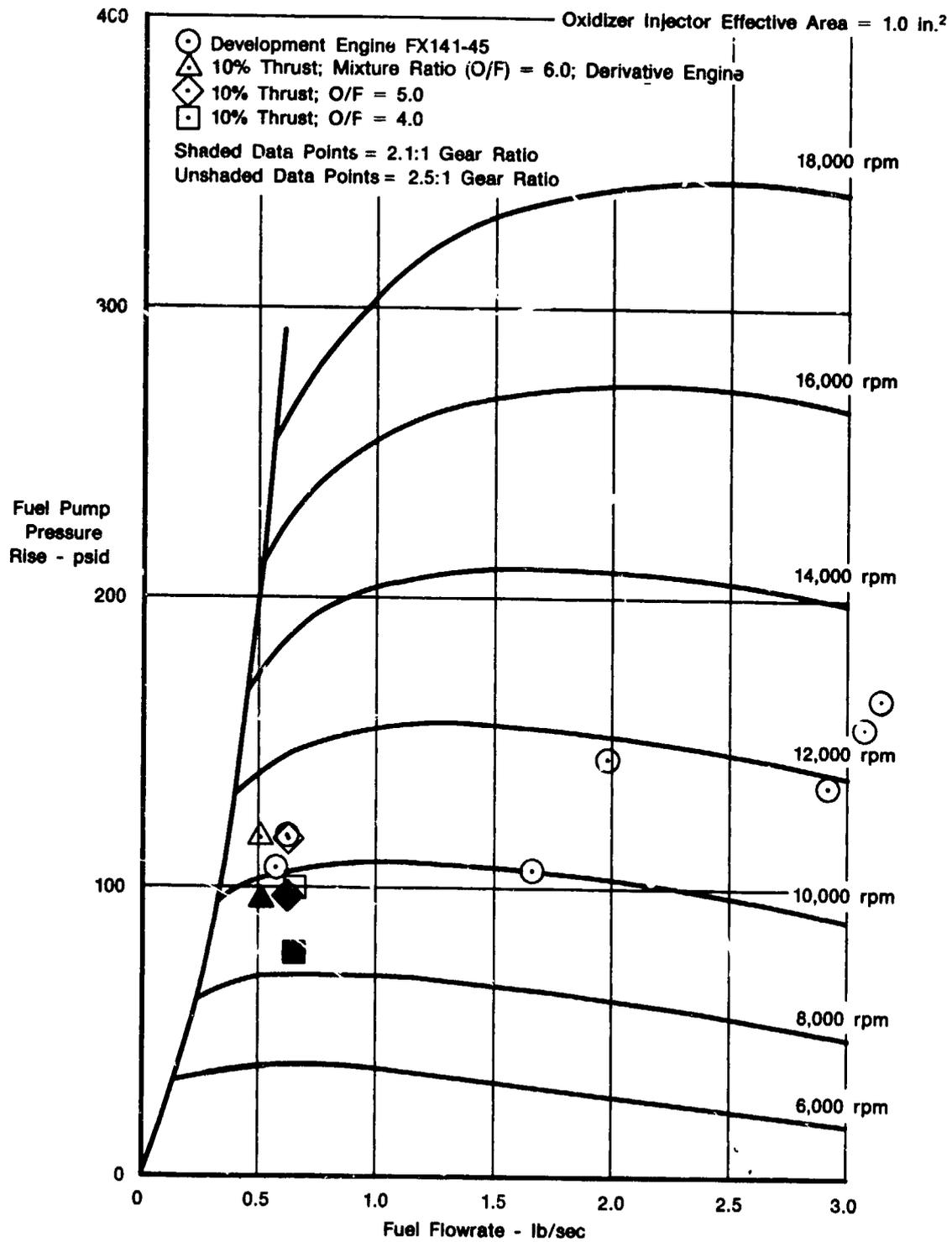
Figure 14. *RL10A-3-3 Fuel Pump Operating Characteristics*

FD 278890

13
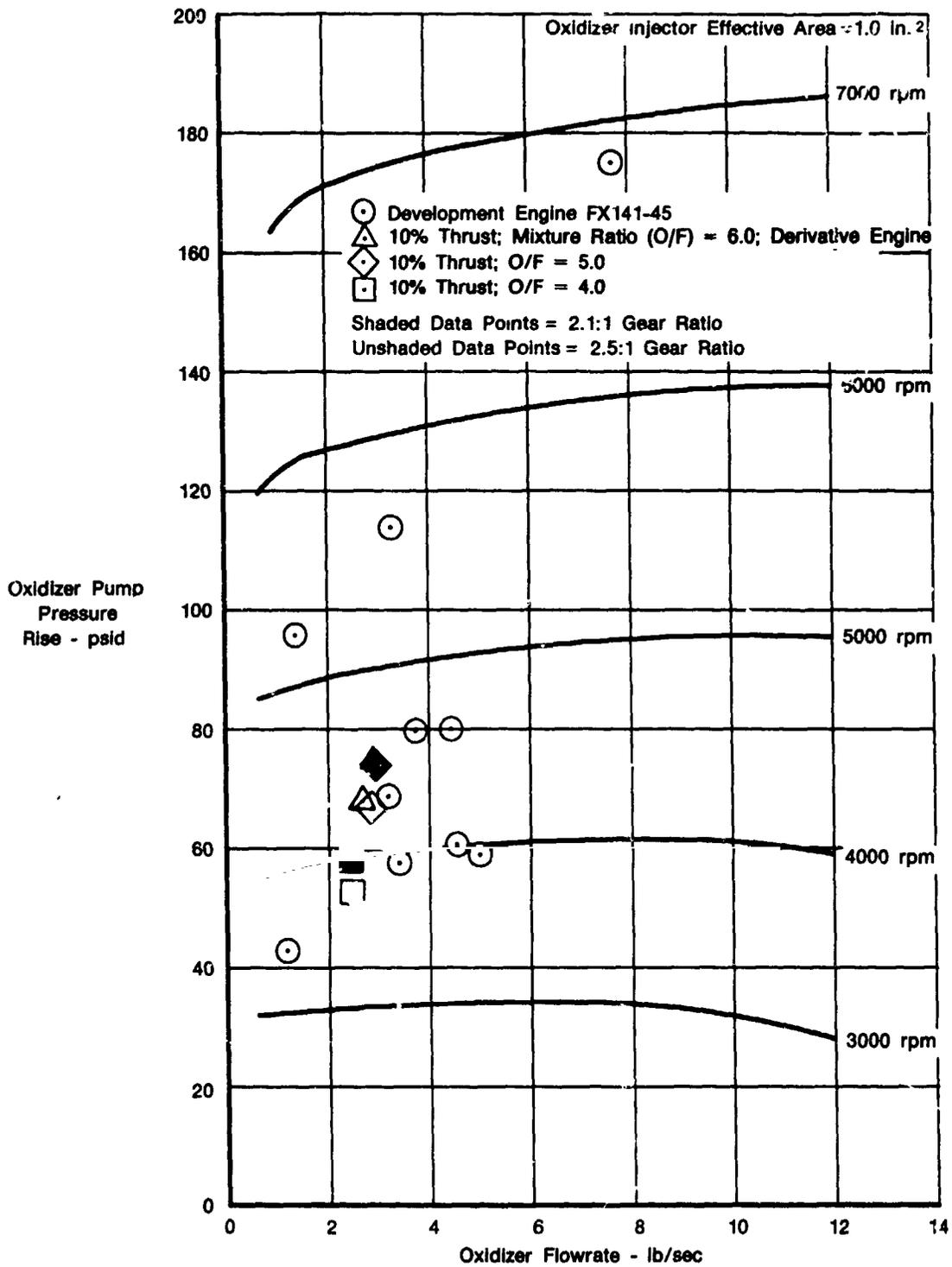
FD 278891

Figure 15. RL10A-3-3 Oxidizer Pump Operating Characteristics
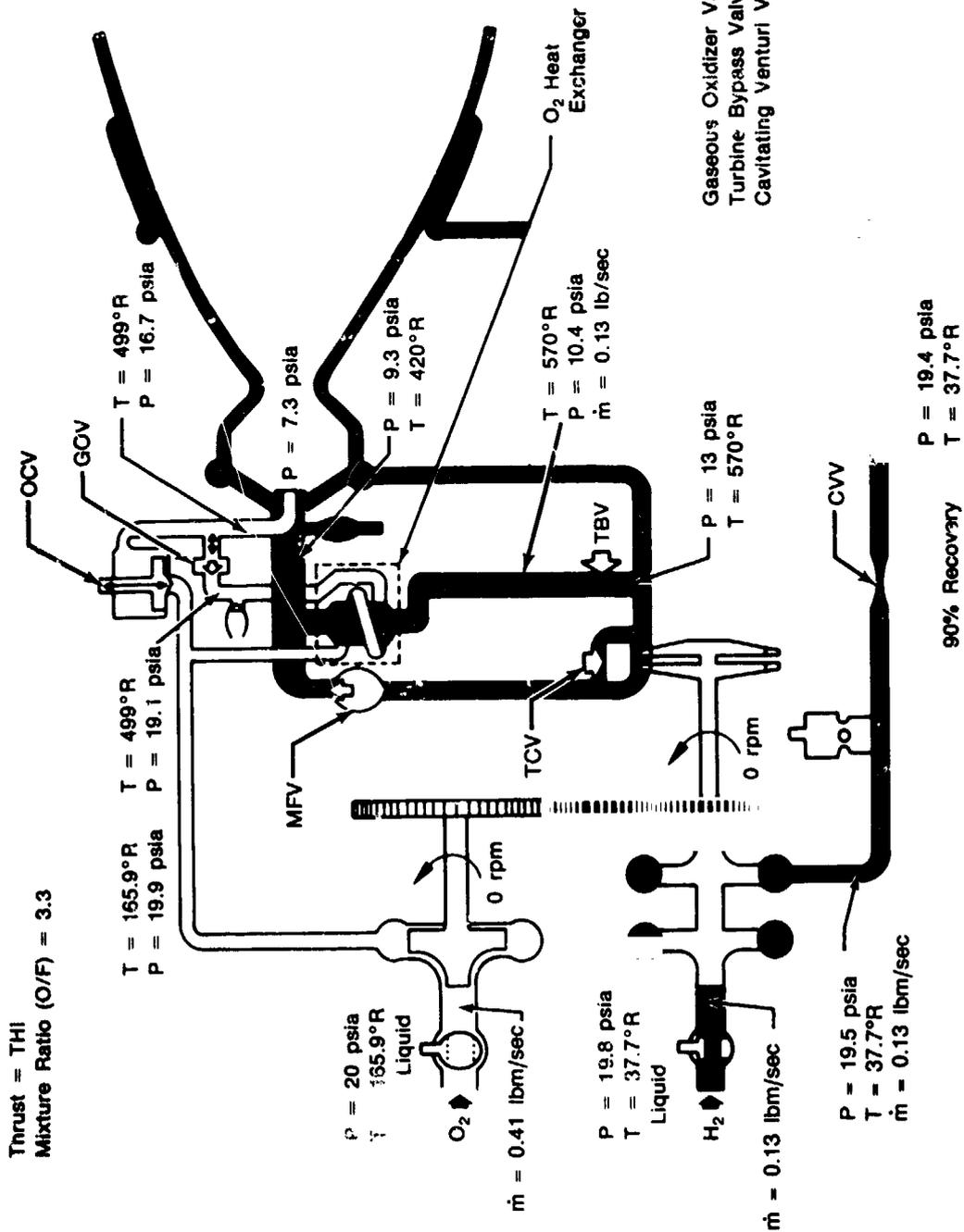
Figure 16. *RL10-IIB Engine Preliminary Configuration — Tank Head Idle (THI) Operating Mode*

	ΔP-psid	Effective Area (A$_{CD}$) - in.2
Gaseous Oxidizer Valve (GOV)	2.4	1.273
Turbine Bypass Valve (TBV)	2.6	2.0
Cavitating Venturi Valve (CVV)	0.1	0.258

Thrust = THI
Mixture Ratio (O/F) = 3.3

FD 278992

15

Thrust Level = 10%
Mixture Ratio (O/F) = 6.0
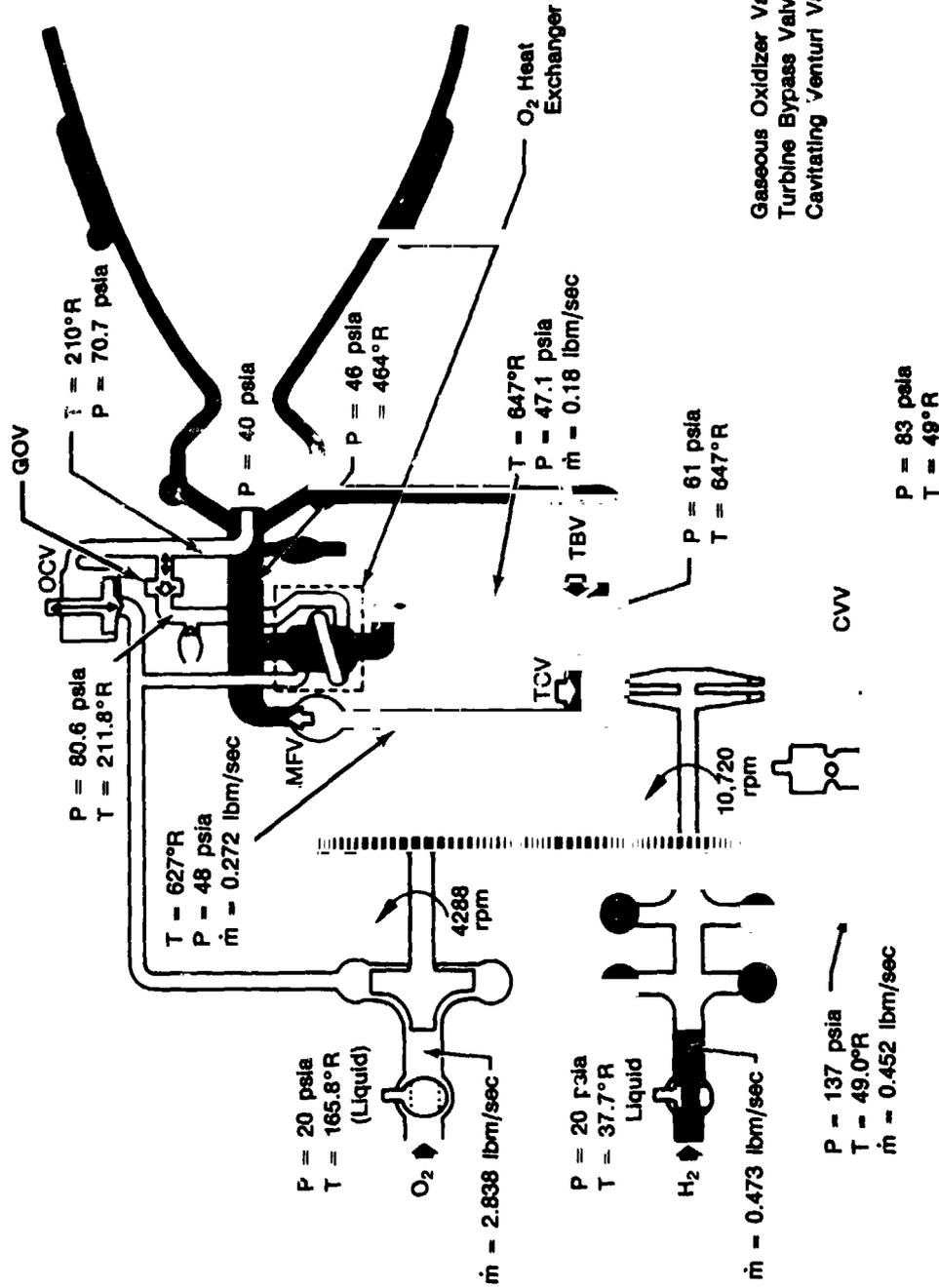
	ΔP-psid	Effective Area (A_{CD}) -in.^{2}
Gaseous Oxidizer Valve (GOV)	9.9	1.273
Turbine Bypass Valve (TBV)	13.9	0.626
Cavitating Venturi Valve (CVV)	54	0.042

Figure 17. RL10-IIB Engine Preliminary Configuration — Pumped Idle (PI) Operating Mode

Thrust Level = 100%
Mixture Ratio (O/F) = 6.0

GOV

OCV

T = 167°R
P = 428 psia

P = 403 psia

P = 459 psia
T = 448°R

O₂ Heat
Exchanger

T = 472°R
P = 460 psia
ṁ = 0.046 lbm/sec

TBV

P = 693 psia
T = 472°R

TCV

CVV

28,654
rpm

T = 167°R
P = 521 psia

T = 447°R
P = 474 psia
ṁ = 4.514 lbm/sec

MFV

11,462
rpm

P = 20 psia
T = 165.8°R
(Liquid)

O₂

ṁ = 27.96 lbm/sec

P = 20 psia
T = 37.0°R
Liquid

H₂

ṁ = 4.66 lbm/sec

P = 865 psia
T = 58.2°R
ṁ = 4.56 lbm/sec

P = 853 psia
T = 58.2°R
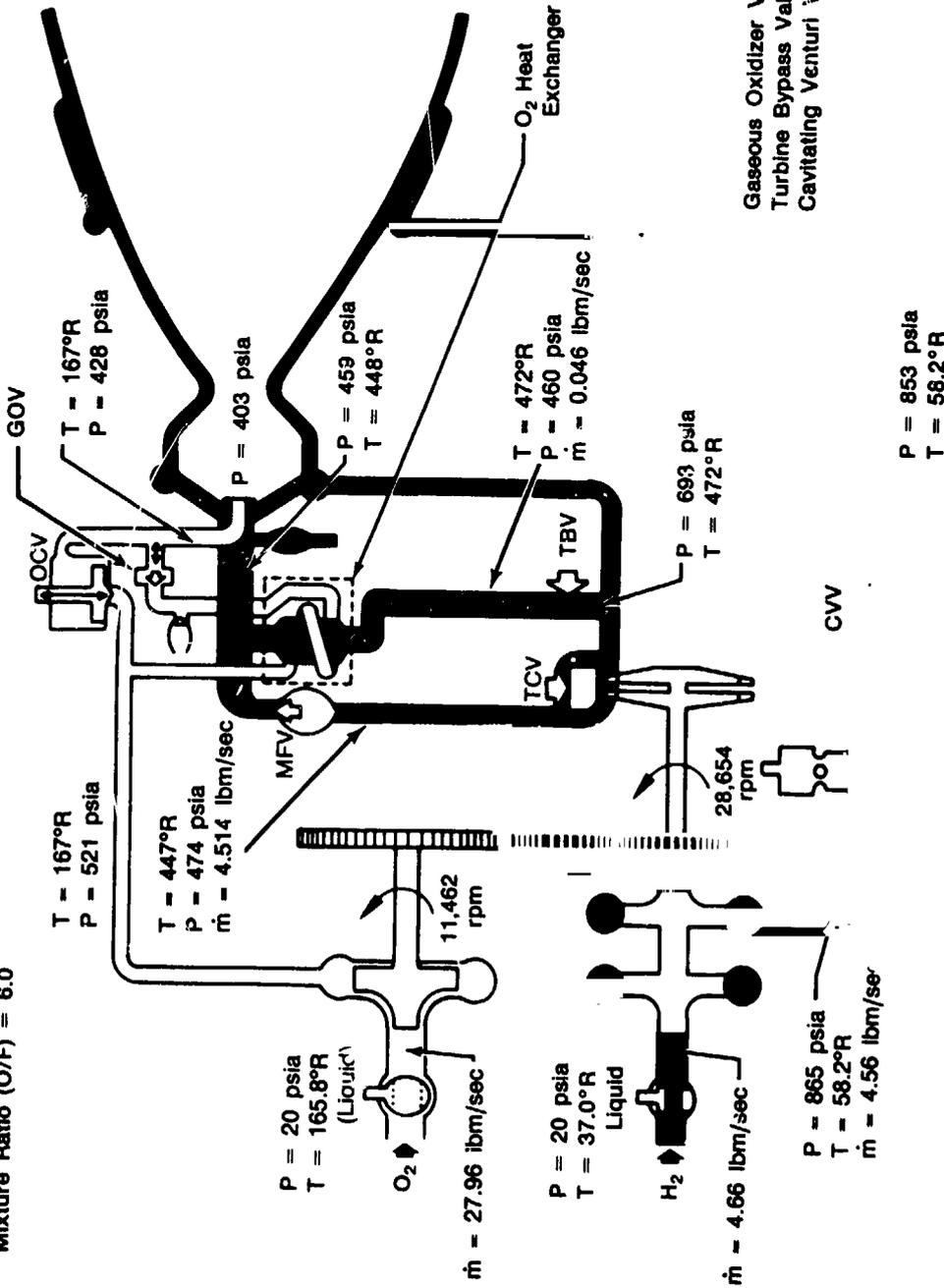
	ΔP-psid	Effective Area (A_{CD}) -In.²
Gaseous Oxidizer Valve (GOV)	-	0
Turbine Bypass Valve (TBV)	233	0.011
Cavitating Venturi Valve (CVV)	7.5	0.258

FD 278894
840412
9992B

Figure 18. RL10-IIB Engine Preliminary Configuration — Full Thrust Level

17

Table 2. *RL10-IIB Engine Cycle Configurations Studied — Preliminary Analysis Summary*

	Configuration Number					
	1	*2*	*3*	*4*	*5*	*6*
Inlet Conditions*	Breadboard	Breadboard	Flight Representative	Flight Representative	Flight Representative	Flight Representative
Gear Ratio (H_2/O_2)	2.5	2.5	2.5	2.1	2.1	2.5
Oxidizer Injector A_{CD} — in.^{2}	0.8	1.0	0.8	0.8	1.0	1.0
Turbine Stators A_{CD} — in.^{2}	0.9	0.9	0.9	0.9	0.9	0.9
Acceptable Gaseous Oxidizer Valve (GOV) Characteristics	Marginal	Yes	No	Yes	Yes	Yes

*Breadboard Tests — Fuel Pump Inlet Pressure (FPIP) = 25 psia Net Positive Suction Pressure (NPSP) = 4.5 psi

— Oxidizer Pump Inlet Pressure (OPIP) = 33 psia Net Positive Suction Pressure (NPSP) = 10 psi

Flight Representative Tests — FPIP = 20 psia NPSP = 2.0 psi

— OPIP = 20 psia NPSP = 2.0 psi

0893C
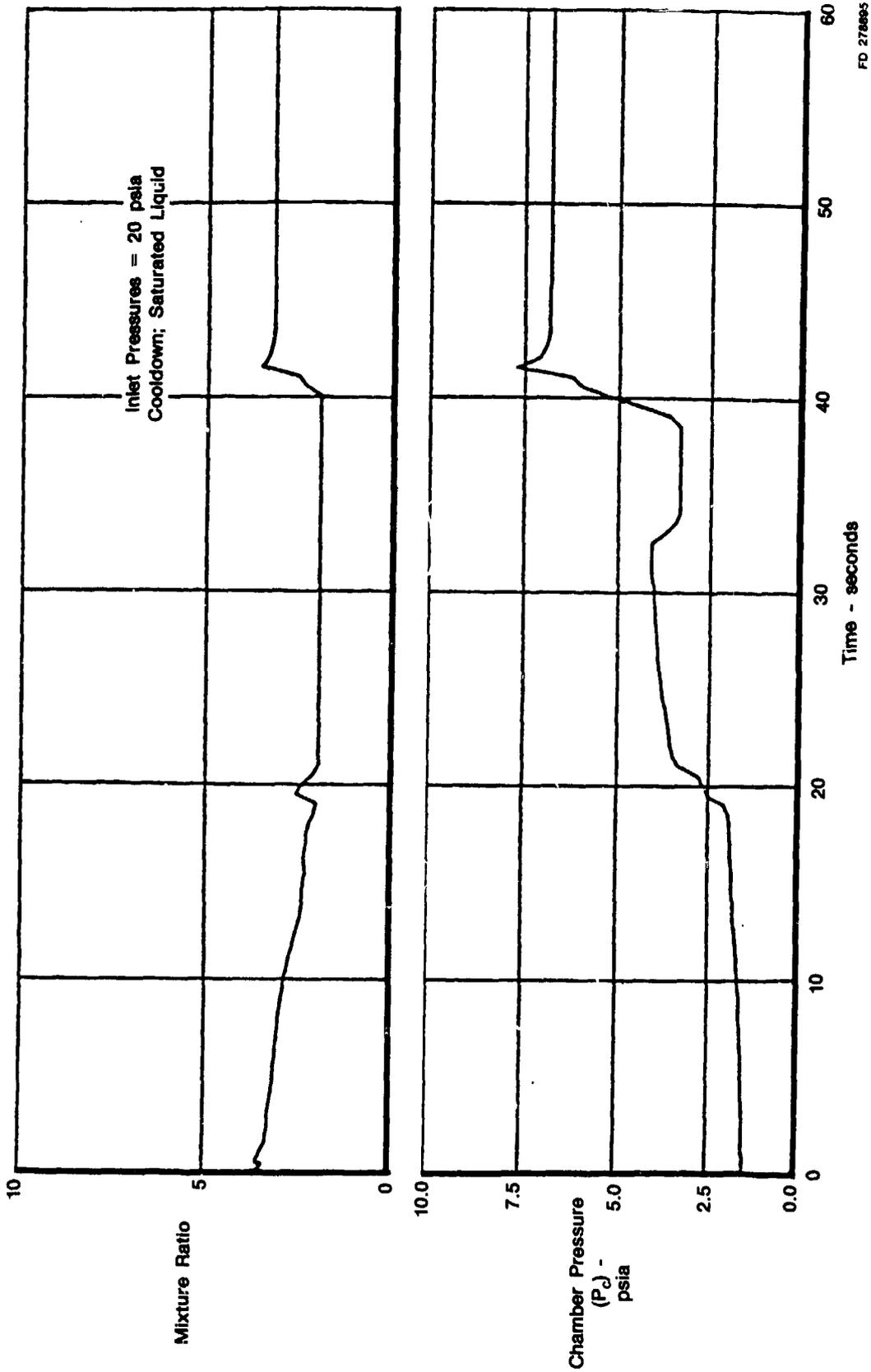
Figure 19. *Preliminary Analysis of RL10-IIB Engine Start to Tank Head Idle Mode Transient (Mixture Ratio and Chamber Pressure versus Time)*

19
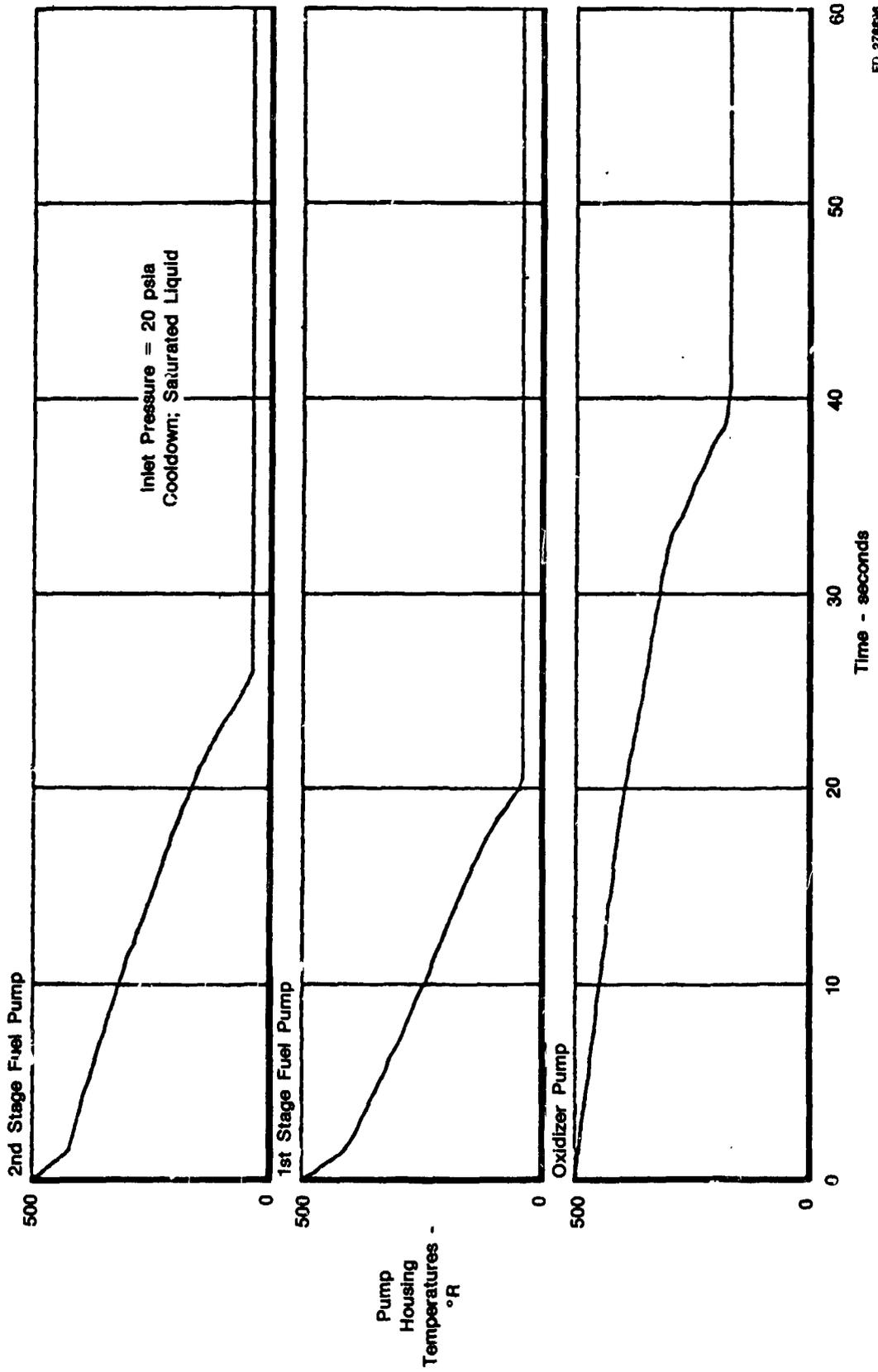
Figure 20. *Preliminary Analysis of RL10-IIB Engine Start to Tank Head Idle Mode Transient (Pump Housing Temperature versus Time)*

Inlet Pressure = 20 psia
Cooldown: Saturated Liquid
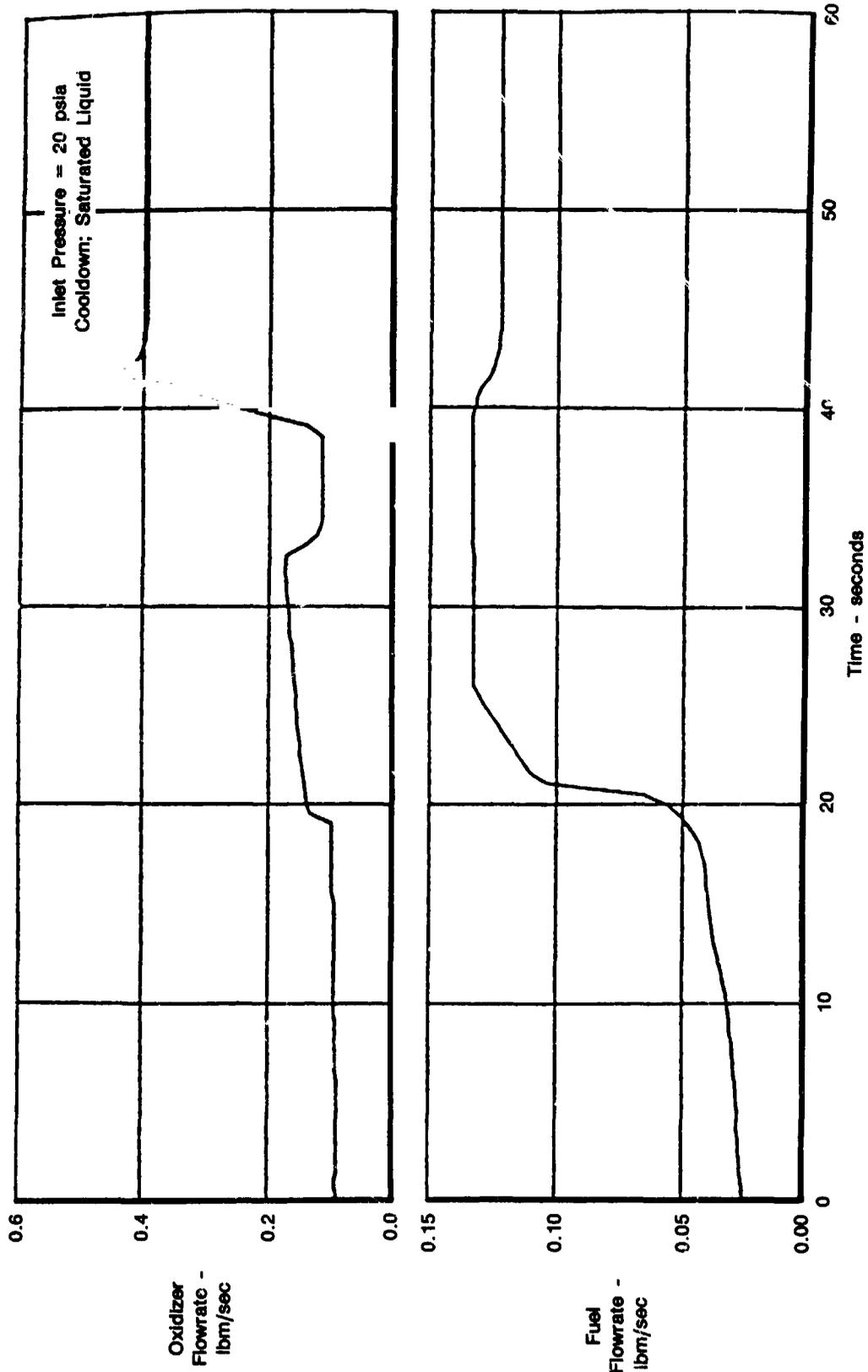
FJ 278697

Figure 21. Preliminary Analysis of RL10-IIB Engine Start to Tank Head Idle Mode Transient (Oxidizer and Fuel Flowrates versus Time)
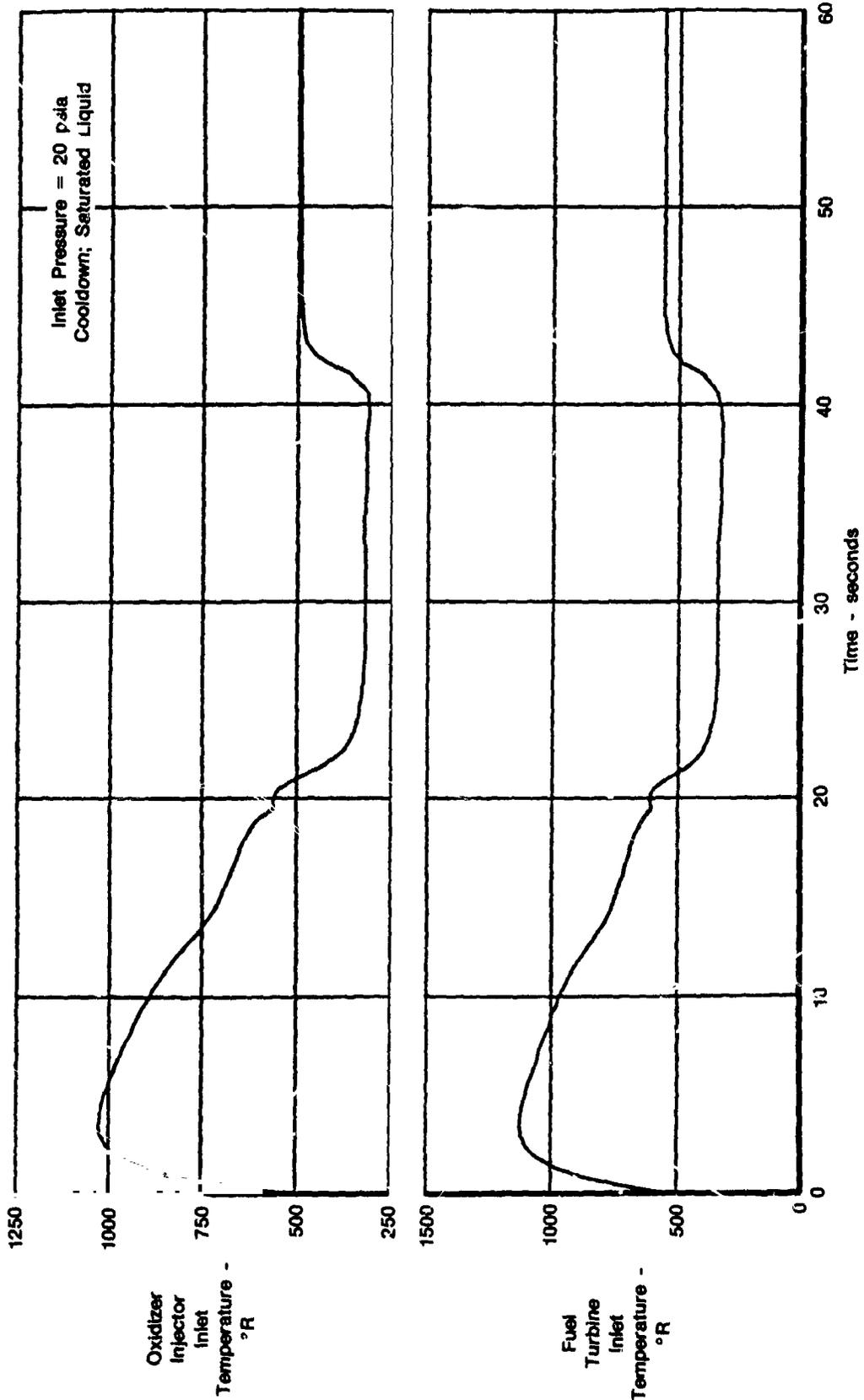
Figure 22. *Preliminary Analysis of RL10-IIB Engine Start to Tank Head Idle Mode Transient (Oxidizer Injector Inlet Temperature and Fuel Turbine Inlet Temperature versus Time)*
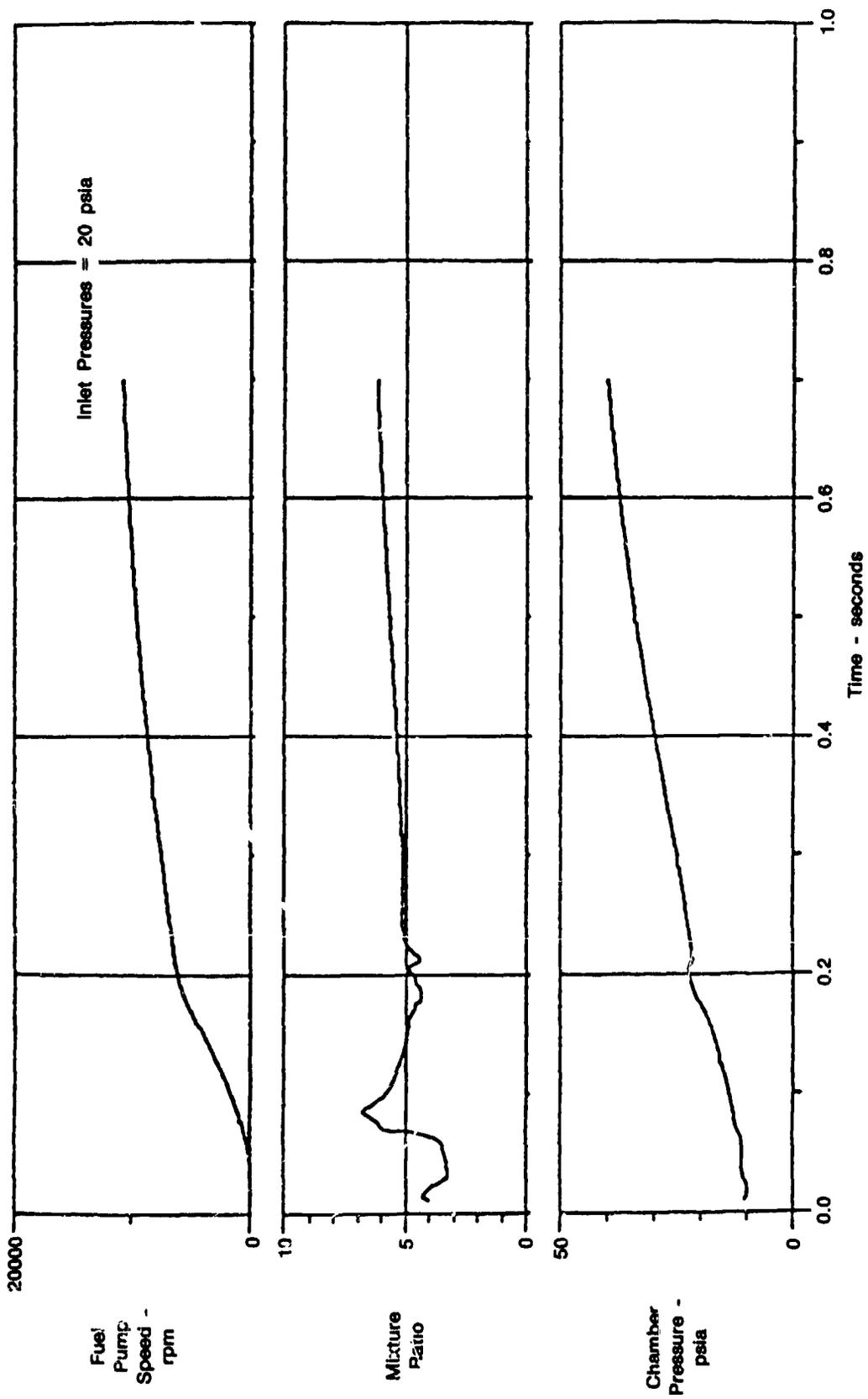
Figure 23. *Preliminary Analysis of RL10-IIB Engine Tank Head Idle to Pumped Idle Mode Transient (Fuel Pump Speed, Mixture Ratio, and Chamber Pressure versus Time)*
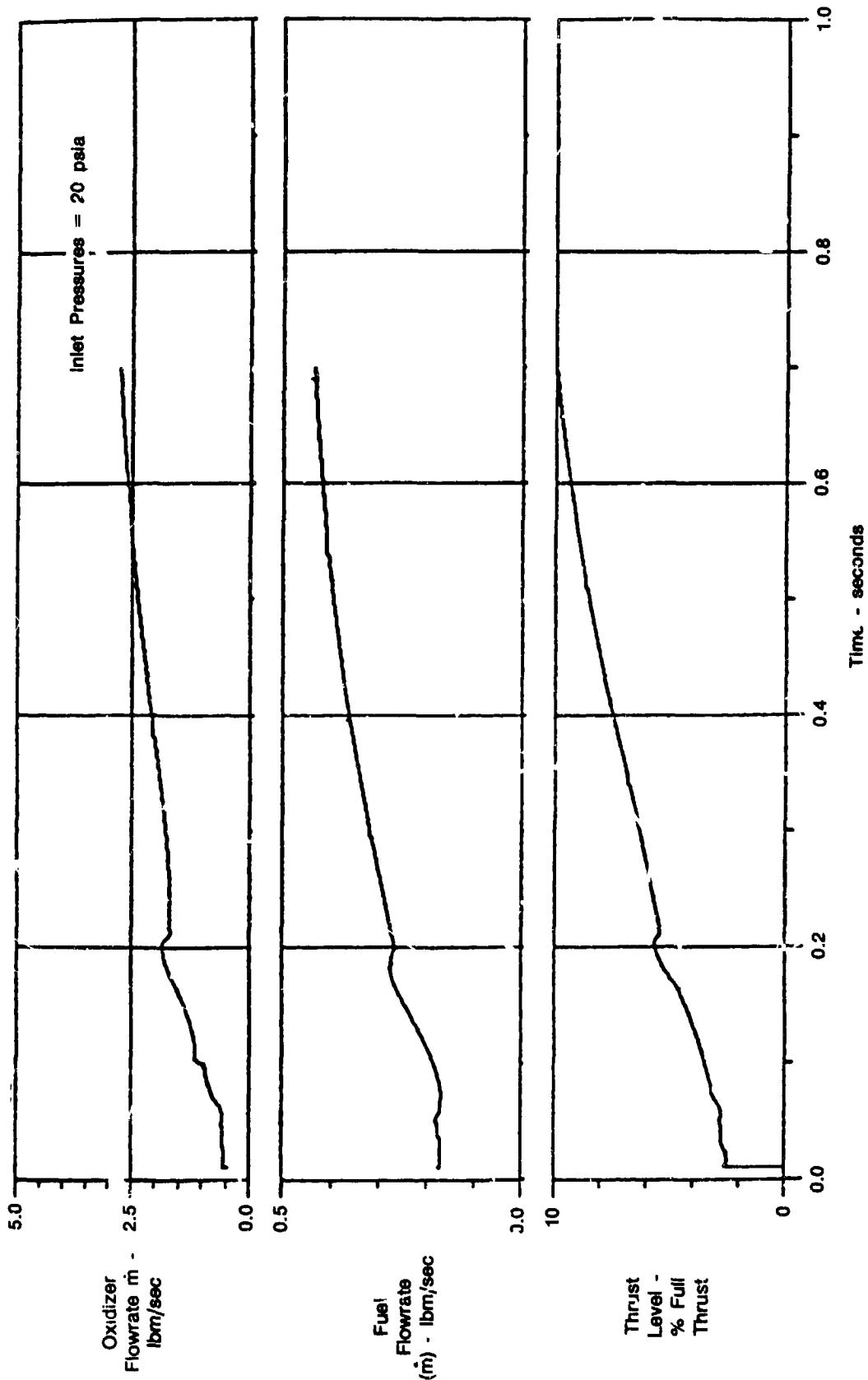
Figure 24. Preliminary Analysis of RL10-IIB Engine-Tank Head Idle to Pumped Idle Mode Transient (Oxidizer Flowrate, Fuel Flowrate, and Thrust Level versus Time)

FD 278900

24
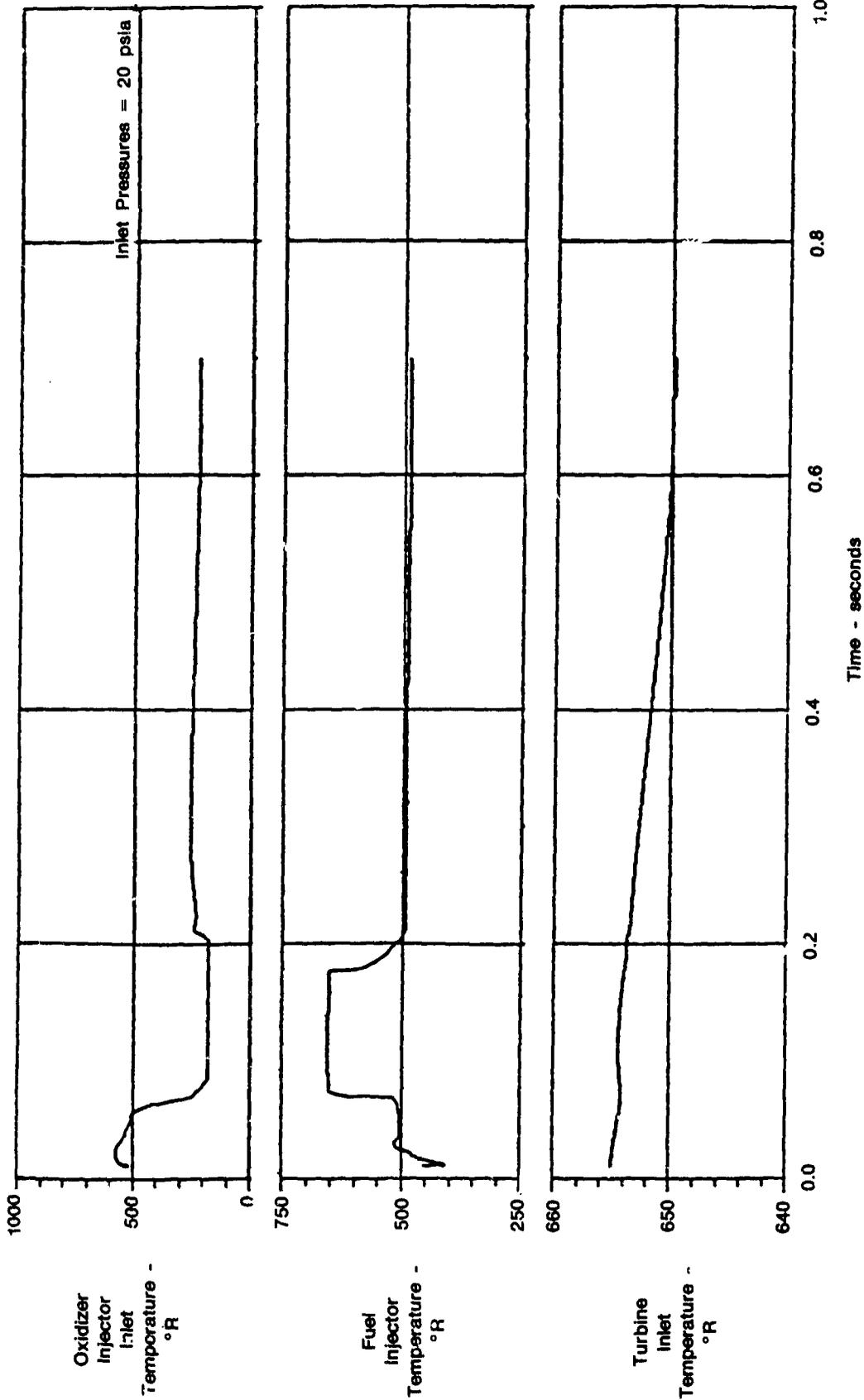
Figure 25. *Preliminary Analysis of RL10-IIB Engine Tank Head Idle to Pumped Idle Mode Transient (Oxidizer Injector Inlet, Fuel Injector, and Turbine Inlet Temperature versus Time)*

FD 27.001
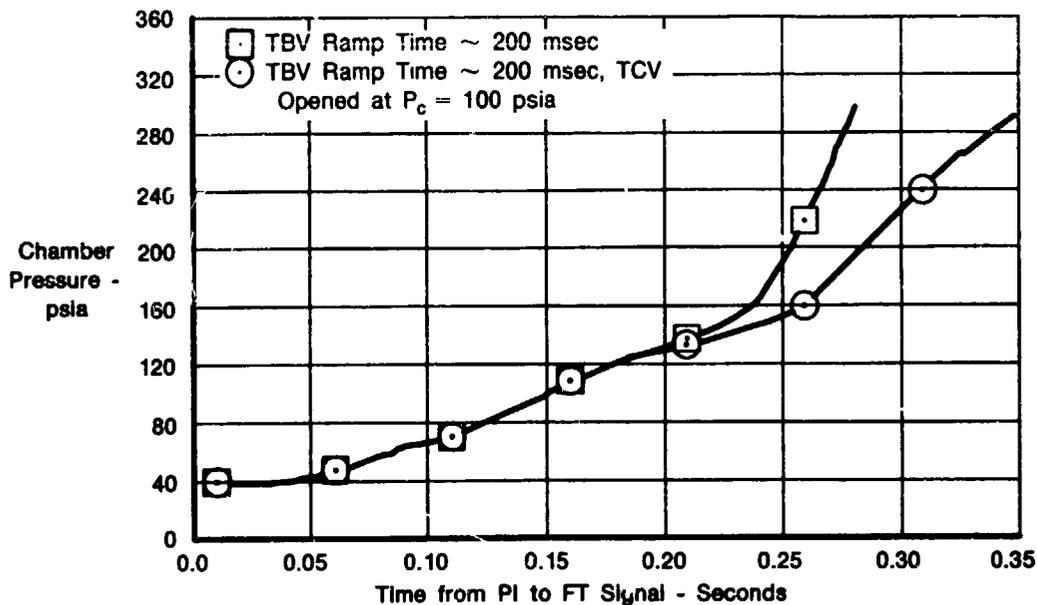
FD 278902

Figure 26. *RL10-IIB Engine Transient — Pumped Idle Mode to Full Thrust (Chamber Pressure versus Time)*
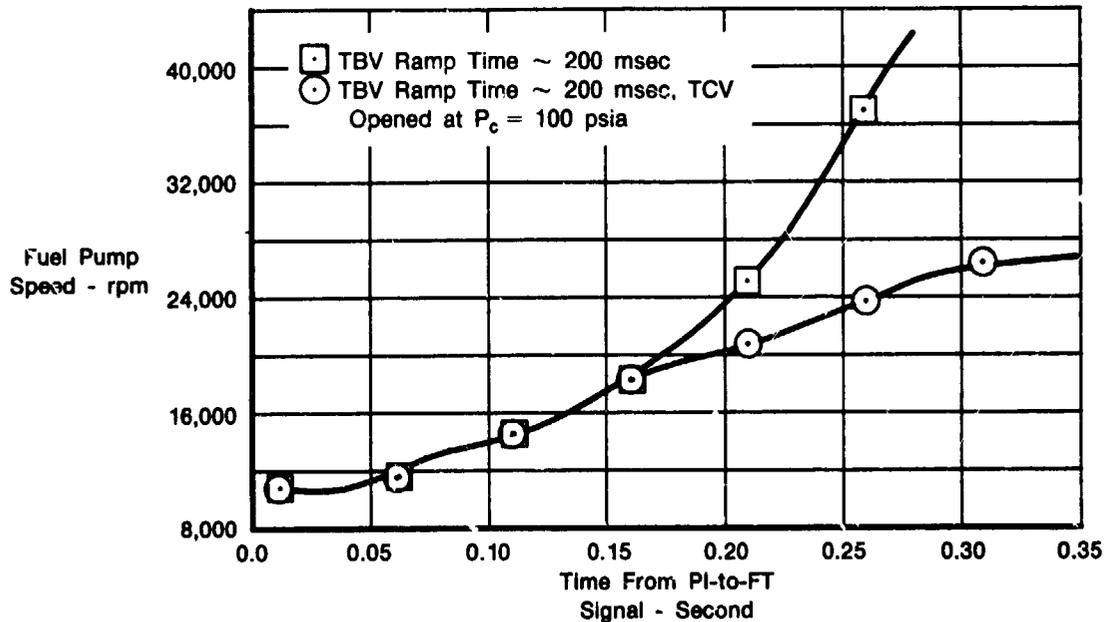
FD 278903

Figure 27. *RL10-IIB Engine Transient — Pumped Idle Mode to Full Thrust (Fuel Pump Speed versus Time)*
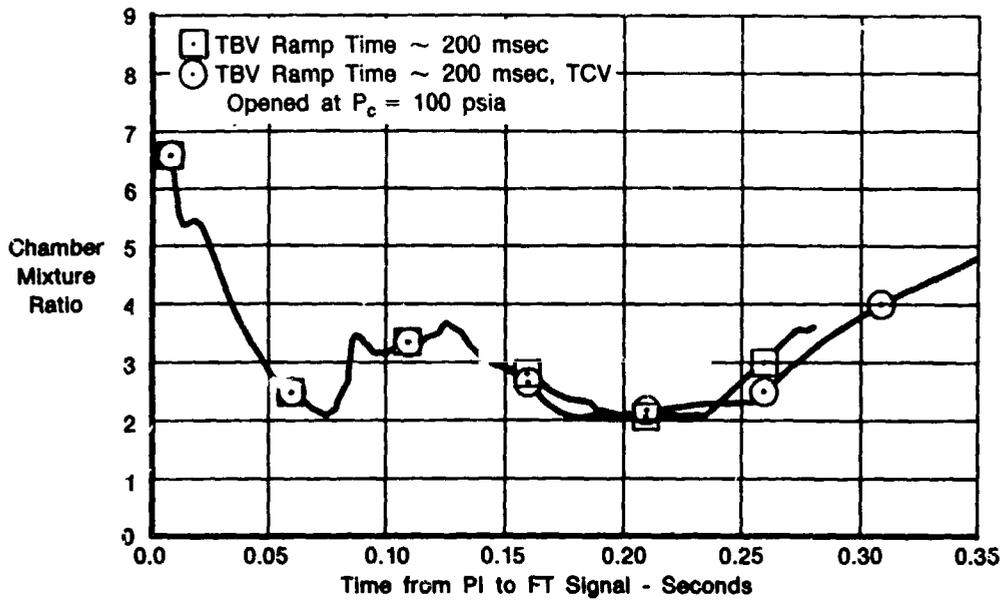
FC 278904

Figure 28. RL10-IIB Engine Transient — Pumped Idle Mode to Full Thrust (Chamber Mixture Ratio versus Time)
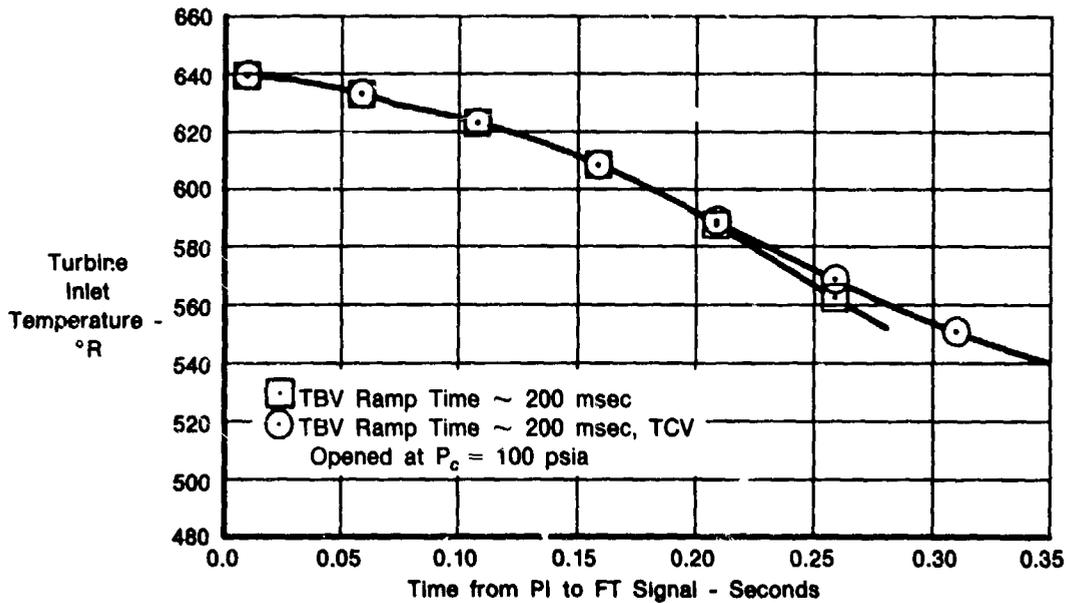
FD 278905

Figure 29. RL10-IIB Transient — Pumped Idle Mode to Full Thrust Level (Turbine Inlet Temperature versus Time)
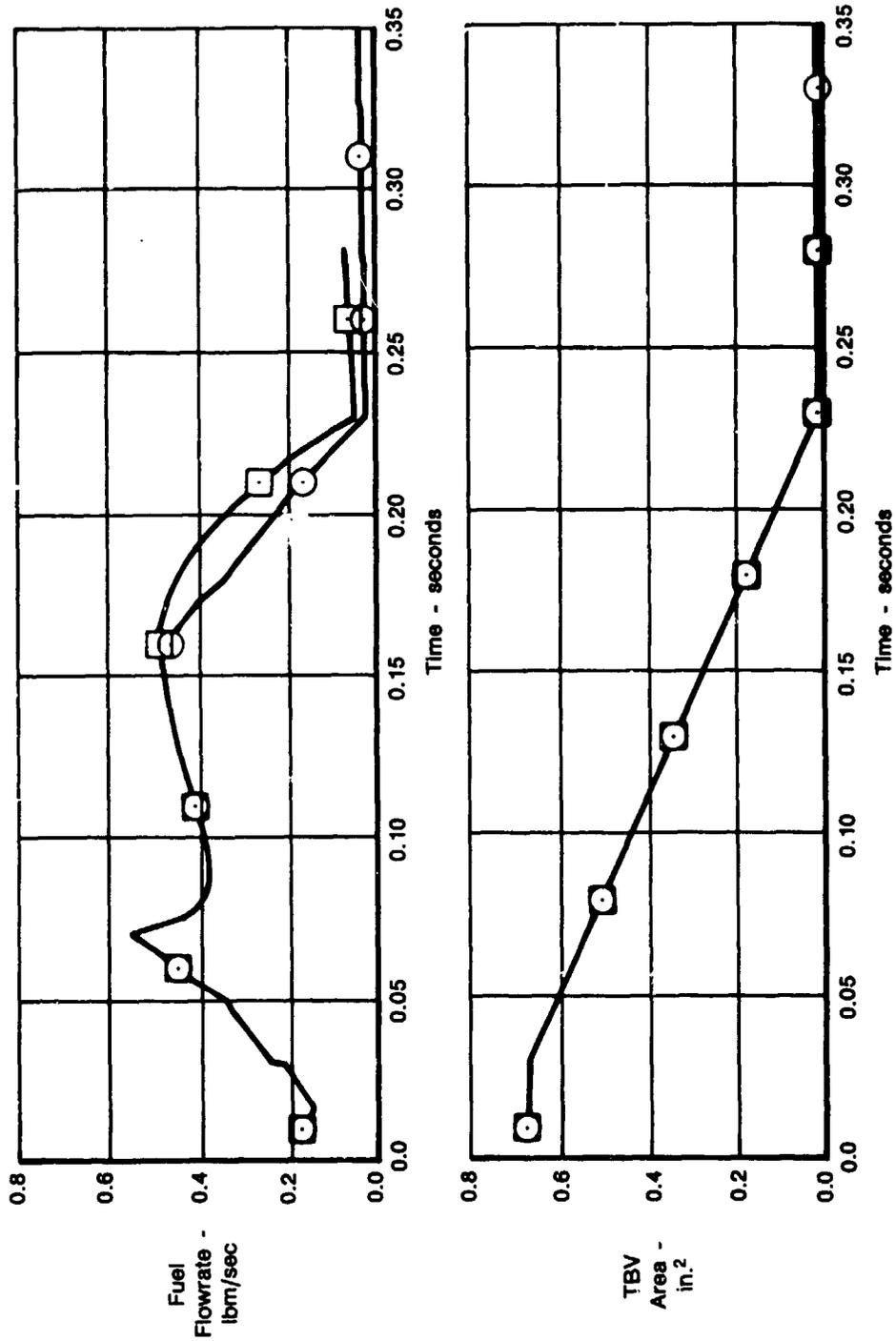
Figure 30. RL10-IIB Engine Transient — Turbine Bypass Valve (TBV) Parameters (Pumped Idle Mode to Full Thrust)
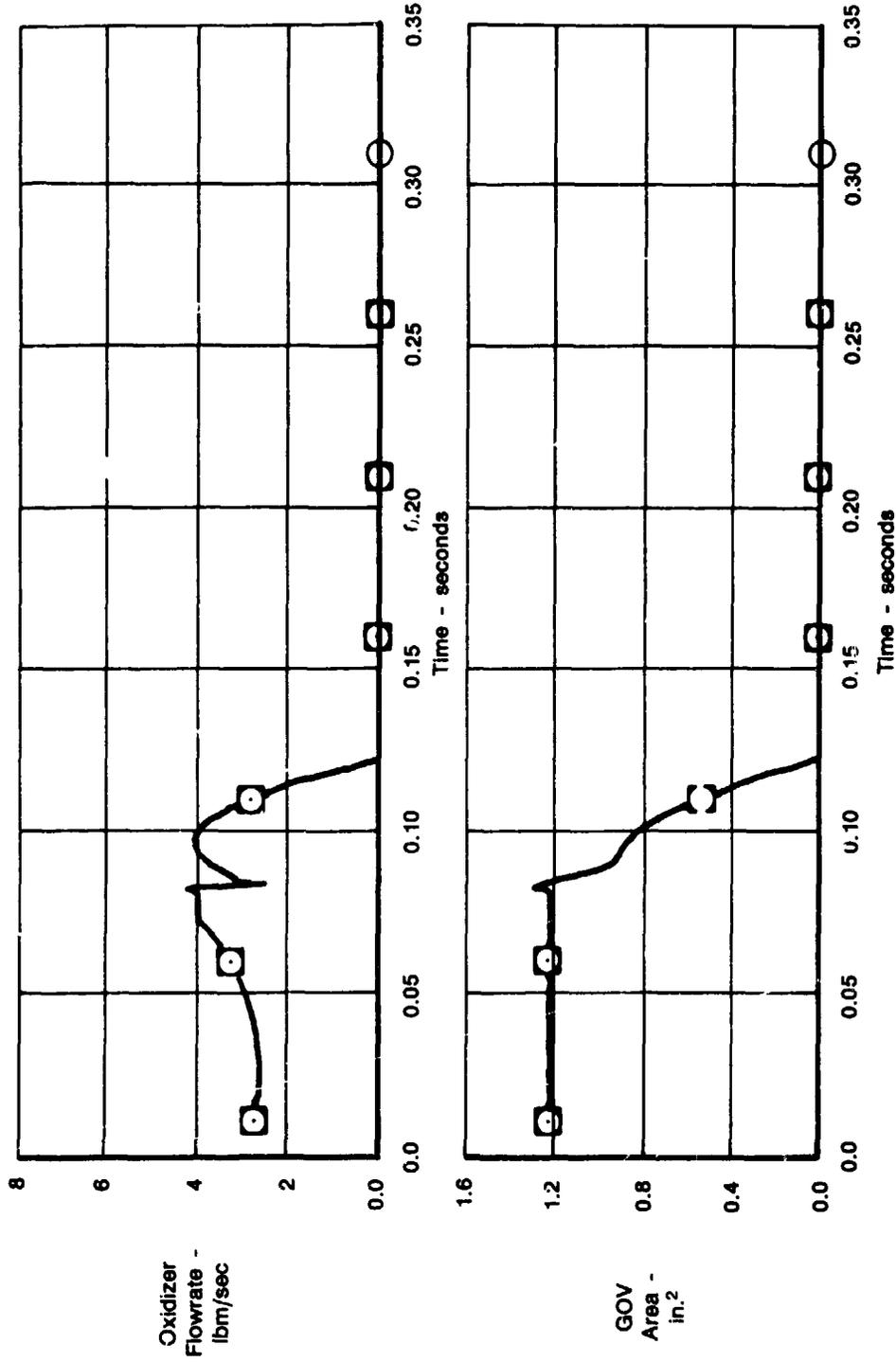
Figure 31. *RL10-IIB Engine Transient — Gaseous Oxidizer Valve (GOV) Parameter (Pumped Idle to Full Thrust)*

FD 276907
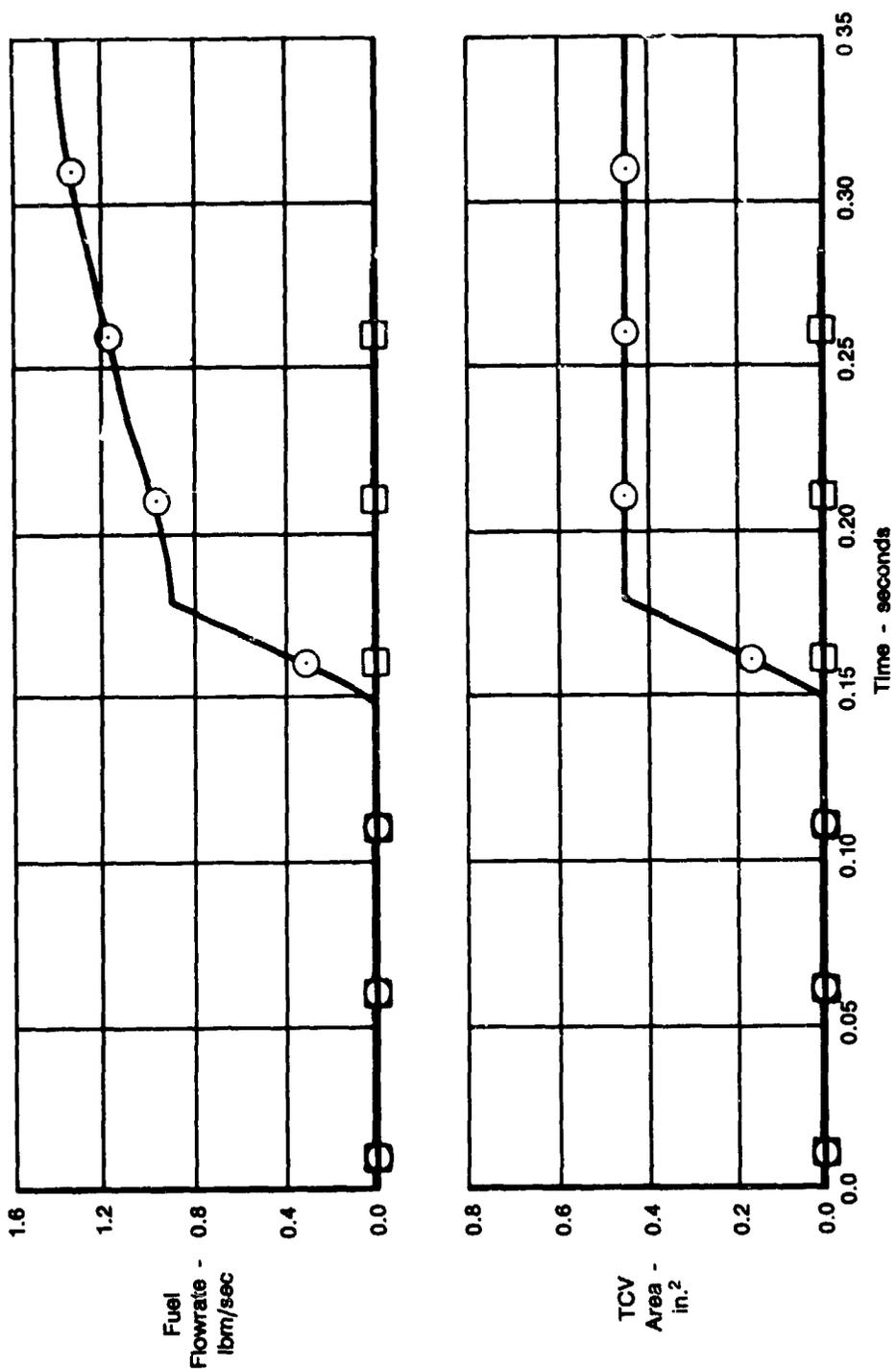
Figure 32. *RL10-IIB Engine Transient — Thrust Control Value (TCV) Parameters (Pumped Idle Mode to Full Thrust)*

FD 27890A

Figure 33. *RL10-IIB Engine Preliminary Updated Configuration — Tank Head Idle (THI) Operating Mode*

Thrust = THI
Mixture Ratio (O/F) = 4.0
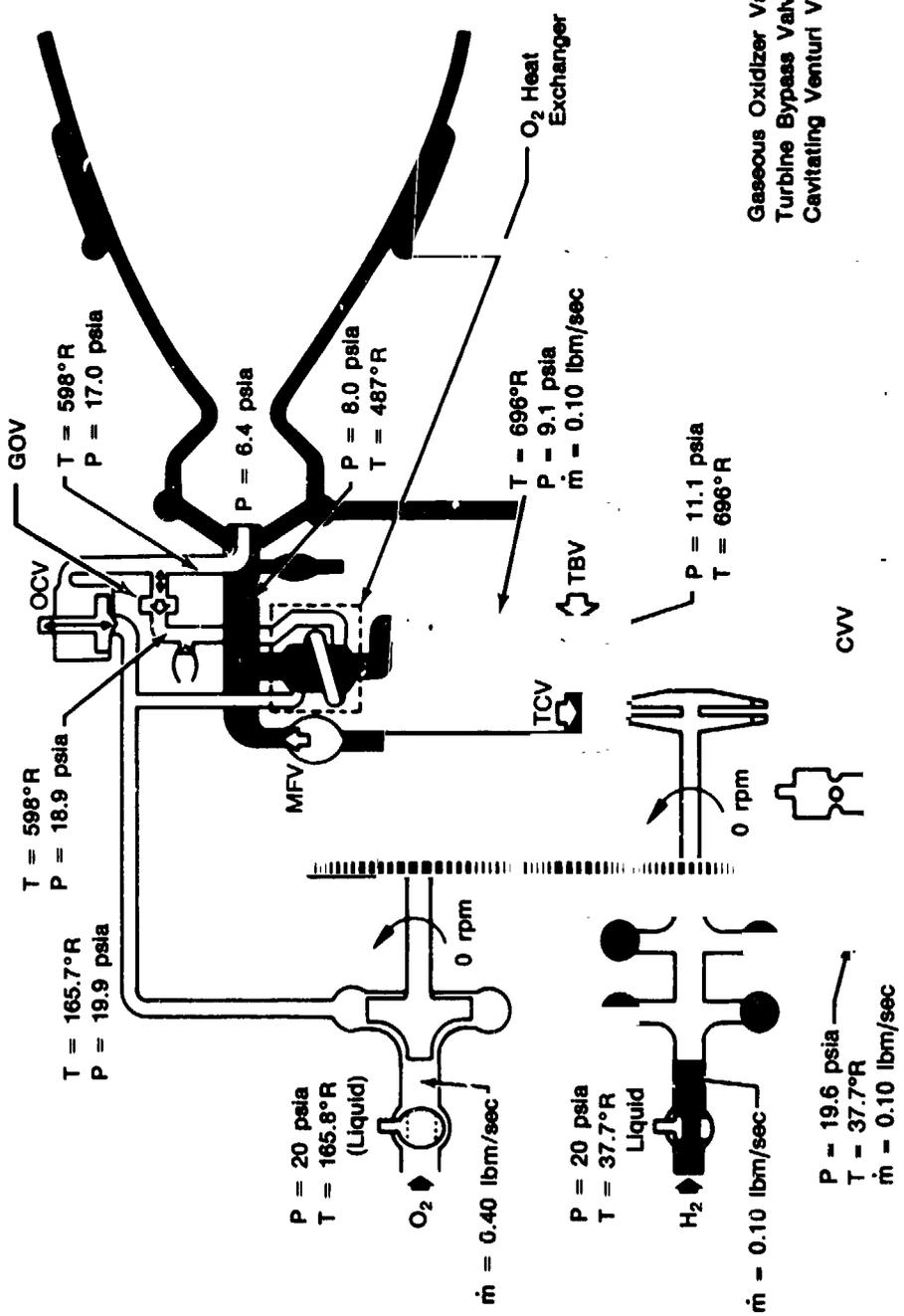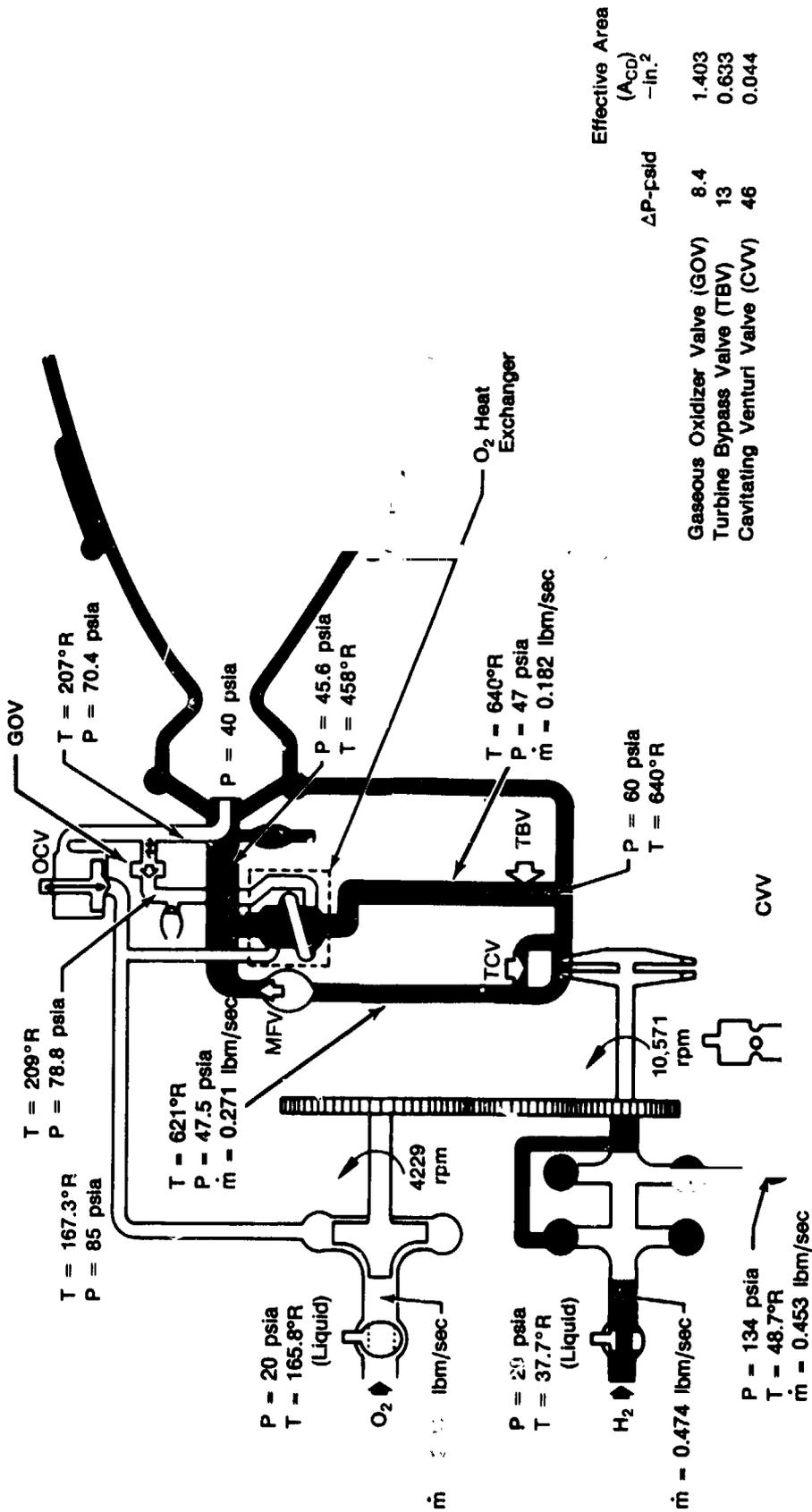
	ΔP-psid	Effective Area (A$_{CD}$) –in.²
Gaseous Oxidizer Valve (GOV)	1.9	1.403
Turbine Bypass Valve (TBV)	2.0	2.0
Cavitating Venturi Valve (CVV)	0.1	0.258

FD 278909

Figure 34. RL10-IIB Engine Preliminary Updated Configuration — Pumped Idle (PI) Operating Mode
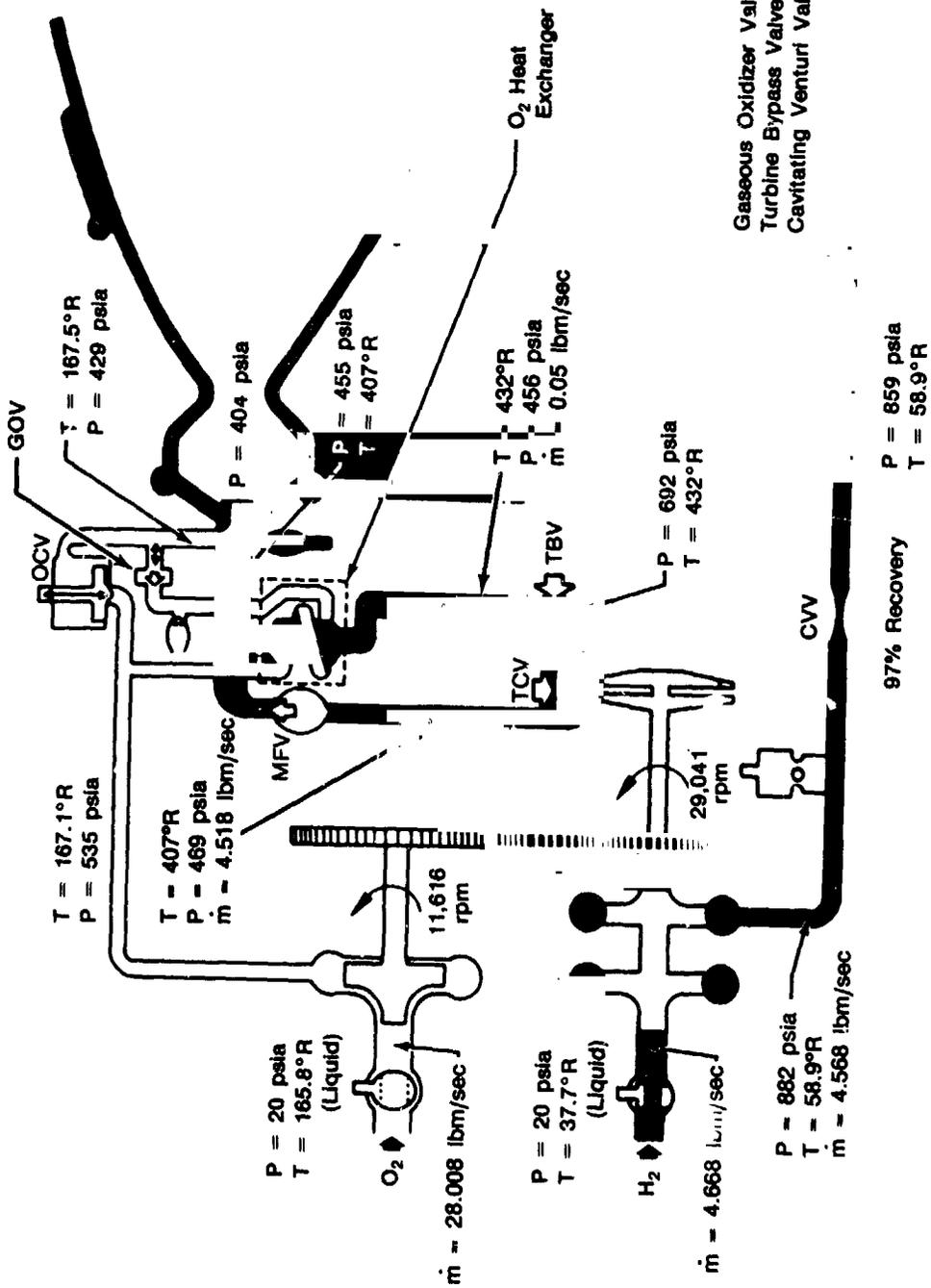
Figure 35. RL10-IIB Engine Preliminary Updated Configuration — Full Thrust Level

33
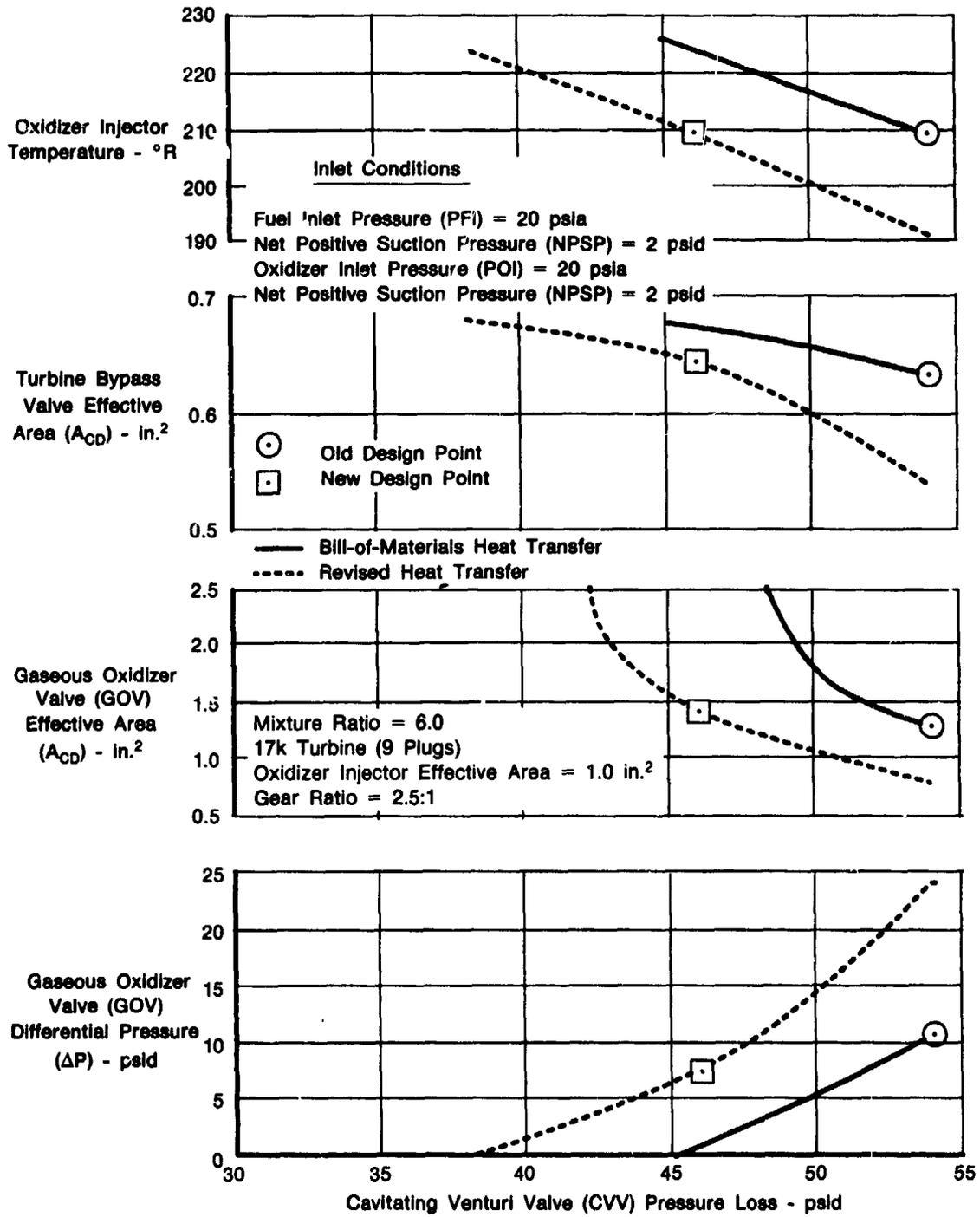
Figure 36. *RL10-IIB Engine Operation (10% Thrust Level)*

FD 278912

C. ALTERNATE GAS/GAS CONFIGURATION

At this point in the analysis a change in the engine's basic flowpath was investigated. The engine, in its preliminary configuration, utilizes the oxygen-hydrogen heat exchanger in the turbine bypass flowpath (Figure 37) to vaporize the liquid oxygen at low thrust levels ($<10\%$), thus providing adequate injector pressure loss to ensure stable combustion. During acceleration to FT, closing the GOV causes the oxygen to be routed through the OCV to the injector where sufficient injector differential pressure (ΔP) is available for stable operation at FT. However, a portion of the preliminary engine acceleration range (between 10% and 40% thrust) may have insufficient injector (liquid oxygen) ΔP to prevent combustion instability with the GOV closed. Therefore, an alternative configuration was conceived to eliminate this possibility. The heat exchanger was moved to the fuel leg downstream of the main shutoff valve (Figure 38) so that both propellants flow through it at all times, thus ensuring sufficient oxidizer injector ΔP and potentially allowing stable engine operation throughout the range from 2% to 100% thrust.

This configuration change would eliminate the liquid oxidizer flow control valve. Ground mixture ratio trim and propellant utilization capability would have to be added to the gaseous oxygen valve (GOV). Then, to accommodate the full thrust (FT) gaseous oxygen flow, the injector's effective area would have to be increased. Initially, an area of 2.0 in.^{2} was investigated, but this area resulted in a marginal fuel pump stall margin. Therefore, to increase fuel pump stall margin, the area was further increased to 3.0 in.^{2} To maximize combustor efficiency, the velocity of the gaseous hydrogen into the chamber was also increased to match the velocity increase that resulted from gaseous oxygen injection at FT. This was achieved by decreasing the fuel injector effective area by approximately 25% to 1.7 in.^{2} To ensure adequate pressure loss on the oxidizer side (for control purposes) and to move the fuel pump operation away from the stall line, the H_2/O_2 pump gear ratio was reduced from 2.5 to 2.1. Pump operating parameters at 10% thrust level are presented in Figures 39 and 40. The effects of varying the mixture ratio and cavitating venturi ΔP on the 10% thrust operation are shown in Figure 41. Engine cycle points for this alternative (gas/gas) configuration are shown in Figures 42 through 44. Table 3 compares the preliminary configuration with this alternative configuration.

D. BASELINE CONFIGURATION

A proposal to build the alternative configuration for testing was rejected because of the significant changes to engine hardware and operations experience not related to low thrust requirements, however the option to implement it later was left open. The same oxygen-hydrogen heat exchanger design requirements apply to either of the low thrust engine configurations. The 2.1:1 gears, however, offer benefits to both the gas/liquid and gas/gas versions of the engine, so a decision was made to incorporate the gears into the gas/liquid engine. These gears also allow the oxidizer injector area to be reduced to 0.8 in.^{2} — the same area as in current RL10A-3-3A production engines. Flow schematics for the resultant "baseline" engine configuration design points at THI, PI, and FT are presented in Figures 45 through 47.

E. UPDATED BASELINE CONFIGURATION

Cycle analysis was continued with updated component operating characteristics as engine design data became available for the current RL10A-3-3A production engine and the RL10-IIB engine. Incorporated into the steady-state cycle deck were: updated RL10A-3-3A turbopump performance characteristics, revised predictions for the 55-inch RL10-IIB thrust chamber/primary nozzle characteristics, and heat transfer and flow characteristics for the RL10-IIB engine 3-stage oxidizer heat exchanger (OHE), such as shown in Figure 48. The resultant cycle data are shown in Figures 49, 50, and 51 for THI, 10% thrust, and FT operating levels, respectively.
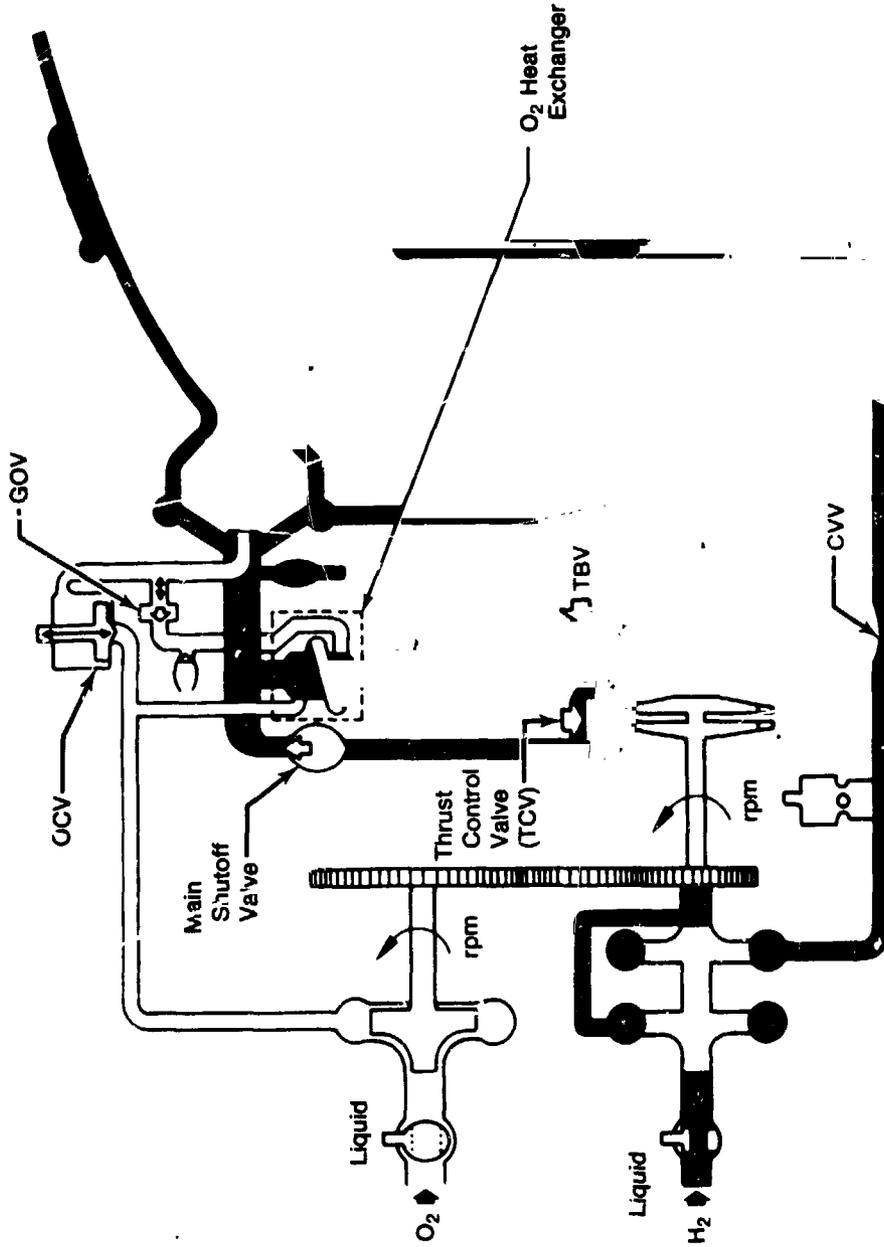
Figure 37. RL10-IIB Engine Preliminary Configuration — Updated Flow Schematic

Gasious
Oxidizer
Valve (GOV)

O₂ Heat
Exchanger

Turbine
Bypass Valve
(TBV)

Cavitating
Venturi Valve
(CVV)

Main
Shutoff
Valve

Thrust
Control
Valve
(TCV)

rpm

rpm

Liquid
O₂

Liquid
H₂
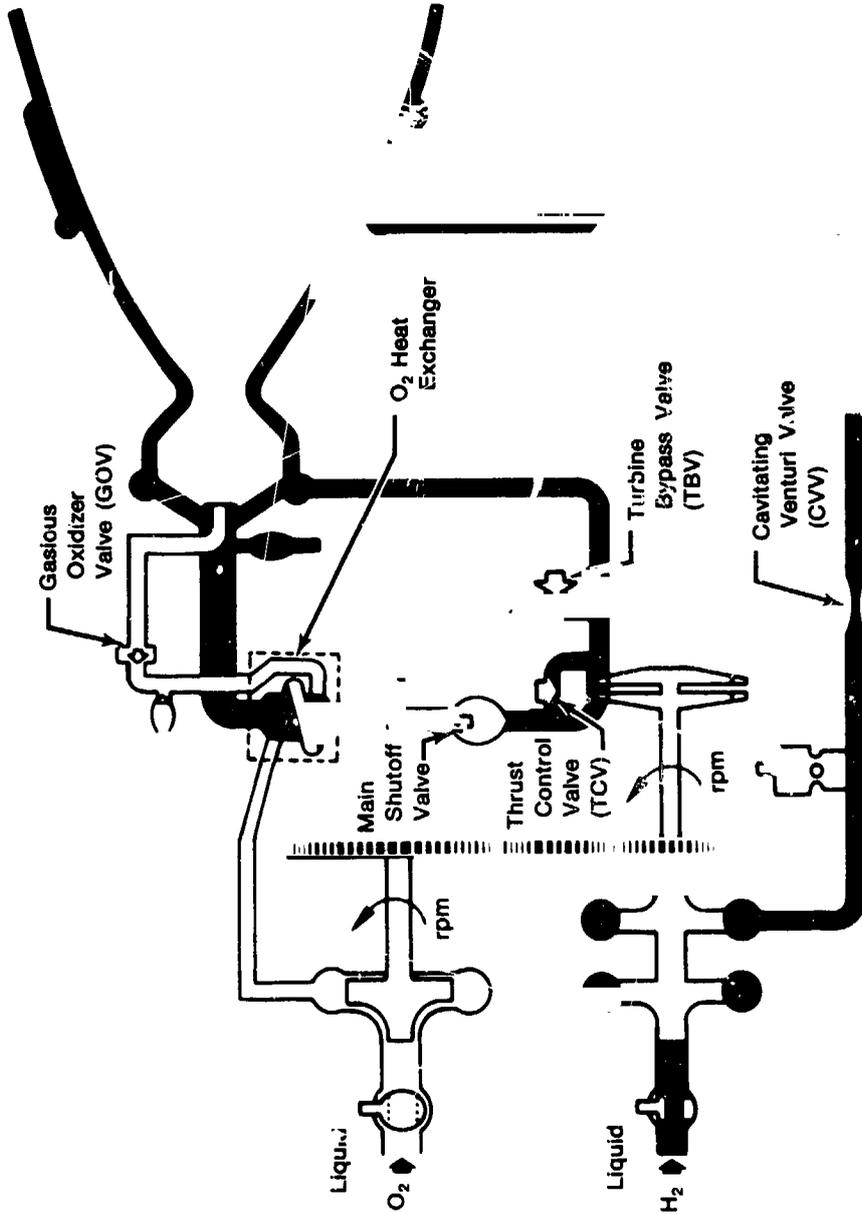
FD 278914

Figure 38. RL10-IIB Engine Alternative Configuration (Gas/Gas) Flow Schematic

Figure 39.   RL10A-3 3 Fuel Pump (2-Stages)

FD 278915

Figure 40. RL10A-3-3 Oxidizer Pump
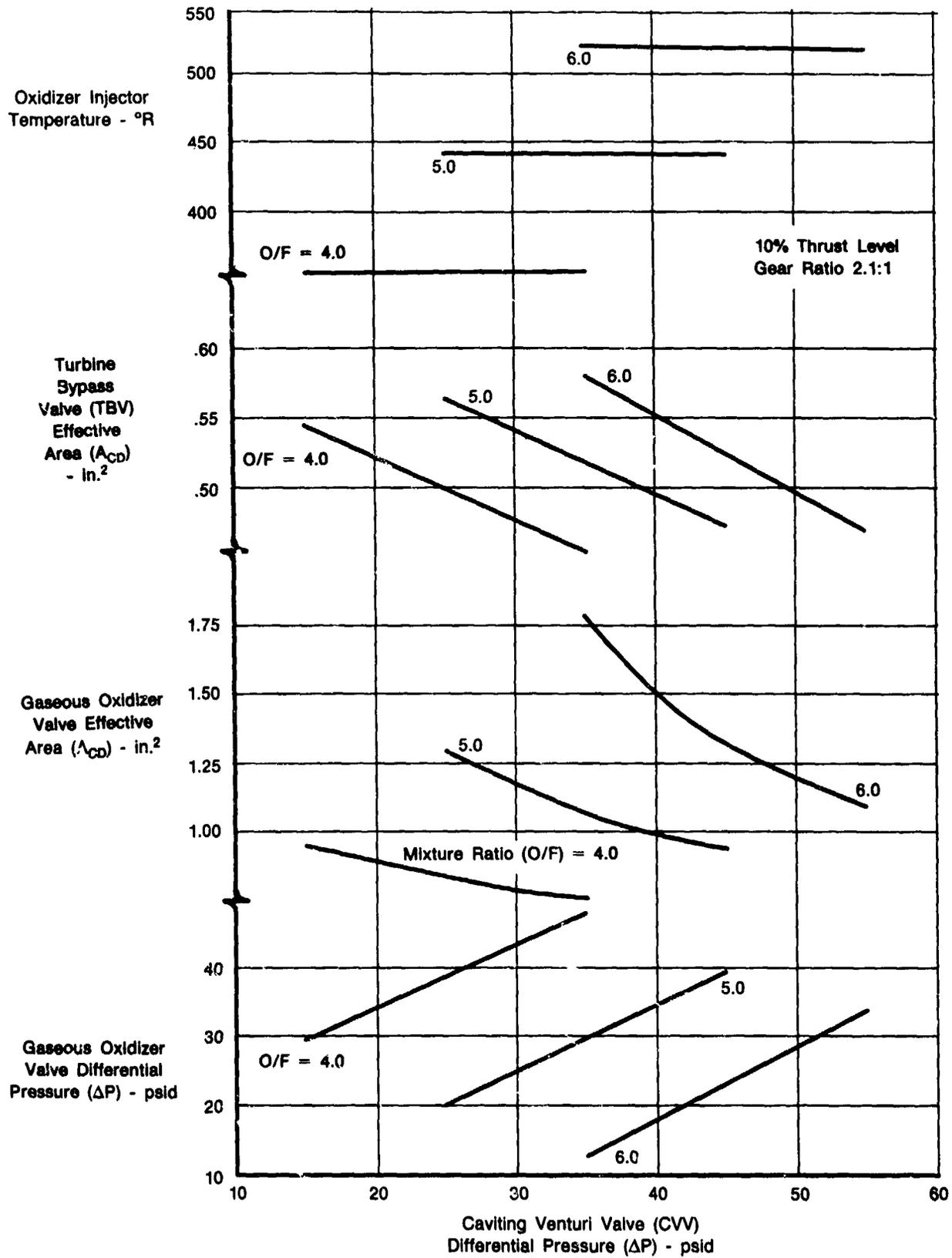
Figure 41. RL10-IIB Alternative Configuration Cycle Deck Results
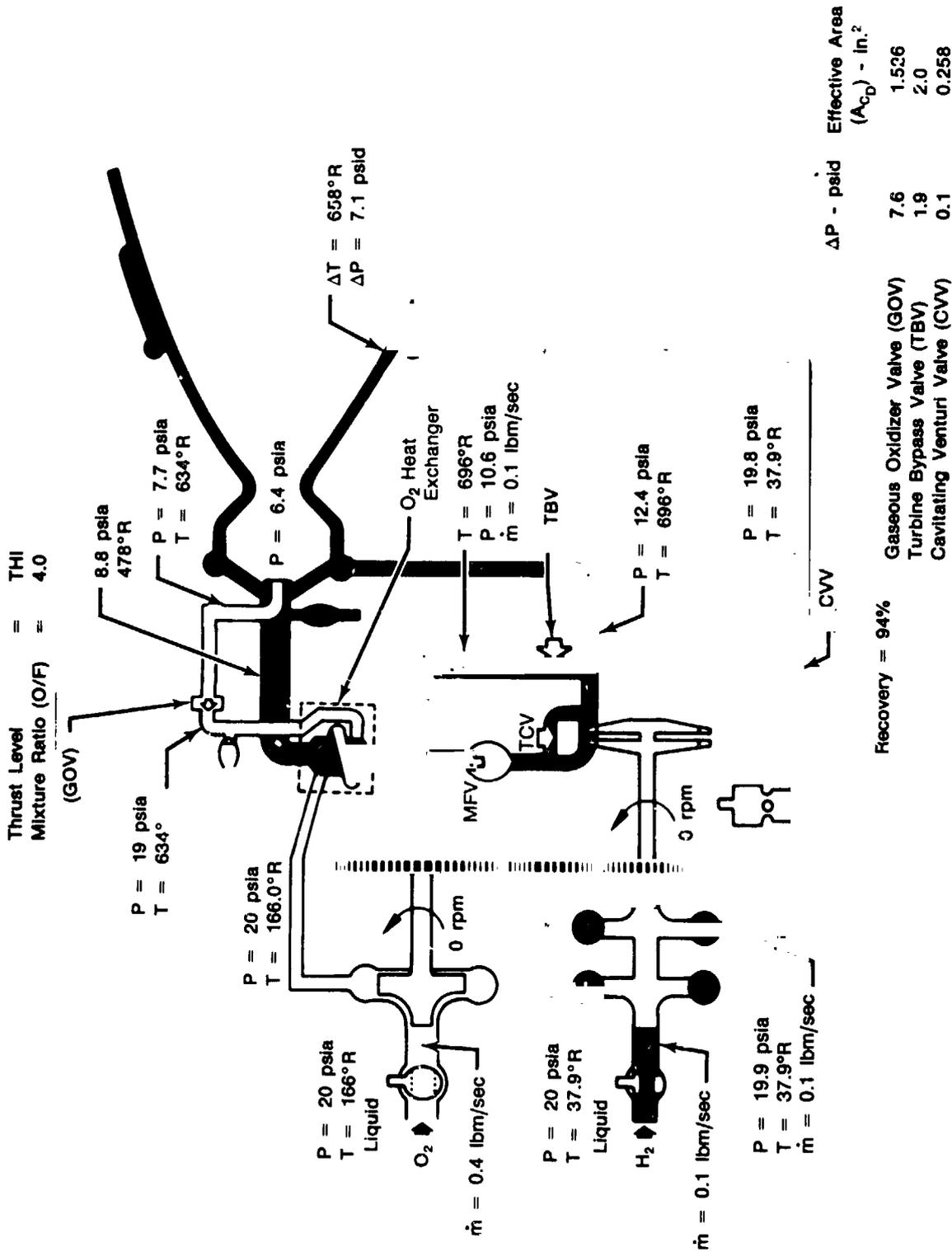
Figure 42. RL10-IIB Engine — Alternative Configuration (Gas/Gas) Flow Schematic — Tank Head Idle (THI) Operating Mode
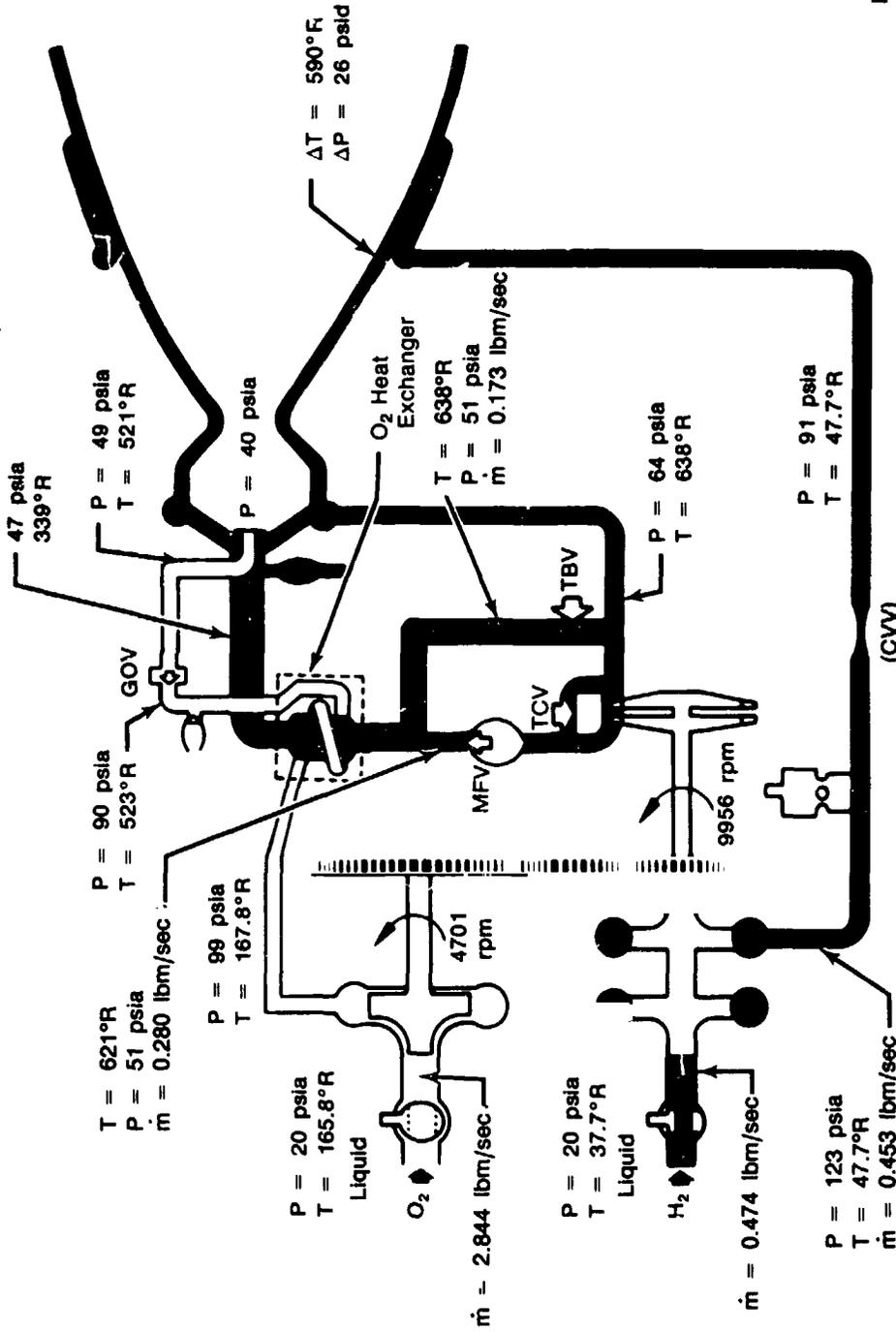
	ΔP - psid	Effective Area (Ac_D) - In.²
Gaseous Oxidizer Valve (GOV)	7.6	1.526
Turbine Bypass Valve (TBV)	1.9	2.0
Cavitating Venturi Valve (CVV)	0.1	0.258

Recovery = 94%

FD 278918

Thrust Level = THI
Mixture Ratio (O/F) = 4.0

Figure 43. RL10-IIB Engine — Alternative Configuration (Gas/Gas) Flow Schematic — Pumped Idle (PI) Operating Mode

Figure 44. RL10-IIB Engine — Alternative Configuration (Gas/Gas) Flow Schematic — (Full Thrust Level)
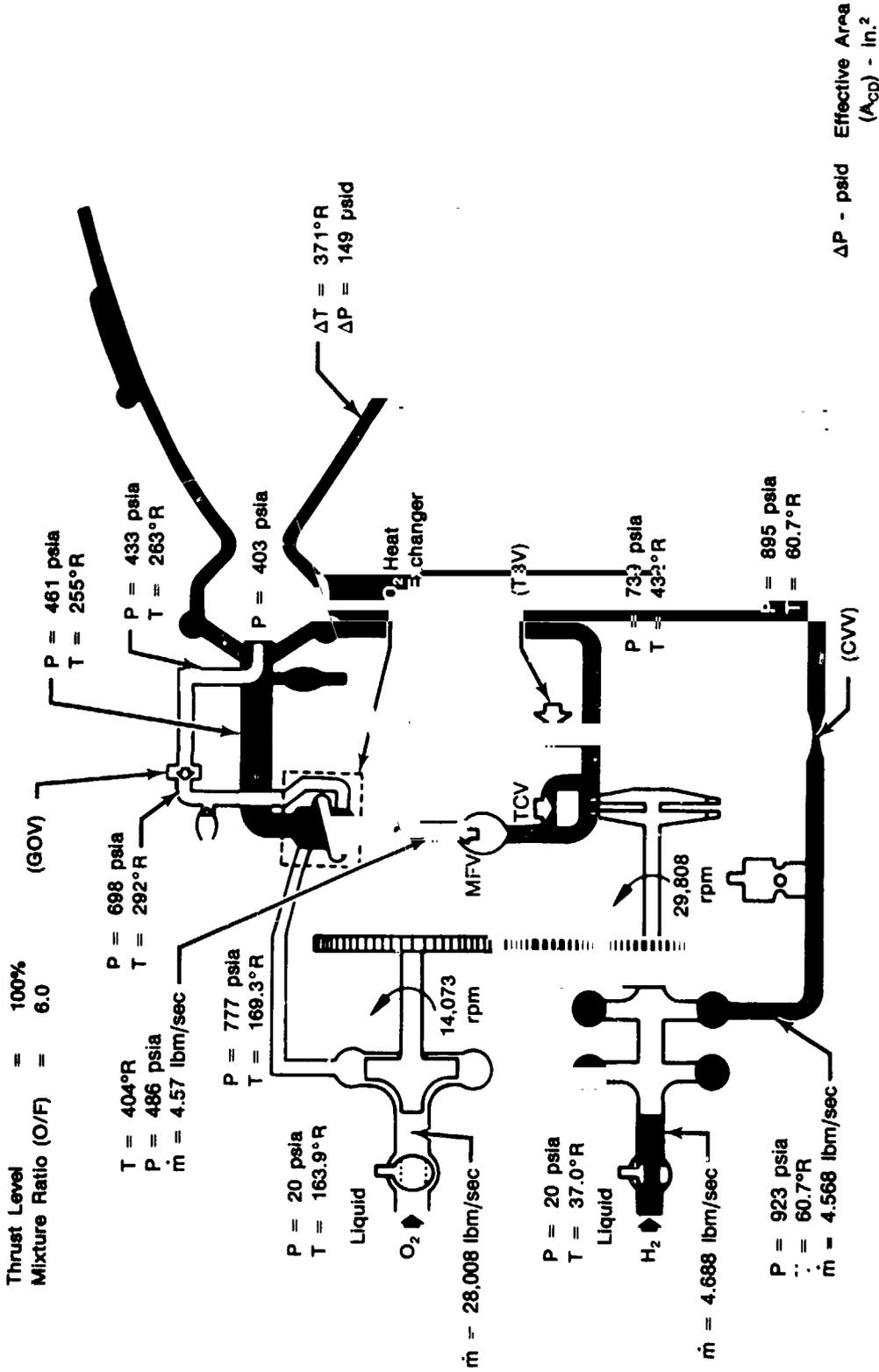
	ΔP - psid	Effective Area (A_{CD}) - in.^{2}
Gaseous Oxidizer Valve (GOV)	142	1.188
Turbine Bypass Valve (TBV)	—	0
Cavitating Venturi Valve (CVV)	20	0.062

Recovery = 90%

Thrust Level = 100%
Mixture Ratio (O/F) = 6.0

FD 278920

43

Table 3. Comparison of the RL10-IIB Engine Preliminary Configuration With the Alternative Configuration

	Preliminary	Alternative
Operating Range — % Full Thrust	2 to 10, 40 to 100	2% — 100%
Oxidizer Control Valve	Yes	No
Gear Ratio	2.5	2.1
Fuel Injector Area — in.^{2}	2.25	1.7
Oxidizer Injector Area — in.^{2}	1.0	3.0
GOX HEX Used — % Full Thrust	2 to 10	2 to 100
Start Transient	Rapid P_c Rise at GOX-to-LOX Point	Smooth and Clean P_c Rise With Constant GOX

Thrust = THI
Mixture Ratio (O/F) = 3.2

T = 517°R
P = 19.6 psia

T = 166.2°R
P = 20 psia

T = 517°R
P = 17.3 psia

P = 6.0 psia

P = 7.7 psia
T = 411°R

T = 559°R
P = 8.6 psia
ṁ = 0.106 lbm/sec
ΔT = 521°R
Δp = 8.7 psid

P = 11.0 psia
T = 559°R

P = 19.7 psia
T = 37.9°R

94% Recovery

O₂ Heat
Exchanger

GOV

OCV

TBV

CVV

TCV

MFV

0 rpm

0 rpm

P = 20 psia
T = 166.2°R
Liquid

O₂
ṁ = 0.339 lbm/sec

P = 20 psia
T = 37.9°R
Liquid

H₂

P = 19.8 psia
T = 37.9°R
ṁ = 0.106 lb/sec

ṁ = 0.106 lb/sec
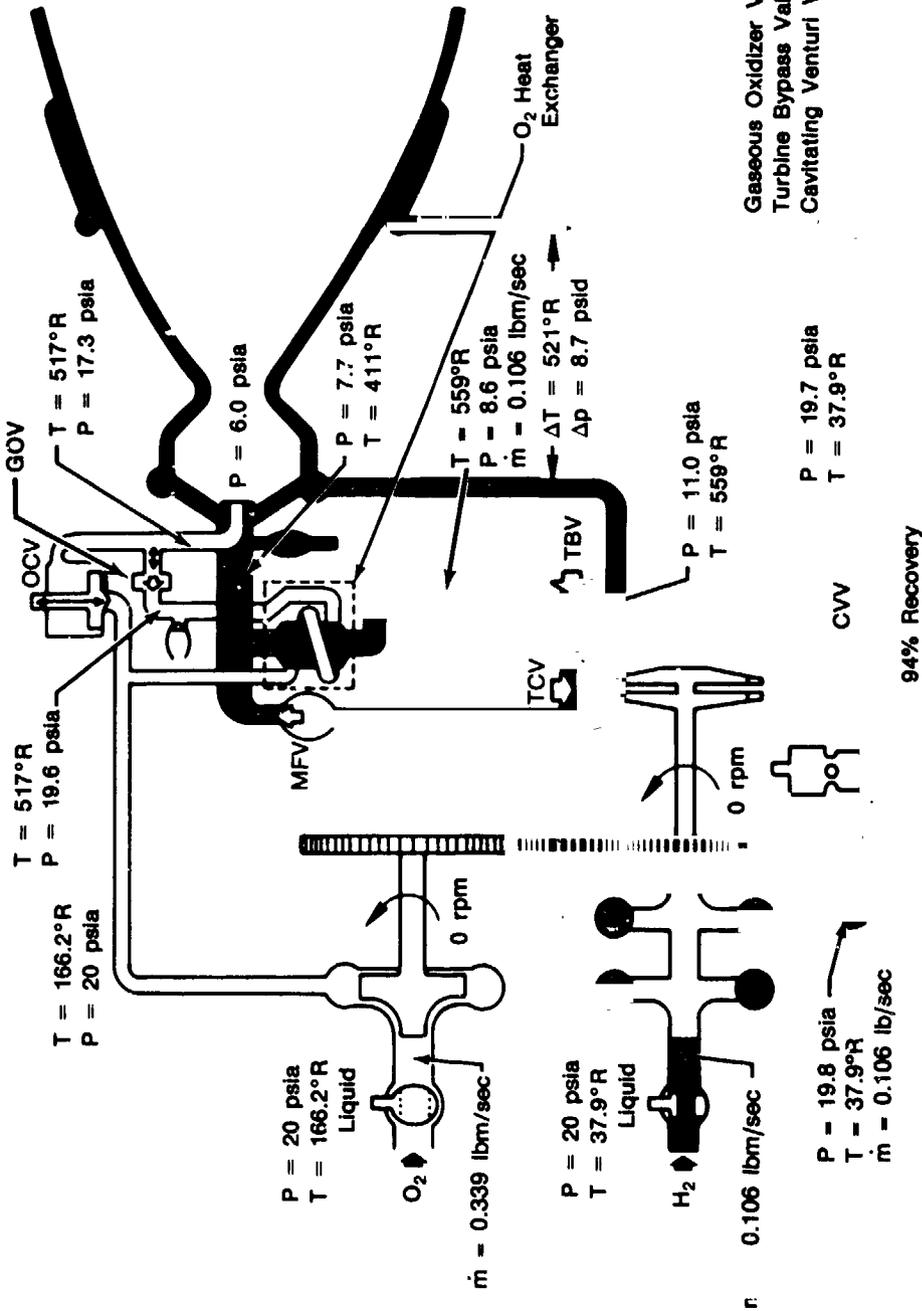
	ΔP-psid	Effective Area (A_{CD}) –in.²
Gaseous Oxidizer Valve (GOV)	1.5	1.268
Turbine Bypass Valve (TBV)	2.0	2.0
Cavitating Venturi Valve (CVV)	0.1	0.258

FD 278921

Figure 45. RL10-IIB Baseline Engine — Tank Head Idle (THI) Operating Mode

45
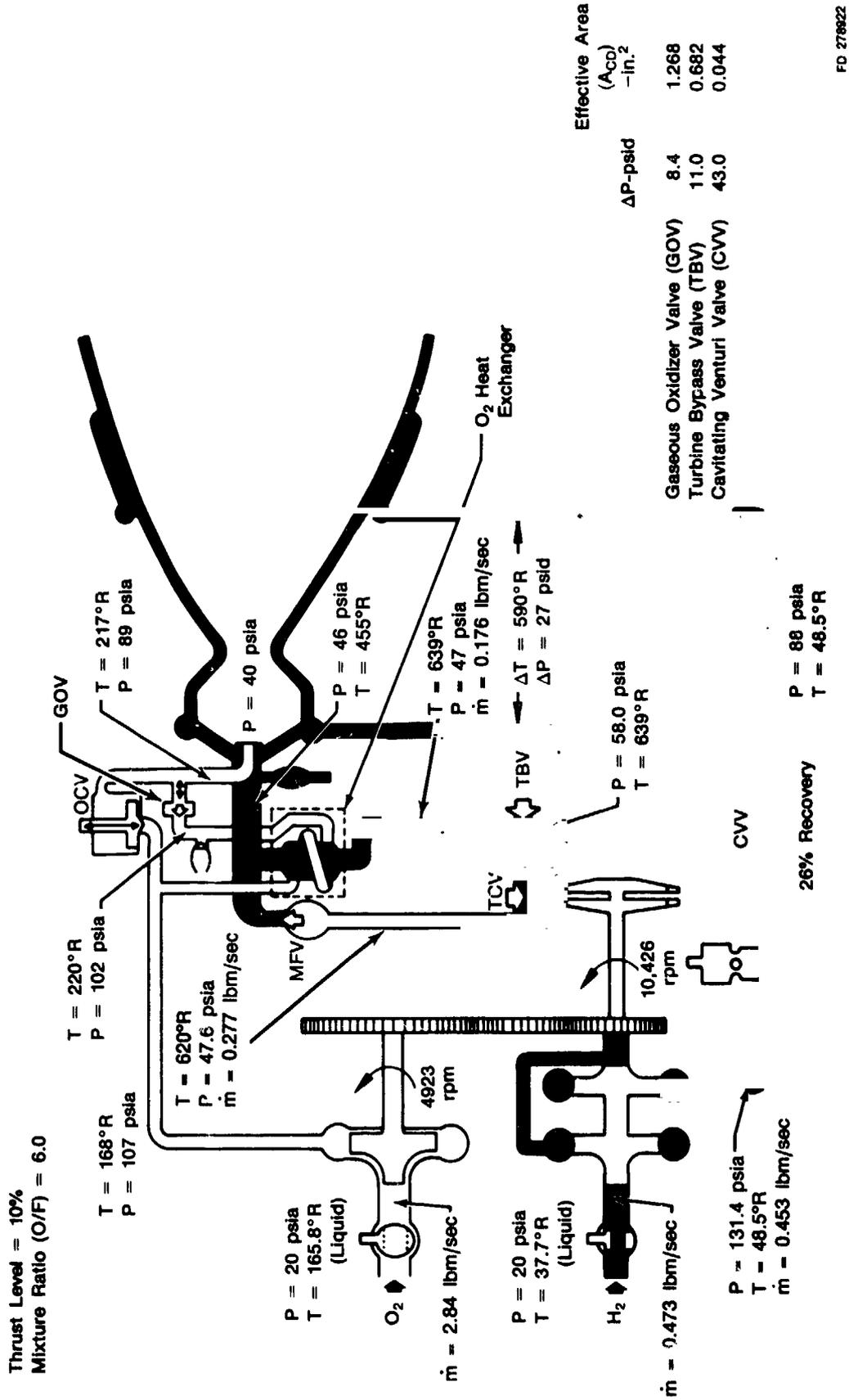
Figure 46. RL10-IIB Baseline Engine — Pumped Idle (PI) Operating Mode
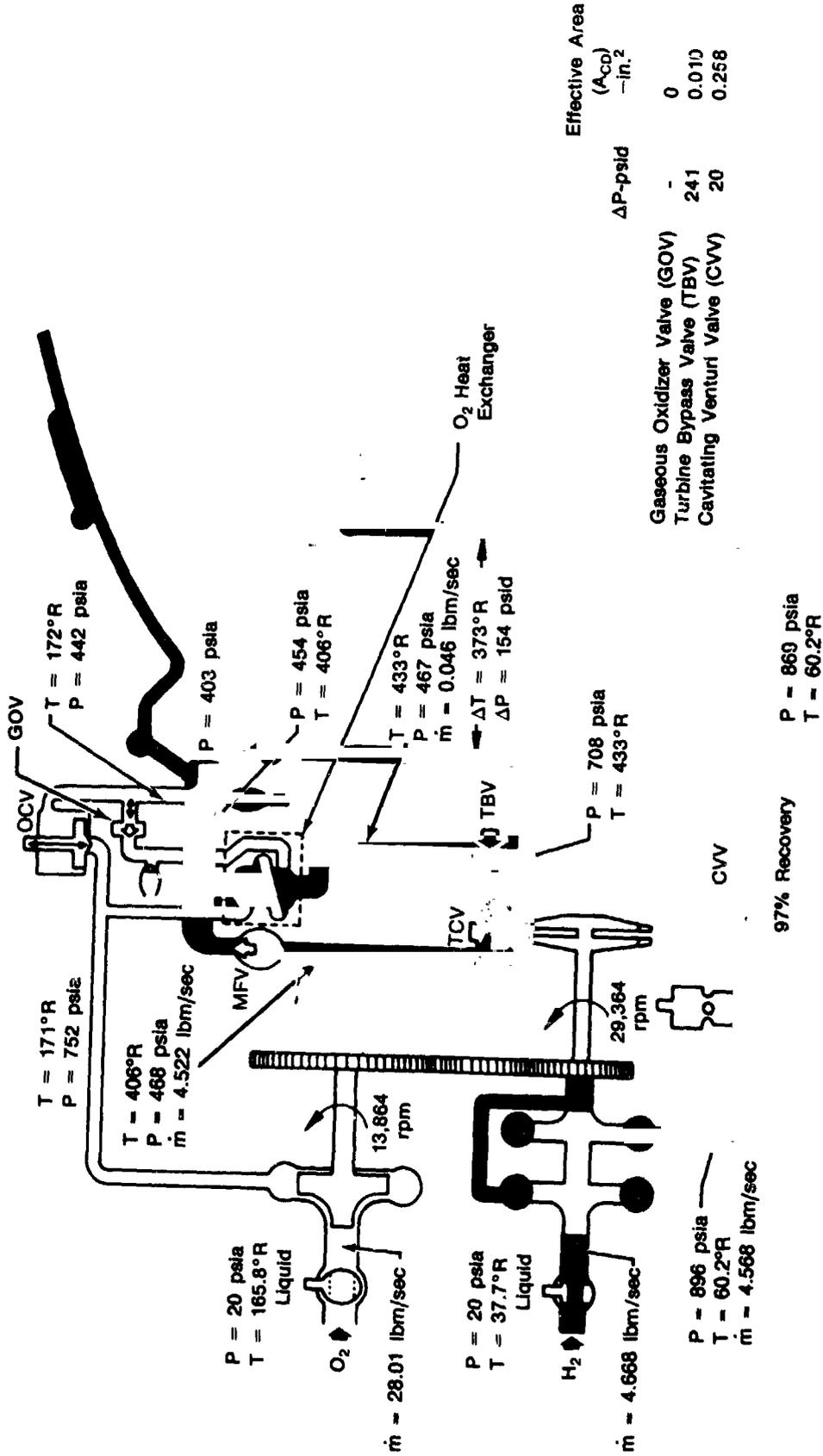
Figure 47. RL10-IIB Baseline Engine — Full Thrust Level

	ΔP-psid	Effective Area (A_CD) –in.²
Gaseous Oxidizer Valve (GOV)	–	0
Turbine Bypass Valve (TBV)	241	0.010
Cavitating Venturi Valve (CVV)	20	0.258

FO 278923

47

Hydrogen Exit
T_{out} = 238°R
P_{out} = 46.4 psia

Stage 1

Oxygen Inlet
T_{in} = 167.3°R
P_{in} = 84.3 psia
$\dot{m}$ = 2.84 lb/sec

Stage 2

Hydrogen Inlet
T_{in} = 639°R
P_{in} = 47.1 psia
$\dot{m}$ = 0.182 lbm/sec

Oxygen Exit
T_{out} = 209°R
P_{out} = 77.2 psia

Stage 3
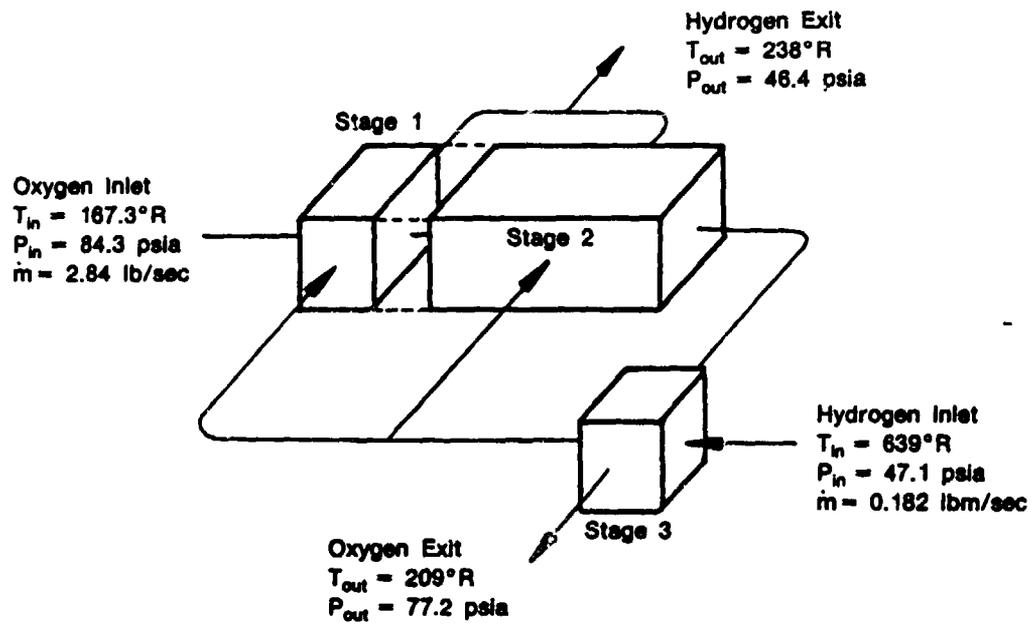
FD 278924

Figure 48. RL10-IIB Engine Oxidizer Heat Exchanger Performance Data — Pumped Idle Mode

0893C

FD 278925

	ΔP-psid	Effective Area (A_{CD}) —in.^{2}
Gaseous Oxidizer Valve (GOV)	1.4	1.23
Turbine Bypass Valve (TBV)	4.1	1.46
Cavitating Venturi Valve (CVV)	0.3	0.258

Thrust = 1.1%
Mixture Ratio (O/F) = 3.2

O$_2$ Heat Exchanger

GOV

T = 512°R
P = 15.5 psia

P = 5.4 psia

OCV

P = 6.9 psia
T = 427°R

T = 575°R
P = 8.1 psia
ṁ = 0.095 lbm/sec

ΔT = 538°R
ΔP = 6.6 psid

T = 512°R
P = 17.6 psia

T = 165.7°R
P = 19.8 psia

MFV

TBV

P = 12.2 psia
T = 575°R

TCV

CVV

P = 19.6 psia
T = 37.7°R

0 rpm

84% Recovery

P = 19.8
T = 165.7°R
Liquid

0 rpm

O$_2$

ṁ = 0.304 lbm/sec

P = 19.9 psia
T = 37.7°R
Liquid

H$_2$

ṁ = 0.095 lbm/sec

P = 19.7 psia
T = 37.7°R
ṁ = 0.095 lbm/sec

Figure 49. RL10-IIB Updated Baseline Engine — Tank Head Idle (THI) Operating Mode

49

Thrust Level = 10%
Mixture Ratio (O/F) = 6.0

	ΔP-psid	Effective Area (A_CD) —in.²
Gaseous Oxidizer Valve (GOV)	8.4	1.23
Turbine Bypass Valve (TBV)	11.4	0.68
Cavitating Venturi Valve (CVV)	48.0	0.043

FD 278926

Figure 50. RL10-IIB Updated Baseline Engine — Pumped Idle (PI) Operating Mode

FD 278927

	ΔP-psid	Effective Area (A_{CD}) —in.^{2}
Gaseous Oxidizer Valve (GOV)	-	0.010
Turbine Bypass Valve (TBV)	232	0.258
Cavitating Venturi Valve (CVV)	20	

Thrust Level = 100%
Mixture Ratio (O/F) = 6.0

O$_2$ Heat Exchanger

T = 171°R
P = 443 psia

P = 451 psia
T = 407°R

P = 403 psia

T = 433°R
P = 466 psia
ṁ = 0.046 lbm/sec

ΔT = 373°R
ΔP = 150 psid

OCV

GOV

T = 1706°R
P = 695 psia

T = 403°R
P = 465 psia
ṁ = 4.524 lbm/sec

MFV

TBV

P = 698 psia
T = 433°R

TCV

CVV

28,768 rpm

13,583 rpm

P = 855 psia
T = 59.4°R

84% Recovery

P = 20 psia
T = 165.8°R
Liquid

O$_2$

ṁ = 28.0 lbm/sec

P = 20 psia
T = 37.7°R
Liquid

H$_2$

ṁ = 4.67 lbm/sec

P = 882 psia
T = 50.4°R
ṁ = 4.57 lbm/sec

Figure 51. RL10-IIB Updated Baseline Engine — Full Thrust Level

51

A subroutine that approximates the thermal inertia of the OHE was then incorporated into the engine transient computer simulation. The model incorporates the effects on propellant temperatures of the heating or cooling of the mass of metal in the OHE. The one-dimensional model of heat flow to and from the metal is based on a multi-point analysis of the heat exchanger at steady-state conditions. Use of the model gives a more realistic representation of transient parameters. Transients were investigated from THI to PI. Significant engine parameters (Pc, O/F, rpm, and FTIT vs time) are shown in Figures 52 through 55. The transient from PI to FT was also investigated to determine valve scheduling. The program was run with ramped input thrust control characteristics because an accurate thrust control transient simulation was not available. Figures 56 through 59 present the same engine parameters listed above versus time. This acceptable transient was achieved by opening the cavitating venturi and main fuel valve, allowing the engine to accelerate to an intermediate thrust level (Pc ~ 160 psia) then closing the turbine bypass valve. This allowed the gaseous oxygen downstream of the (liquid) OFC to be removed from the system before the transition to full turbine power, thus preventing the excessive fuel pump overspeed seen on previous transient simulations. (c.f. Figure 27, Preliminary RL10-IIB Configuration.)
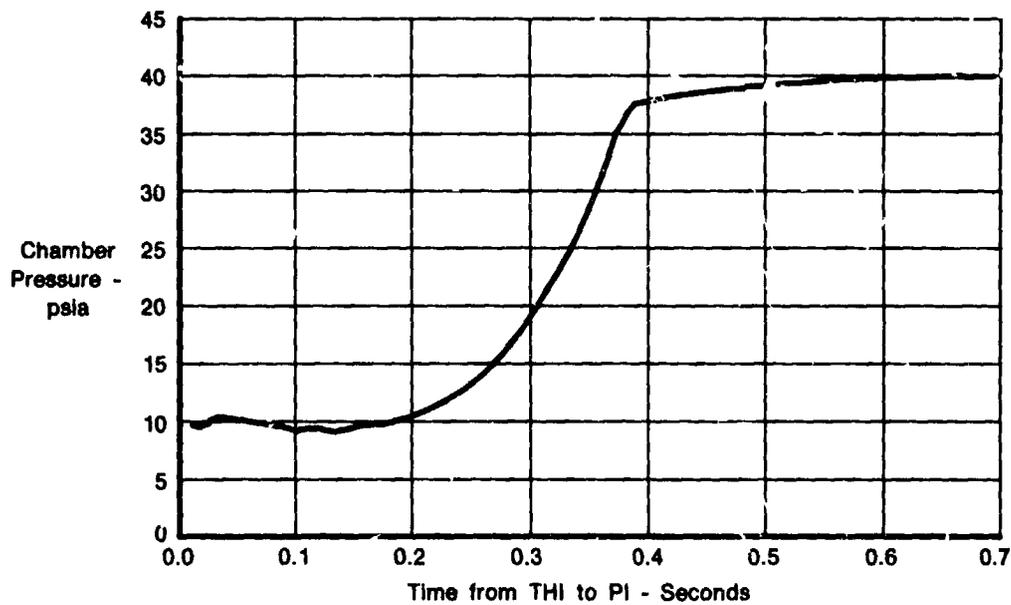
FD 278928

Figure 52. RL10-IIB Engine — Tank Head Idle to Pumped Idle Transition (Chamber Pressure versus Time)
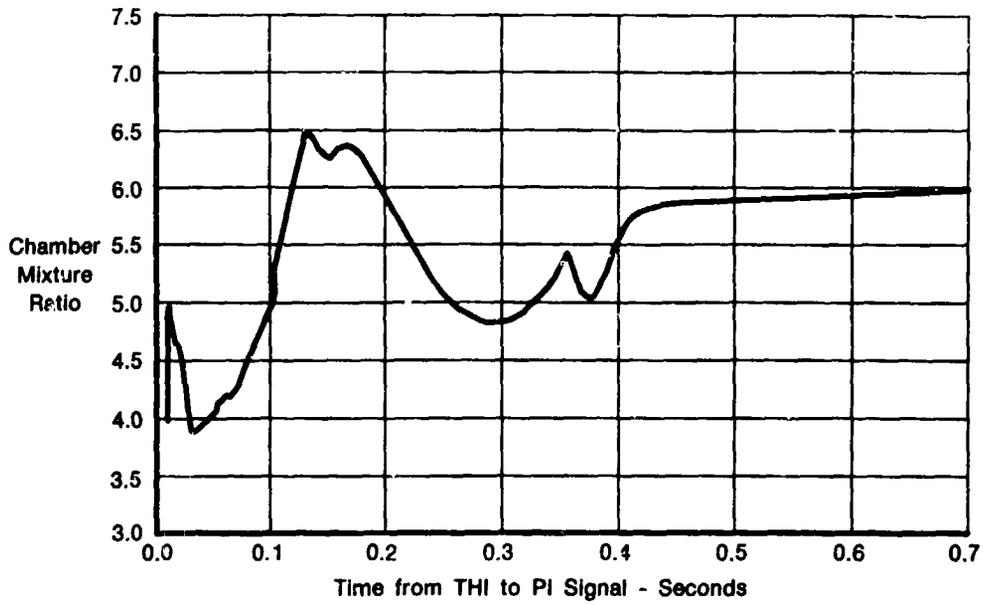
FD 278929

Figure 53. RL10-IIB Engine — Tank Head Idle to Pumped Idle Transition (Chamber Mixture Ratio versus Time)
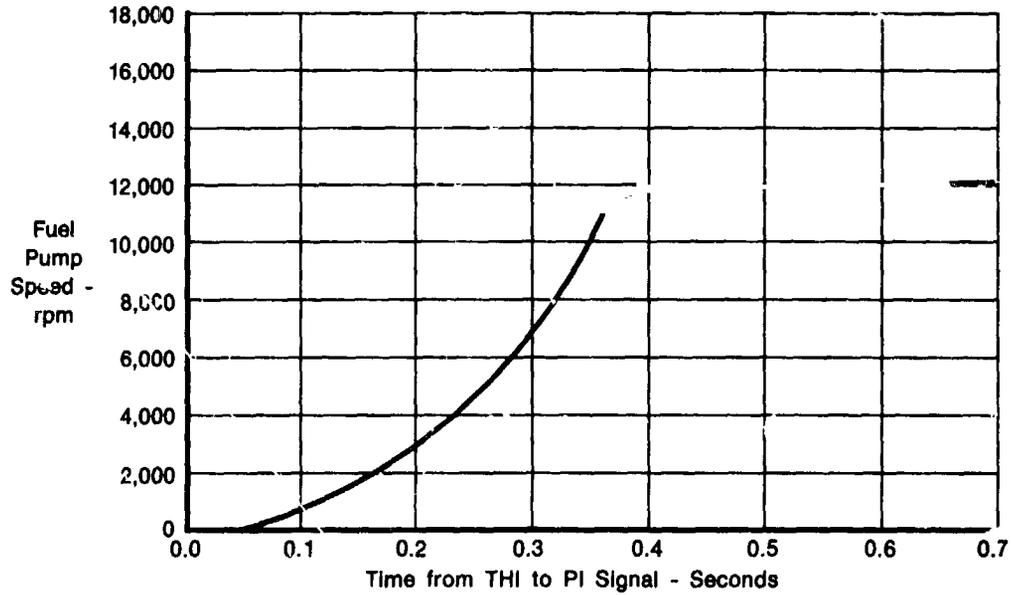
FD 278930

Figure 54. RL10-IIB Engine — Tank Head Idle to Pumped Idle Transition (Fuel Pump Speed versus Time)
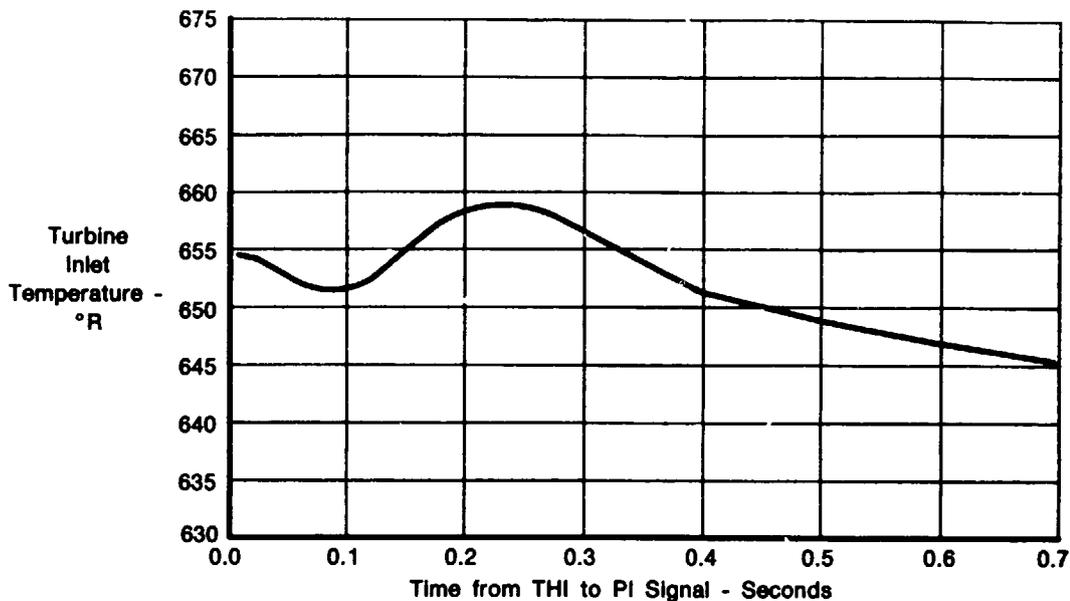
Figure 55. RL10-IIB Engine — Tank Head Idle to Pumped Idle Transition (Turbine Inlet Temperature versus Time)
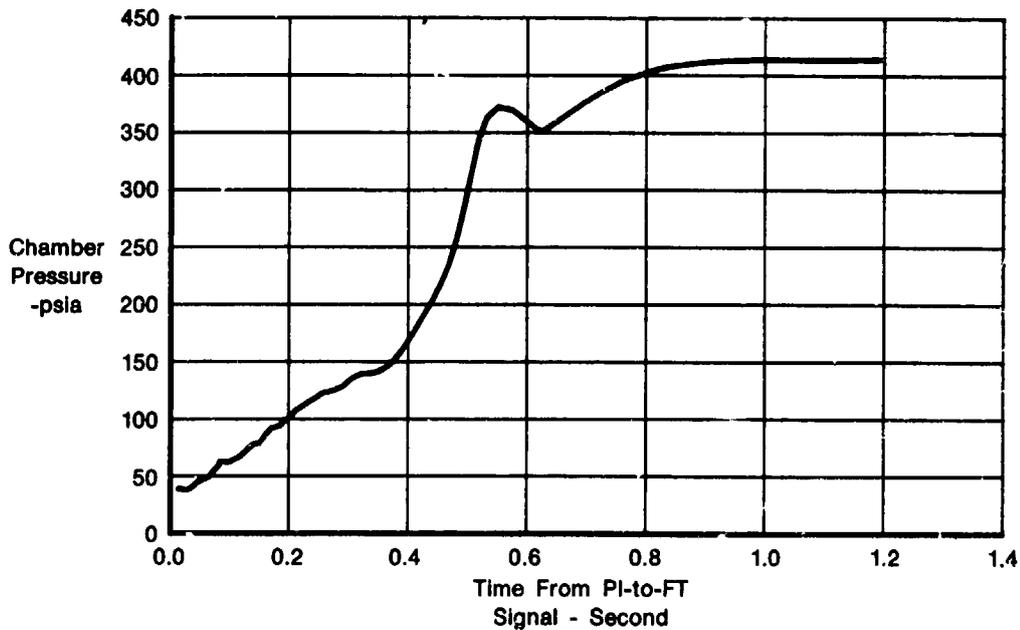
Figure 56. RL10-IIB Engine — Pumped Idle to Full Thrust Transition (Chamber Pressure versus Time)
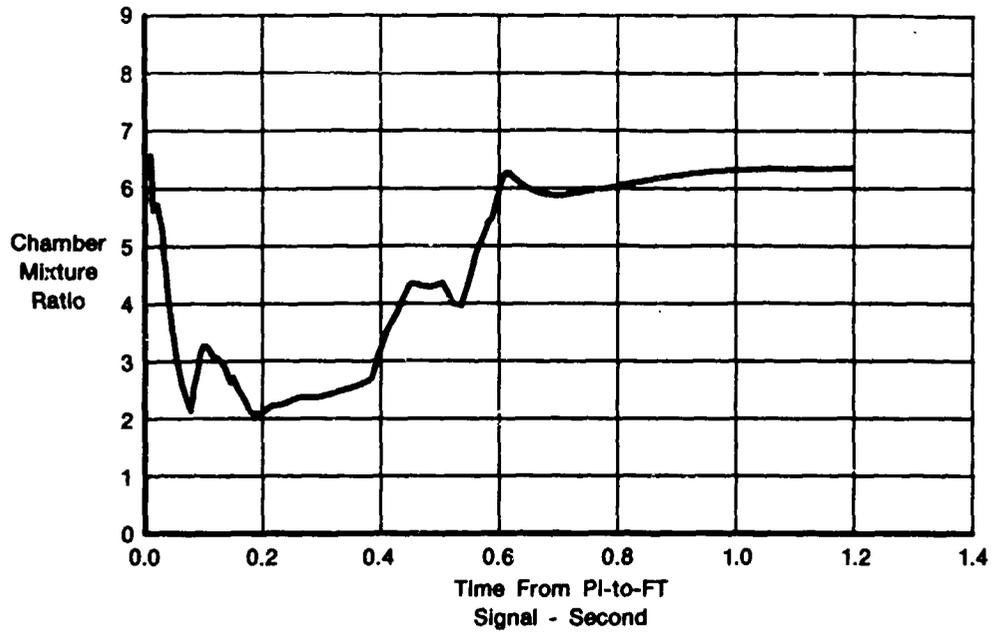
FD 278933

Figure 57. *RL10-IIB Engine — Pumped Idle to Full Thrust Transition (Chamber Mixture Ratio versus Time)*
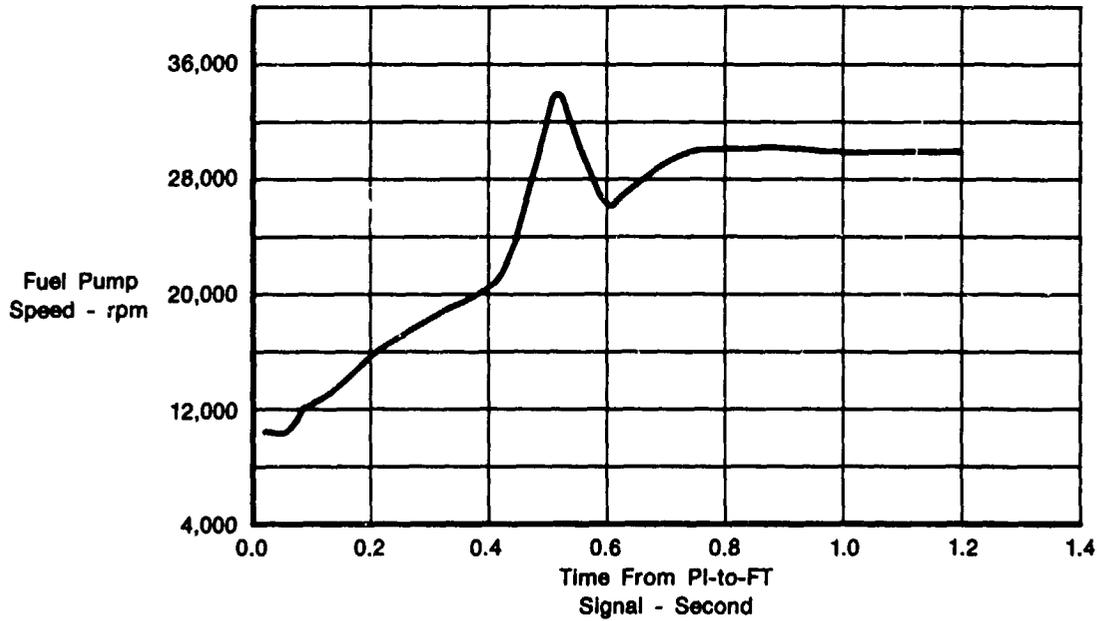
FD 278934

Figure 58. *RL10-IIB Engine — Pumped Idle to Full Thrust Transition (Fuel Pump Speed versus Time)*

55
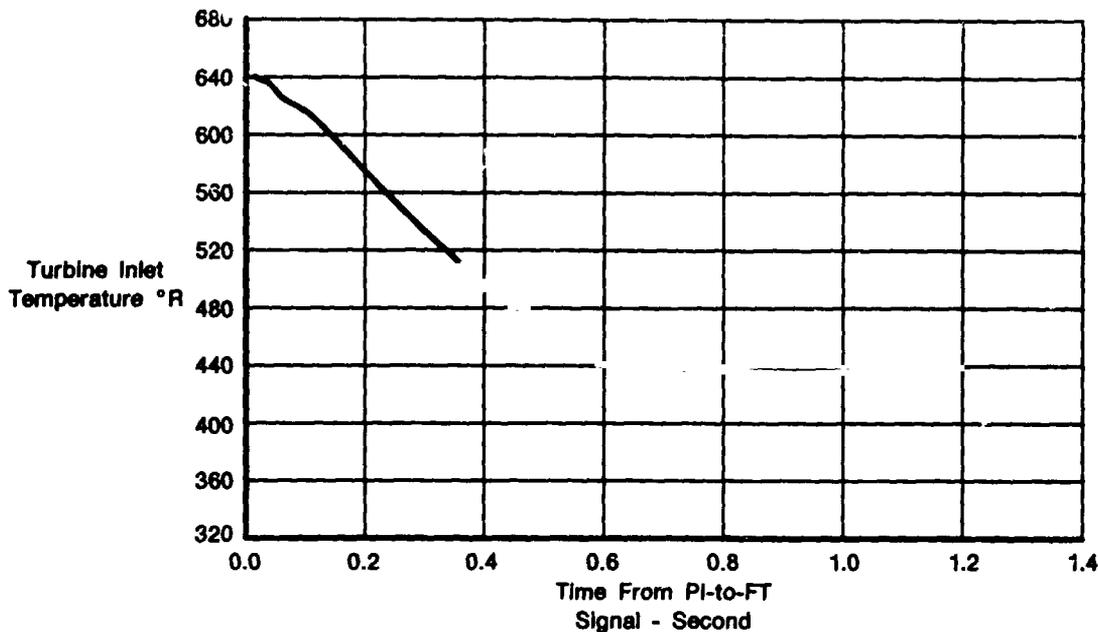
FD 278936

Figure 59. RL10-IIB Engine — Pumped Idle to Full Thrust Transition (Turbine Inlet Temperature versus Time)

An effort was made to write a thrust control simulation for use in the RL10-IIB engine transient program. The RL10 thrust control valve (TCV) (Figure 60) limits thrust overshoot during engine start and controls turbopump power to maintain chamber pressure at steady-state. A spring-mass model and a two-volume dynamic model were combined to simulate the transient response of the thrust control. The spring-mass model determines the shear orifice and bypass valve displacements as functions of time and fluid system driving forces. The two-volume fluid dynamics model calculates flows and pressures in the thrust control to determine those forces.

Various iterations of the thrust control simulation ˄ ˅un with input engine acceleration test data from P&W experimental engine FX143-33 (Run ˄. 436.01), which had been fitted with high response instrumentation to measure TCV input parameters. This produced thrust control simulation results that compared favorably to engine test data (Figures 61 and 62). However, when this simulation was used with the RL10-IIB engine transient program, unstable operation was indicated during engine acceleration to full thrust from pumped idle. Many i˄˅rations of the basic thrust control simulation ar d a simplified version failed to provide either engine operation consistent in all respects with measured data or stable engine operation after acceleration. A modification to the engine simulation to incorporate a gas venturi between the fuel bypass tee and turbine inl˅˅ appeared t˄ reduce the chamber pressure oscillation duration but did not eliminate it entirely (Figures 63 and 64). Since rated thrust demonstration was not a primary goal of the first test series, the TCV simulation effort was terminated.

0893C
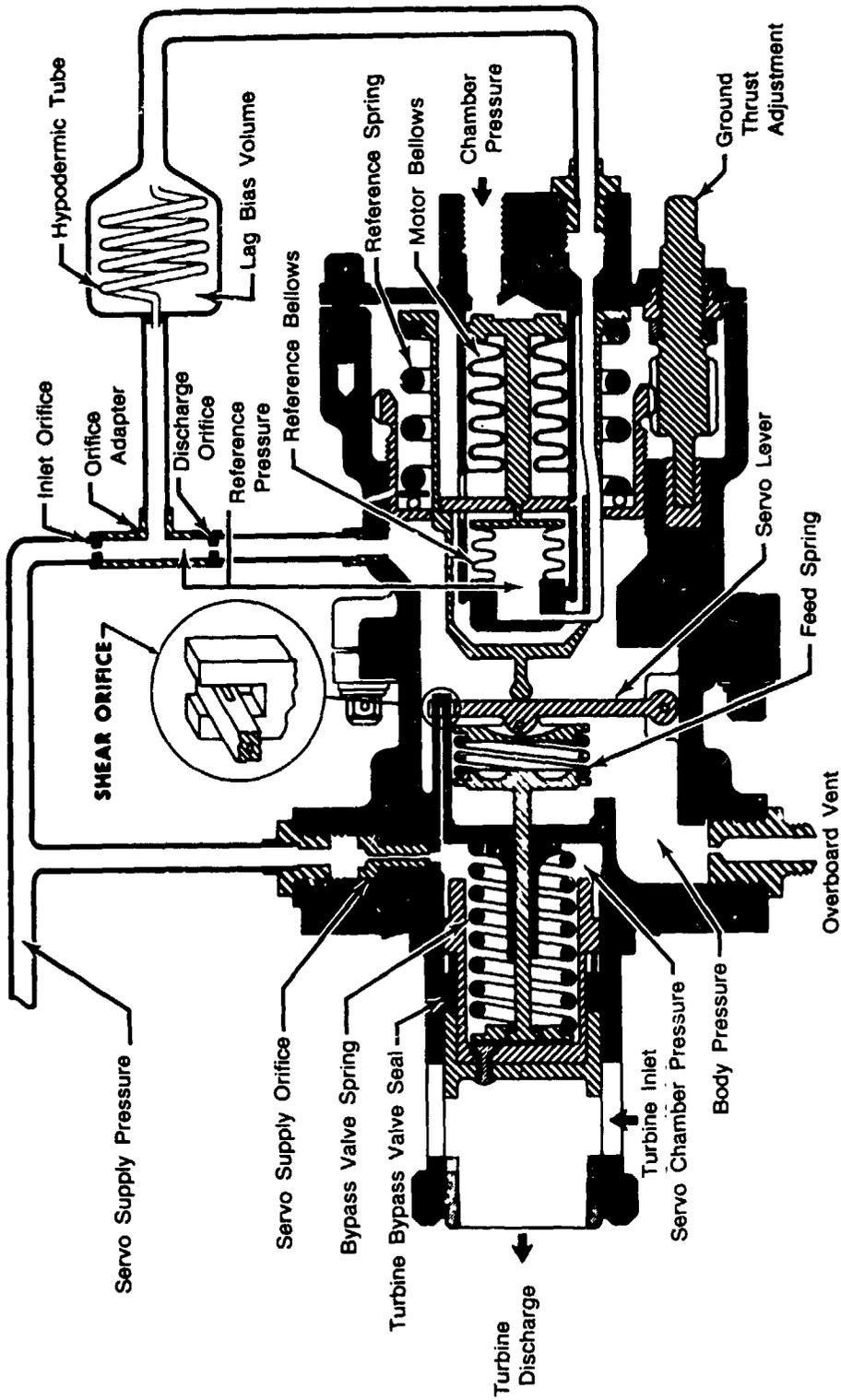
FD 8769

Figure 60. RL10 Thrust Control (P/N 2105497)
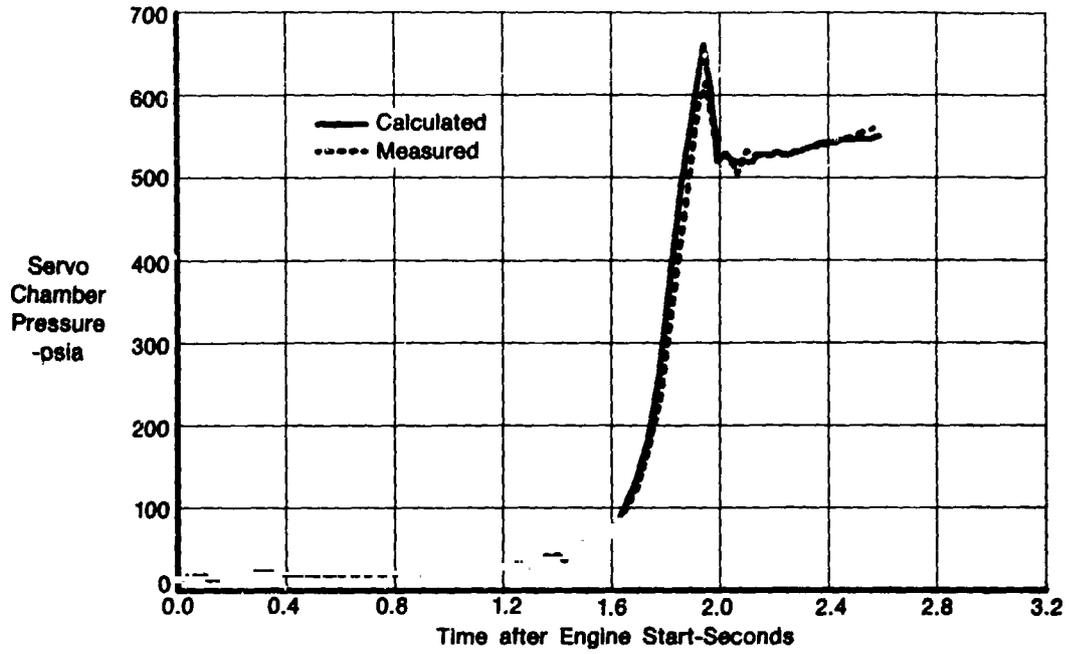
FD 278937

Figure 61. RL10-IIB Engine Start Transient (Servo Chamber Pressure versus Time)
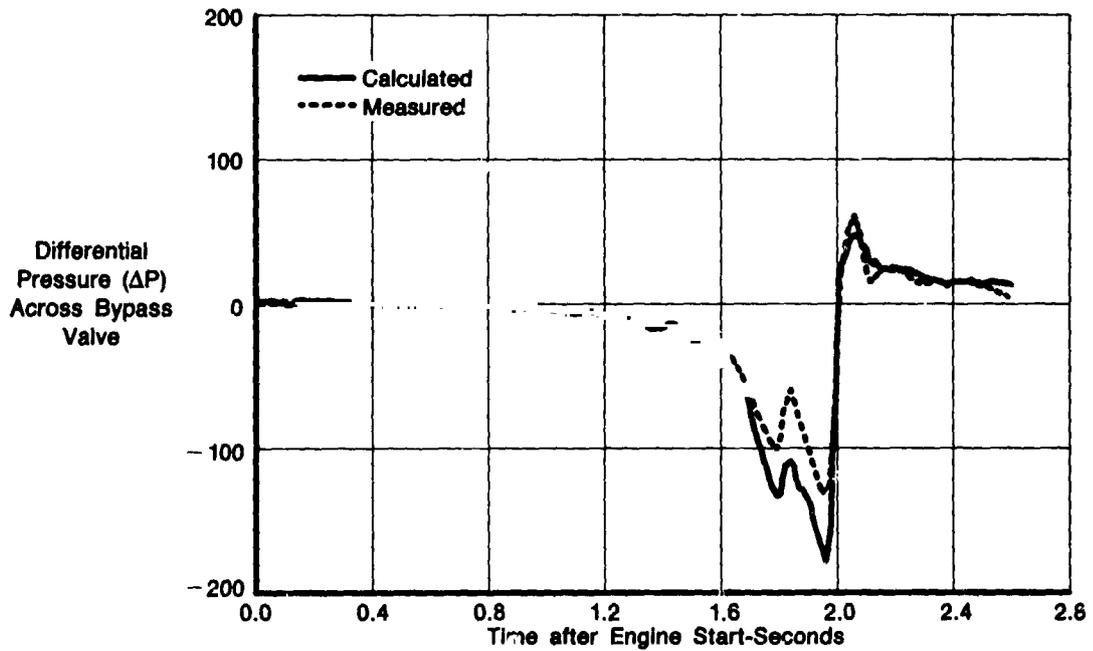
FD 278938

Figure 62. RL10-IIB Engine Start Transient (Differential Pressure Across Bypass Valve versus Time)
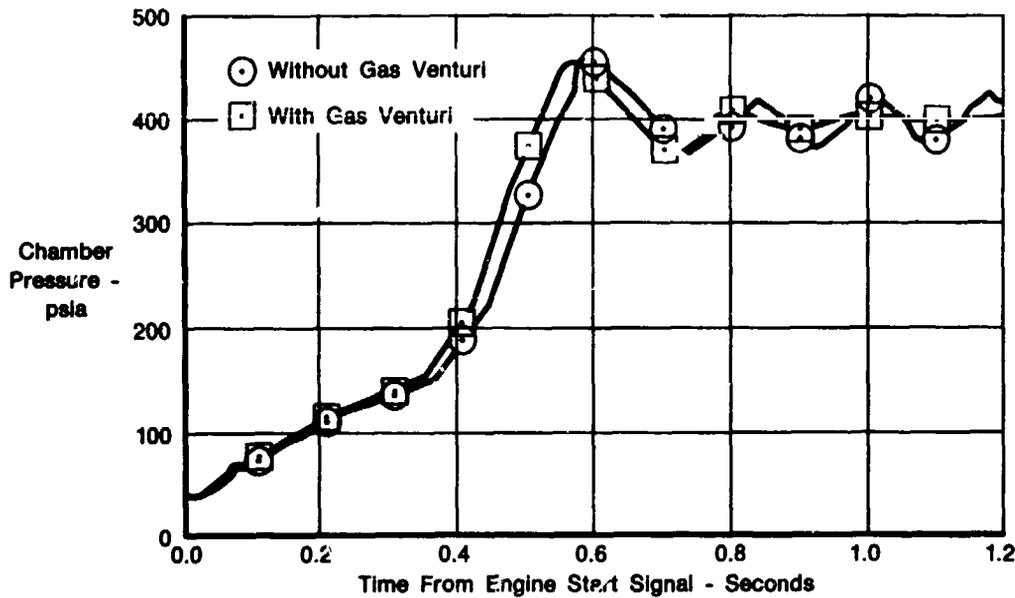
FD 278939

Figure 63. *RL10-IIB Engine Start Transient — Pumped Idle Operating Mode to Full Thrust Level (Chamber Pressure versus Time)*
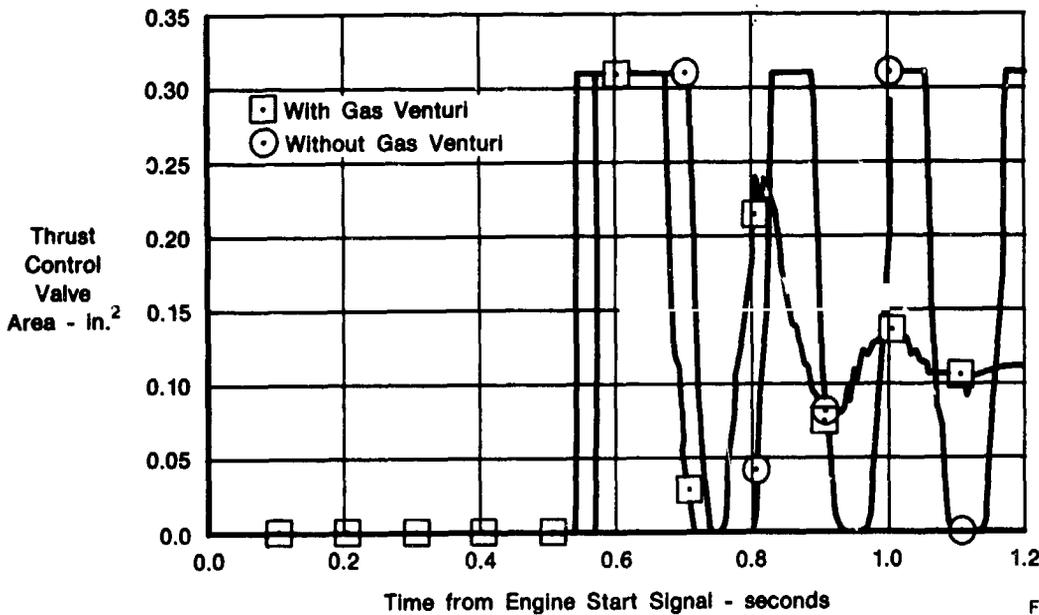
FD 278940

Figure 64. *RL10-IIB Engine Start Transition — Pumped Idle Operating Mode to Full Thrust Level (Thrust Control Valve Area versus Time)*

F. FINAL BASELINE AND BREADBOARD CONFIGURATIONS

After the designs of the flight representative controls and the design and heat transfer analyses of the OHE were completed, the characteristics of the "reversed" flow OHE model (Figure 65) were incorporated in the cycle deck. As explained in Section IV, and Appendix C, the reverse flow concept permitted reduction in 3rd-stage heat transfer without redesign of the heat

exchanger. This became the final configuration. The results are shown in Figures 66 through 68. The cycle deck was then run with propellent inlet conditions and corresponding valve settings planned for the breadboard low thrust engine test program. These results are shown in Figures 69 and 70.

Mixture Ratio (O/F) = 6.0
Stage 2 Insulation Conductivity = 0.033 Btu/ft-hr°R

Hydrogen Inlet
T_{out} = 639°R
P_{out} = 47.1 psia

Oxygen Inlet
T_{in} = 167°R
P_{in} = 84.3 psia
$\dot{m}$ = 2.84 lbm/sec

Stage 1

Oxygen
T = 199°R
P = 90.8 psia
Quality = 0.12

Stage 2

Hydrogen
T = 547°R
P = 46.6 psia

Stage 3

Hydrogen Exit
T_{in} = 230°R
P_{in} = 46.2 psia
$\dot{m}$ = 0.182 lbm/sec

Oxygen Exit
T_{out} = 198°R
P_{out} = 78.3 psia
Quality = 0.95
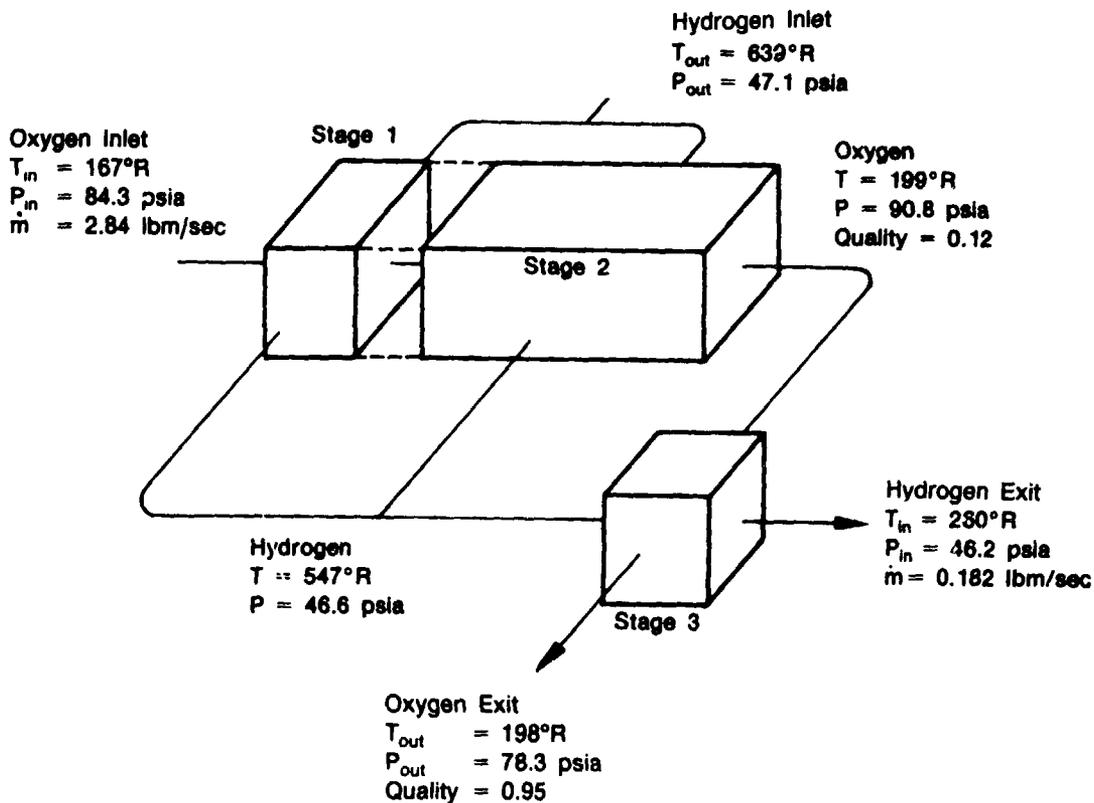
FD 278950

Figure 65. RL10-IIB Oxidizer Heat Exchanger — Pumped Idle Performance (Reversed Hydrogen Flow)

Thrust = THI
Mixture Ratio (O/F) = 3.3

T = 165.8°R
P = 20 psia

T = 445°R
P = 17.5 psia

445°R
14.6 psia

P = 5.4 psia

P = 6.9 psia
T = 454°R

OCV

GOV

O₂ Heat
Exchanger

MFV

TCV

TBV

P = 12.7 psia
T = 594°R

CVV

P = 19.8 psia
T = 37.7°R

0 rpm

0 rpm

P = 20 psia
T = 165.8°R
Liquid

O₂

ṁ = 0.31 lbm/sec

P = 20 psia
T = 37.7°R
Liquid

H₂

ṁ = 0.094 lbm/sec

P = 19.9 psia
T = 37.7°R
ṁ = 0.094 lbm/sec
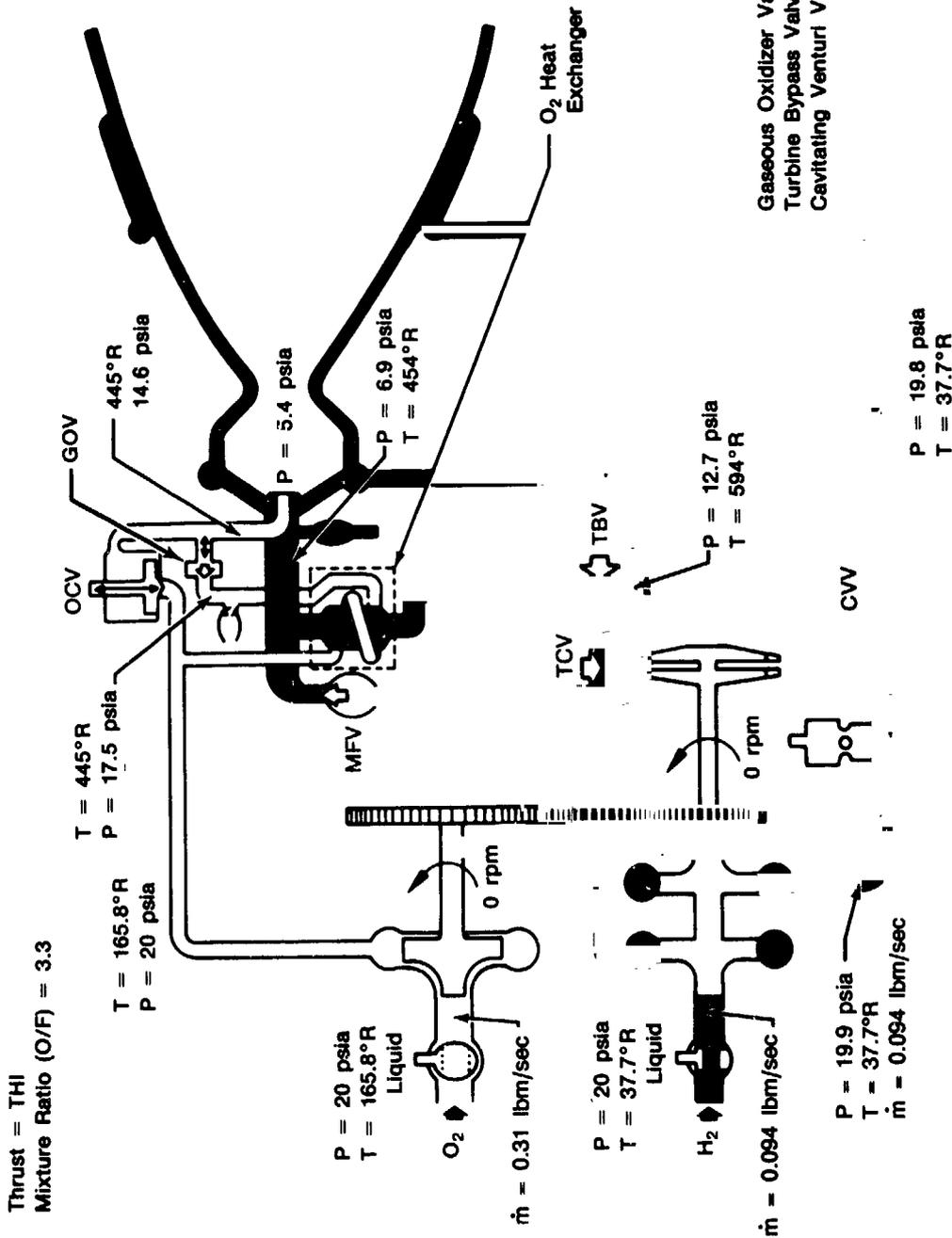
	ΔP-psid	Effective Area (A_{CD}) –in.²
Gaseous Oxidizer Valve (GOV)	2.2	0.980
Turbine Bypass Valve (TBV)	3.6	1.40
Cavitating Venturi Valve (CVV)	0.1	0.22

FD 276941

Figure 66. RL10-IIB Engine (Final Baseline) — Tank Head Idle (THI) Operating Mode

61

Figure 67. RL10-IIB Engine (Final Baseline) — Pumped Idle

Thrust Level = 10%
Mixture Ratio (O/F) = 6.0

T = 207°R
P = 97.3 psia

P = 40 psia

P = 45.4 psia
T = 479°R

O₂ Heat Exchanger

T = 659°R
P = 47.7 psia
ṁ = 0.187 lbm/sec

GOV

OCV

T = 211°R
P = 104 psia

T = 168°R
P = 110 psia

T = 640°R
P = 46.2 psia
ṁ = 0.265 lbm/sec

MFV

TBV

P = 57.1 psia
T = 659°R

TCV

CVV

10,700 rpm

5052 rpm

P = 20 psia
T = 165.8°R
Liquid

O₂

ṁ = 2.84 lbm/sec

P = 20 psia
T = 37.7°R
Liquid

H₂

ṁ = 0.473 lbm/sec

P = 138 psia
T = 48.3°R
ṁ = 0.452 lbm/sec

P = 88 psia
T = 48.3°R

27% Recovery

	ΔP-psid	Effective Area (A_{CD}) –in.²
Gaseous Oxidizer Valve (GOV)	12.9	0.980
Turbine Bypass Valve (TBV)	9.3	0.802
Cavitating Venturi Valve (CVV)	50	0.041

FD 278942

62

Thrust Level = 100%
Mixture Ratio (O/F) = 6.0

	ΔP-psid	Effective Area (A_{CD}) -in.^{2}
Gaseous Oxidizer Valve (GOV)	257	0.010
Turbine Bypass Valve (TBV)	231	0.010
Cavitating Venturi Valve (CVV)	20	0.22

FD 278943

T = 187°R
P = 444 psia

P = 403 psia

451 psia
406°R

O₂ Heat
Exchanger

T = 430°R
P = 452 psia
ṁ = 0.046 lbm/sec

T = 430°R
P = 701 psia

GOV

OCV

T = 171°R
P = 701 psia

T = 405°R
P = 464 psia
ṁ = 4.514 lbm/sec

MFV

TCV

TBV

P = 683 psia
T = 430°R

28,495
rpm

P = 841 psia
T = 56.7°R

CVV

97% Recovery

3,454
rpm

P = 20 psia
T = 165.8°R
Liquid

O₂

ṁ = 27.98 lbm/sec

P = 20 psia
T = 37.7°R
Liquid

H₂

ṁ = 4.66 lbm/sec

P = 868 psia
T = 56.7°R
ṁ = 4.56 lbm/sec

Figure 68. RL10-IIB Engine (Final Baseline) — Full Thrust Level

Thrust = THI
Mixture Ratio (O/F) = 4.3
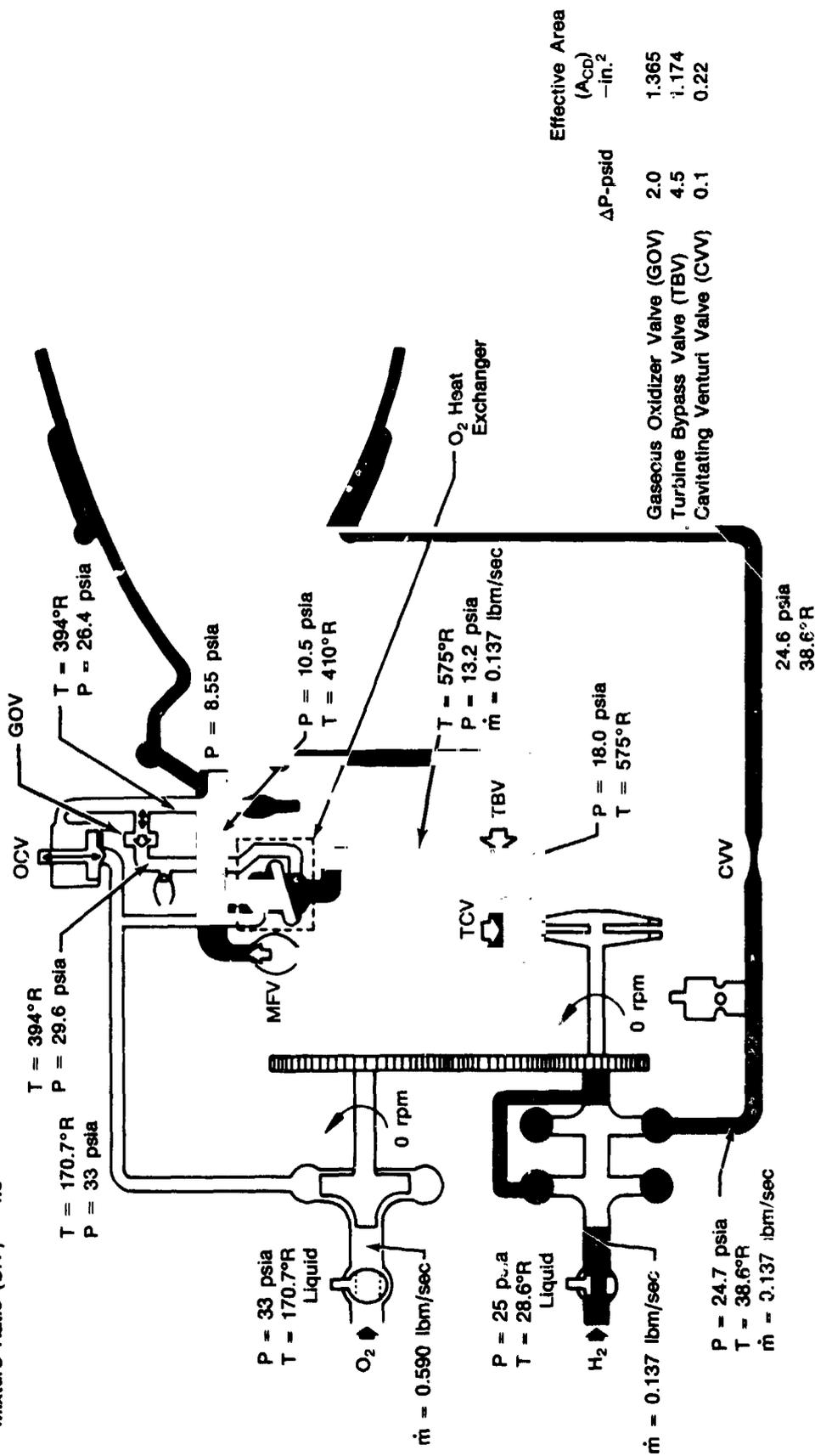
Effective Area

	ΔP-psid	(A_{CD}) —in.^{2}
Gaseous Oxidizer Valve (GOV)	2.0	1.365
Turbine Bypass Valve (TBV)	4.5	1.174
Cavitating Venturi Valve (CVV)	0.1	0.22

FD 27894

Figure 69. RL10-IIB Breadboard Engine — Tank Head Idle (THI) Operating Mode

Thrust Level = 10%
Mixture Ratio (O/F) = 6.0

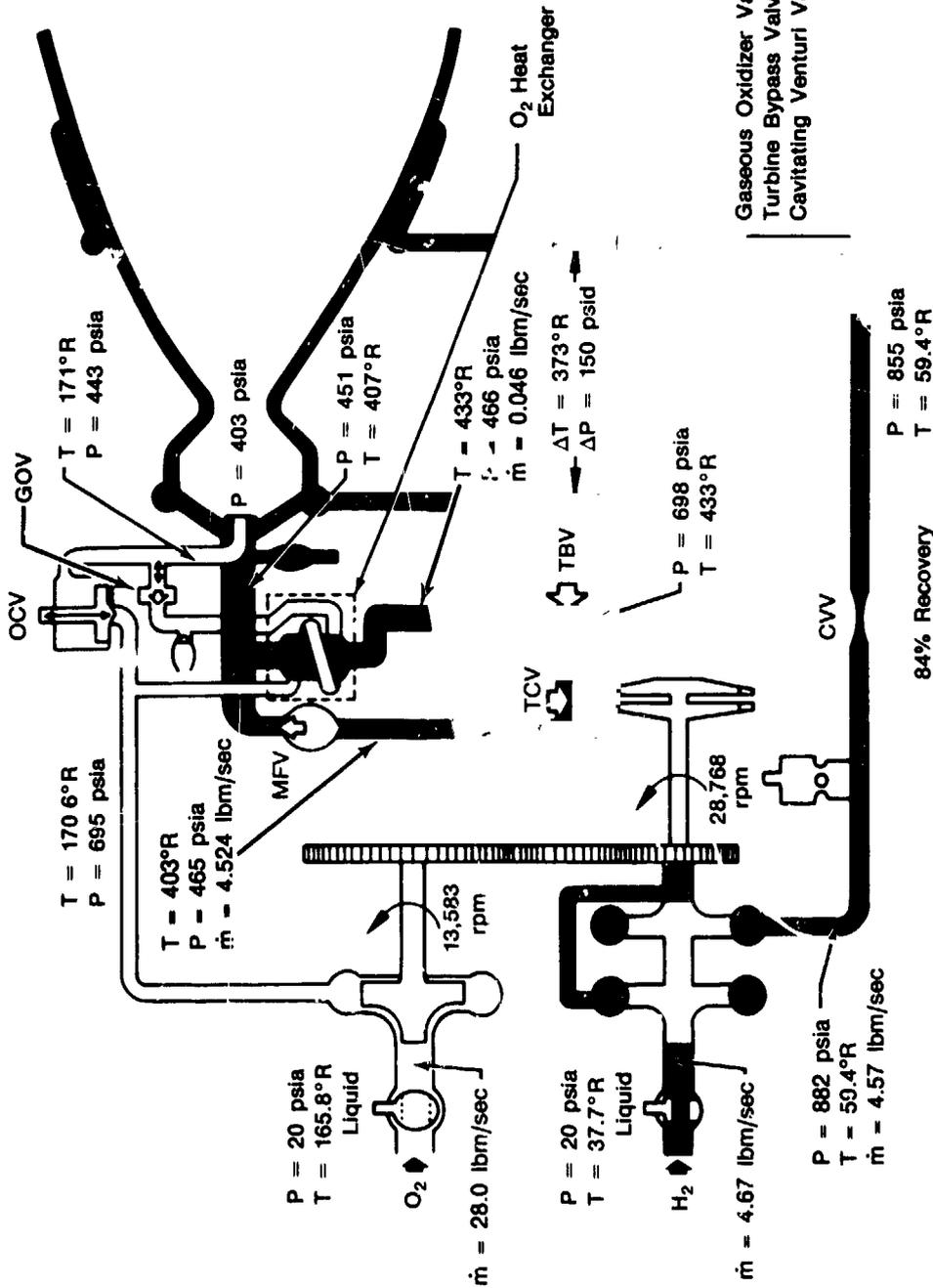|	ΔP-psid	Effective Area (A_{CD}) $-in.^2$
Gaseous Oxidizer Valve (GOV)	6.9	1.365
Turbine Bypass Valve (TBV)	8.3	0.965
Cavitating Venturi Valve (CVV)	52.0	0.045
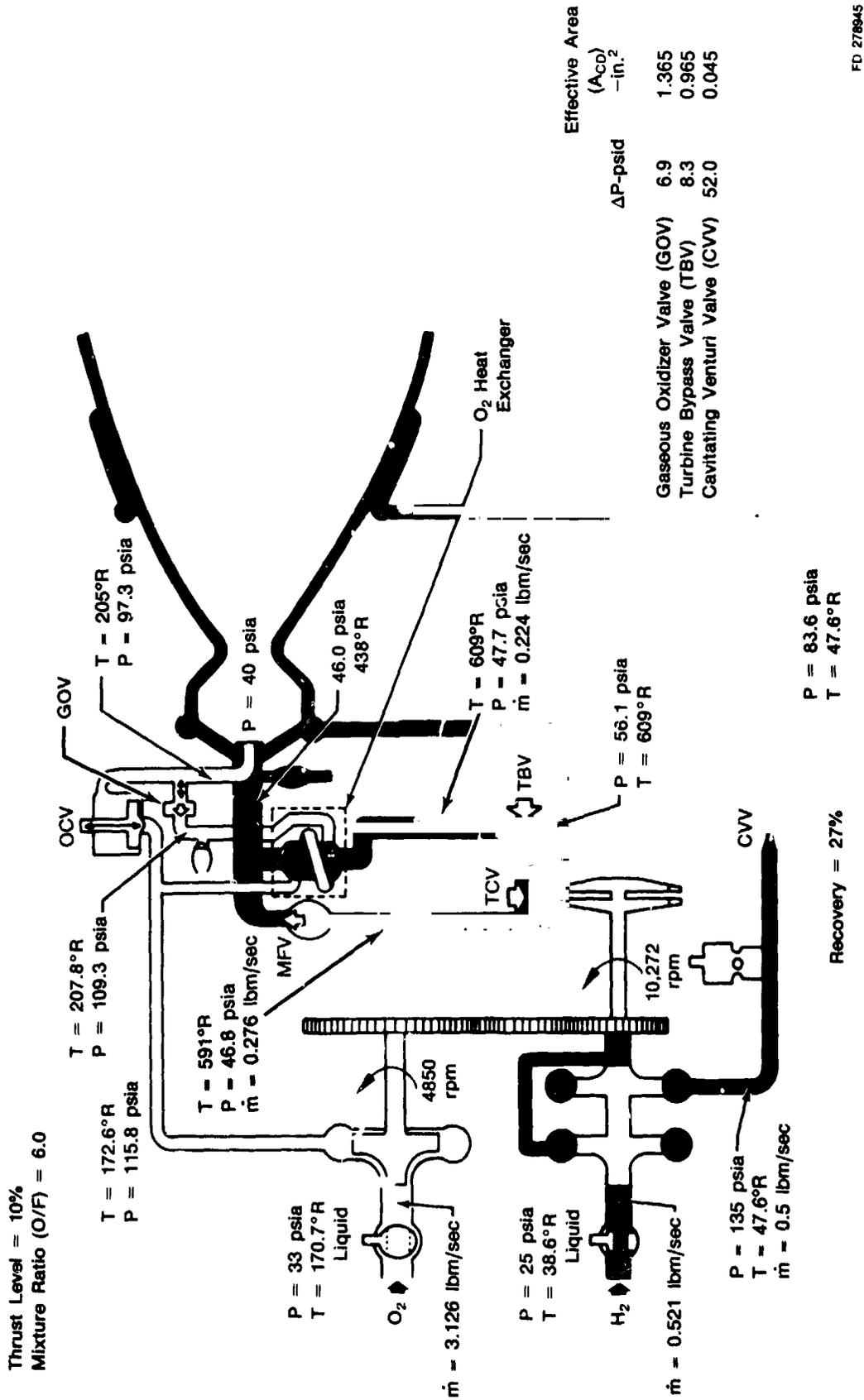
FD 278945

Figure 70. RL10-IIB Engine Breadboard Configuration — Pumped Idle (PI) Operating Mode

65

SECTION IV
HEAT EXCHANGER ANALYSIS AND DESIGN

The Oxidizer Heat Exchanger (OHE) heat transfer analyses that provided the basic OHE design requirements and those for subsequent design iterations were based on limiting the heat input to the liquid oxygen during both THI and PI operation until a 5% to 10% oxidizer quality (percent vapor by weight) is achieved. Increased heat transfer rates could then be applied without causing unstable boiling. These requirements had been established during the tests and studies leading to the Space Tug Engine Report (P&W Report No. FR-7498, 21 May 1976), and the Orbit Transfer Vehicle Advanced Expander Cycle Engine Point Design Study (P&W Report No. FR-14615, 15 March 1981). The maximum allowable heat flux values for the liquid oxygen at THI and PI conditions were calculated accordingly.

The basic RL10-IIB OHE design fluid conditions are shown in Table 4. The same inlet flowrates, temperatures and pressures were maintained for all OHE design analyses. The initial heat transfer analysis defined a three-stage cross-flow heat exchanger. Figure 71 shows the initial three-stage heat exchanger arrangement with the 10% Pumped Idle design point performance parameters; the THI and FT off-design performance parameters are also given.

*Table 4. RL10-IIB Engine Heat Exchanger Design
Fluid Conditions*

| | 10% Thrust | |
Oxygen	Heat Exchanger Inlet	10% Quality Point
Flowrate — lbm/sec	2.84	2.84
Pressure — psia	84.3	—
Temperature — °R	167.3	—
Enthalpy — Btu/lbm	63.2	84.9
Hydrogen		
Flowrate — lbm/sec	0.182	0.182
Pressure — psia	47.1	—
Temperature — °R	679.0	—
Enthalpy — Btu/lbm	2161.0	1822.0

The initial OHE was designed to supply slightly-superheated oxygen at 209°R and 77.2 psia at the exit. Stages 1 and 2 are of etched or milled-channel stainless steel (Thermal Skin®) construction with metal felt insulation between the plates. Stage 3 is of stainless steel Thermal Skin construction with no insulation between the plates. Detailed geometry and performance information for the individual stages can be found in Figures 72 through 74.

Stage 1 was designed to assure stable boiling of the liquid oxygen at the conditions experienced during THI operation. The metal felt insulation density and thickness were selected to keep the heat flux to the oxygen below the maximum allowable heat flux for stable boiling (0.95 Btu/ft^2 sec) at THI. The calculated conductivity of the compressed metal felt insulation used in the analysis was 0.041 Btu-ft/ft^2-hr-°F.

PRECEDING PAGE BLANK NOT FILMED

PAGE 66 INTENTIONALLY BLANK

Hydrogen Exit
T_{out} = 238°R
P_{out} = 46.4 psia

Stage 1

Oxygen Inlet
T_{in} = 167.3°R
P_{in} = 84.3 psia
$\dot{m}$ = 2.84 lb/sec

Oxygen
T = 199°R
P = 82.1 psia

Stage 2

Hydrogen
T = 324°R
P = 46.8 psia

Hydrogen Inlet
T_{in} = 639°R
P_{in} = 47.1 psia
$\dot{m}$ = 0.182 lbm/sec

Stage 3

Oxygen Exit
T_{out} = 209°R
P_{out} = 77.2 psia
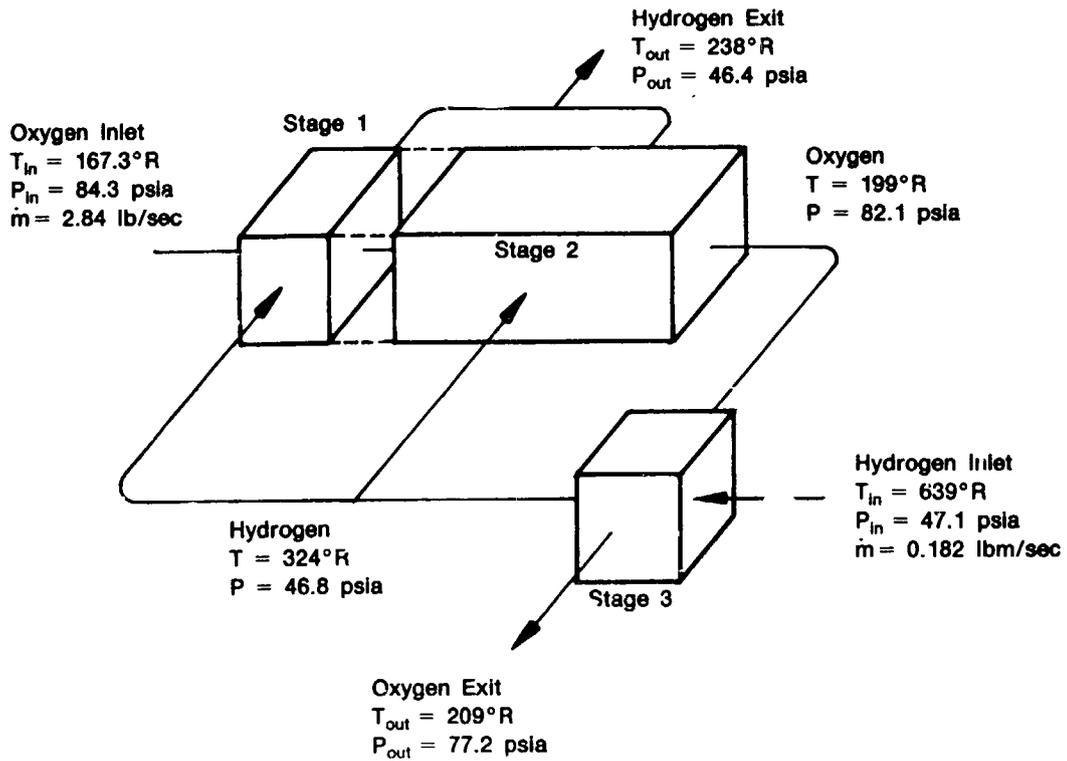
Heat Exchanger Performance at Off-Design Conditions

		Tank Head Idle Mode	Full Thrust Level
Oxygen	- T_{in} - °R	166.0	167.0
	T_{out} - °R	539.0	263.0
	P_{in} - psia	20.0	538.8
	P_{out} - psia	17.3	534.0
	ΔP - psid	2.67	4.8
	Exit Quality	1.0	0.1
Hydrogen	- T_{in} - °R	559.0	431.5
	T_{out} - °R	404.9	214.1
	P_{in} - psia	8.6	692.0
	P_{out} - psia	7.25	692.0
	ΔP - psid	1.35	0.0

FD 278946

Figure 71. RL10-IIB Engine —Gaseous Oxygen Heat Exchanger Geometry (At Pumped Idle Design Point)

Dimensions of Core

3.5

3.125

9.0

O_2 In. →

H_2 In.

Thermal Skin Geometry Blow-Up

H_2 Plate

0.015 — 0.04 — 0.08 — 0.015 ⌐0.010

Insulation 0.015 0.084

O_2 Plate (Turned 90°)

0.015 — 0.02 — 0.08 — ⌐0.010

All Dimensions Are In Inches
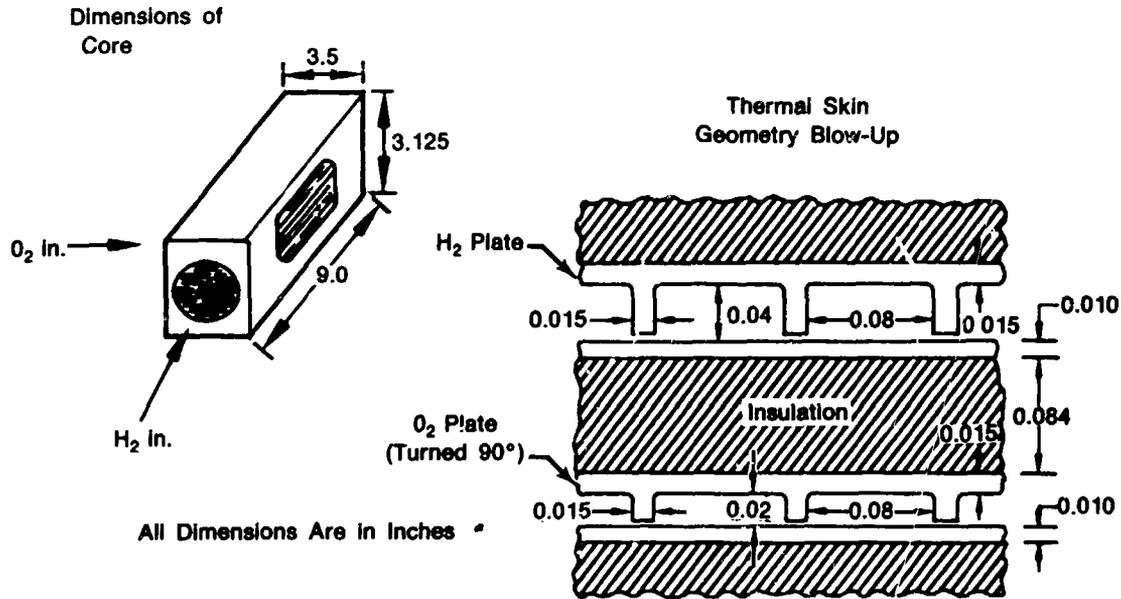
Geometry	H_2 Plate	O_2 Plate
No. Plates	12.0	11.0
Passage Diameter, in.	0.0513	0.0336
Flow Area, in.^{2}	1.213	1.602
Heat Transfer Area, ft^2	5.2	
Core Weight, lb	7.5	
Insulation Type	2% Dense Metal Felt (0.150 inches compressed to 0.084 inches)	
Insulation Material	300 Series Stainless Steel	

Heat Exchanger Performance

	Design Point	Off Design	
	Tank Head Idle	Pumped Idle	Full Thrust
$\dot{m}(H_2)$, - lbm/sec	0.0106	0.0182	0.006
$\dot{m}(O_2)$, - lbm/sec	0.339	2.84	1.00
$T_{in}(H_2)$ - °R	538.0	324.0	261.0
$T_{in}(O_2)$ - °R	166.0	167.0	167.0
$T_{out}(H_2)$ - °R	476.0	310.0	236.0
$T_{out}(O_2)$ - °R	168.0	168.0	168.0
$\Delta P(H_2)$ - psi	0.5	0.1	~0.0
$\Delta P(O_2)$ - psi	0.354	0.7	0.09
O_2 Exit Quality	0.1	0.0	0.0
Q - Btu/sec	2.4	1.0	0.55
Q/A, Average - Btu/ft$^2 \cdot$sec	0.56	0.19	0.102

FD 278947

Figure 72. RL10-11B Engine — Gaseous Oxygen Heat Exchanger (Stage 1 Core)

Dimensions of Core

9.0

14.0

O₂ In

3.125

H₂ In

All Dimensions Are In Inches

Thermal Skin
Geometry Blow-Up

H₂ Plate

O₂ Plate (Turned 90°)
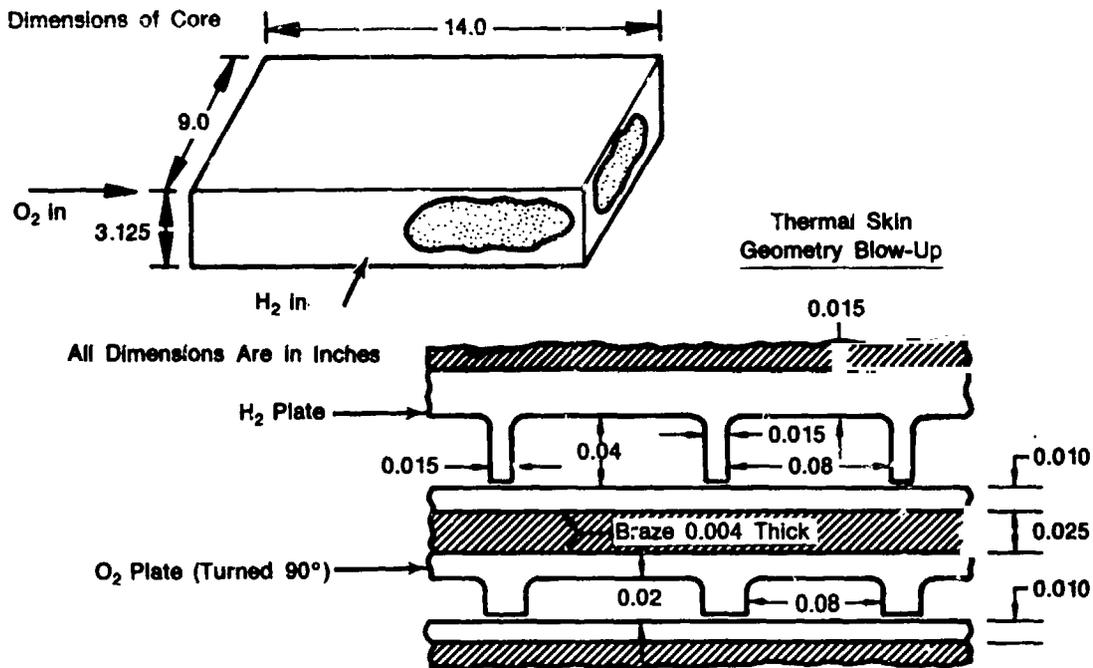
Geometry	H₂ Plate	O₂ Plate
No. Plates	20.0	19.0
Passage Diameter, in.	0.0513	0.0336
Flow Area, in.²	8.199	2.77
Heat Transfer Area, ft²	36.6	
Core Weight, lb	53.3	
Insulation Type	5% Dense Metal Felt	
Insulation Material	Nickel 200	

Heat Exchanger Performance

	Design Point	Off Design	
	Pumped Idle	Tank Head Idle	Full Thrust
$\dot{m}(H_2)$, - lbm/sec	0.1638	0.098	0.054
$\dot{m}(O_2)$, - lbm/sec	2.84	0.339	1.00
$T_{in}(H_2)$ - °R	324.0	538.0	260.9
$T_{in}(O_2)$ - °R	168.1	168.0	168.3
$T_{out}(H_2)$ - °R	230.0	397.0	211.7
$T_{out}(O_2)$ - °R	199.0	449.0	195.5
$\Delta P(H_2)$ - psi	0.10	0.53	~0.0
$\Delta P(O_2)$ - psi	1.50	1.72	0.08
O_2 Exit Quality	0.1	1.0	0.0
Q - Btu/sec	60.5	65.34	10.89
Q/A, Average - Btu/ft²·sec	1.653	1.785	0.297

FD 278948

Figure 73. RL10-IIB Engine — Gaseous Oxygen Heat Exchanger (Stage 2 Core)

Dimensions of Core

Thermal Skin
Geometry Blow-Up

H₂ Plate

O₂ Plate
(Turned 90°)

All Dimensions Are in Inches
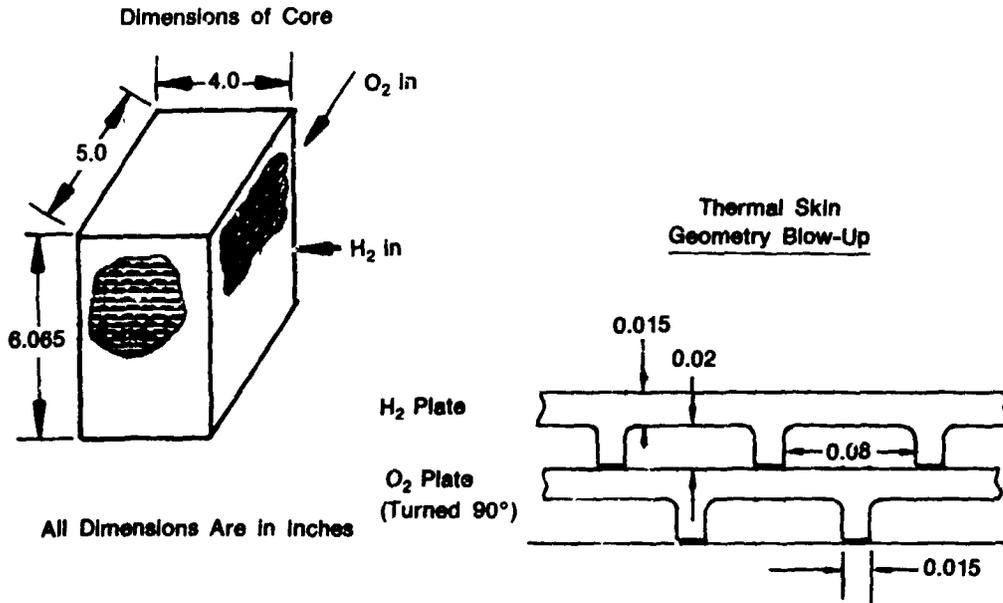
Geometry

	H₂ Plate	O₂ Plate
No. Plates	87.0	86.0
Passage Diameter, in.	0.0336	0.0336
Flow Area, in.^{2}	6.475	5.180
Heat Transfer Area, ft^2	21.3	
Core Weight, lb	19.3	

Heat Exchanger Performance

	Design Point	Off Design	
	Pumped Idle	Tank Head Idle	Full Thrust
$\dot{m}(H_2)$, - lbm/sec	0.182	0.109	0.06
$\dot{m}(O_2)$, - lbm/sec	2.840	0.339	1.000
$T_{in}(H_2)$ - °R	639.0	559.0	431.5
$T_{in}(O_2)$ - °R	199	449.0	195.5
$T_{out}(H_2)$ - °R	324.0	538.0	260.9
$T_{out}(O_2)$ - °R	209.0	539.0	263.2
$\Delta P(H_2)$ - psi	0.30	0.82	0.0
$\Delta P(O_2)$ - psi	4.28	0.30	0.02
O_2 Exit Quality	1.0	1.0	0.1
Q - Btu/sec	213.0	14.197	40.2
Q/A, Average - Btu/ft^2·sec	10.0	0.666	1.887

FD 278949

Figure 74. RL10-IIB Engine — Gaseous Oxygen Heat Exchanger (Stage 3 Core)

Stage 2 was designed so that no unstable boiling of the liquid would occur at pumped idle flow conditions. It required 40% dense metal fiber insulation between the hydrogen and oxygen plates. This insulation is too stiff to conform to the plate surface and therefore must be brazed to the plates. The calculated equivalent conductivity of the 0.025 inch thick insulation and braze is 0.294 Btu-ft/ft^2-hr-°F. The maximum allowable heat flux for stable boiling at PI is 2.62 Btu/ft^2 sec. The calculated maximum heat flux for this configuration is 2.41 Btu/ft^2 sec at PI.

Stage 3 of the OHE was designed to deliver 209°R superheated oxygen at the PI design point. The oxygen that flows through stage 3 is always above 5% quality so no insulation is used. The average heat flux at pumped idle is 10.0 Btu/ft^2 sec.

The pressure drop calculations for the RL10-IIB OHE are also based on work done in the P&W Space Tug Engine Study (P&W Report No. FR-7498). The hydrogen flow is all single-phase and the pressure drop calculations were straightforward. The oxygen flow is a combination of single-phase flow and two-phase flow at the PI design point. Oxygen single-phase flow occurs in stage 1, the first half of stage 2, and the end of stage 3. Two-phase oxygen flow occurs in the last half of stage 2 and most of stage 3. Two methods were used to calculate the two-phase flow pressure drops. The homogeneous model is most accurate at low vapor qualities and the separated flow model, with the Martinelli-Lockhart correlation, is more accurate at higher qualities (and also gives higher pressure losses). The total oxygen pressure drops at PI using the homogeneous and separated-flow models are 4.4 psid and 7.1 psid, respectively. Since the Martinelli-Lockhart separated flow model is the more conservative method, it was used for calculation of all two-phase oxygen pressure drops.

The initial design of the OHE, based on the above analyses, was a silver-brazed Type 347 stainless steel cores and end closures. The calculated weight of the design was 130 pounds (Ref. Layout Drawing No. L-238388, Sheets 1-3). This weight was unacceptable to NASA, even for a demonstration unit. An engineering review of the design indicated that it could be changed to 6061T-6 aluminum with minor design modifications. The calculated weight of the aluminum OHE was 51 pounds, but there was reluctance to make the change because of the potentially more difficult fabrication (very limited P&W experience with aluminum welding and brazing). However, after weighing the known risks and benefits the decision was made to go with aluminum and the redesign was accomplished (Ref. Layout Drawing No. L-238388, Sheets 5-7). Predicted heat transfer performance was essentially the same as for the stainless steel design, but the second stage insulation had to be changed to compressed nickel felt to obtain the required heat transfer coefficient with metal-to-metal contact instead of brazed surfaces.

Concerns with producibility of design tolerances for photo-etched flow passage dimensions, insulation conductivities, fluxless vacuum brazed construction, and the heat transfer analysis resulted in unplanned design support efforts to determine their validities. As a result, modifications to the flow passage groove dimensions and shapes were found necessary through sample panel etchings to assure producibility for the required flow areas. Flow passage geometry was revised accordingly.

Also, conductivity data could not be found on metal felts used to limit heat transfer at the OHE Stages 1 and 2 operating conditions. Contacts with various testing laboratories resulted in the selection of Dynatech, Inc., Cambridge, Mass. to perform conductivity testing. A decision had been made early in the OHE design effort to provide access to the insulation spaces for venting during brazing, and allow the use of vacuum or pressurized gases to tailor insulation conductivities if necessary. Accordingly, the conductivity tests of stainless steel and nickel felts by Dynatech covered vacuum, Nitrogen and Helium atmospheres at OHE design thicknesses. A schematic of the test setup is shown in Figure 75. The results are given in Table 5. They showed that the effective conductivities in the planned Nitrogen atmosphere was far below the values

predicted during the design and   es, but by varying the atmosphere acceptable results could be produced (Ref. Dynatech Report No. PRA-105, October 1983).

Initial contacts with potential aluminum heat exchanger fabrication vendors resulted in design changes to improve the producibility of the aluminum OHE designs. Modifications to increase stages 1 and 2 thermal skin cover panel thickness were made to reduce the possibility of braze alloy silicon diffusion through the parent material (potential porosity) and to provide raised edges to allow for weld repair of the panel-to-header slot braze joints, if necessary. These modifications however increased both the size of the OHE and the calculated weight from 51 to 55 pounds. The modifications are shown on P&W Layout Drawing No. L-238388, sheets 8-10. Sheet 4 of drawing L-238388 presents the OHE mount provisions for the breadboard engine.

An independent heat transfer analysis of the initial stainless steel designs was conducted by Optics and Applied Technology Laboratory (OATL), a division of United Technologies Research Center (UTRC). The same propellant supply conditions, flow rates, and insulation conductivities used for the design analysis were specified. A 100 node finite element cross flow heat exchanger computer analysis program previously developed by UTRC was modified by OATL to utilize the OHE design configuration, propellant conditions and characteristics, and insulation conductivities. This computer code provides a more detailed analysis since it separates each stage of the heat exchanger into a nodal array and computes the heat transfer and pressure drop for the volume represented by each node based on local flow conditions. This is of particular importance during oxygen vaporization (two phase flow) when the fluid properties can vary dramatically. This analysis, as summarized in OATL Report No. 83R-280169-3, dated 24 August 1983, predicted higher heat transfer rates than the original design analysis in the two-phase flow regions of the OHE. Consequently, the higher heat transfer in Stage 3 at PI would cool the fuel too much and prevent sufficient heat transfer in stage 2. As in the design analysis, the substitution of aluminum for stainless steel had a negligible effect on core performance. However, the possibility of excessive conductive heat transfer in stages 1 and 2 oxidizer inlets, where the hydrogen panels were brazed to the oxygen headers, was recommended for additional analysis. The OATL computer program was furnished to P&W for analysis review and development of design modifications.

The design reanalysis (reported in R. J. Peckham to J. S. Henderson memorandum of 2 / August 1983 and included in this report as Appendix C), recommended a 12% increase in Stage 2 insulation conductivity, and a reduction in Stage 3 heat transfer by plugging approximately 9% of the propellant flow passages. An alternative solution that involved reversing the hydrogen flow path and a reducing stage 2 insulation conductivity by a factor of 9 with no change to stage 3 was also included in the memorandum. Subsequent nickel felt insulation conductivity tests showed only 5% of the predicted (initial design) value in a nitrogen atmosphere, but twice the required reversed-flow configuration conductivity in helium. Entrance conductivity was reduced by spacing the internal H_2 panels away from the O_2 headers and plugging two of the H_2 passages of the two external panels at the edges where they are brazed to the O_2 headers. The resultant breadboard configuration schematic and predicted fluid conditions are shown in Figure 76 and the stage 2 computer program results at PI are shown in Figure 77. The final design is shown on P&W Layout Drawing No. L-238388, sheets 8 through 10.
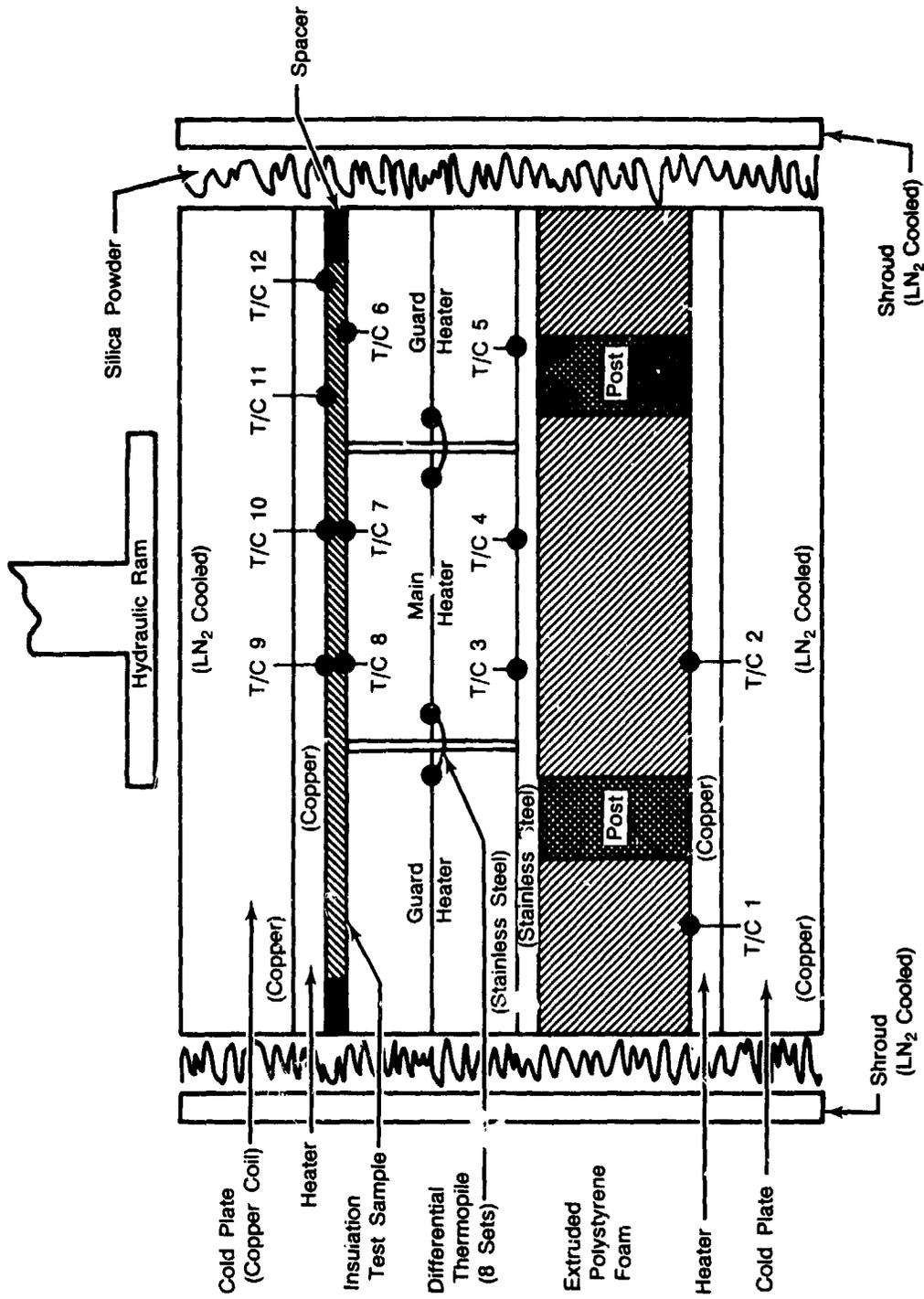
Figure 75. Schematic Representation of Single Sample Guarded Hot Plate Test Apparatus

74

Table 5.   Thermal Conductivity Test Results

	Hot Plate Temperatures (Part a. Test Material: 2% 304 SST FeH)					
	$T_1 = 370°R$ $\Delta T_1 = 241°R$		$T_2 = 393°R$ $\Delta T_2 = 264°R$		$T_3 = 417°R$ $\Delta T_3 = 288°R$	
Nitrogen	0.01108	$\dfrac{Btu}{hr\text{-}ft\text{-}°R}$	0.01125	$\dfrac{Btu}{hr\text{-}ft\text{-}°R}$	0.01217	$\dfrac{Btu}{hr\text{-}ft\text{-}°R}$
Helium			0.0526	$\dfrac{Btu}{hr\text{-}ft\text{-}°R}$		
Vacuum			0.001175	$\dfrac{Btu}{hr\text{-}ft\text{-}°R}$		

Other Conditions:

Material Thickness (Uncompressed): 0.150 in. nom.
Material Thickness (Compressed): 0.084 ± 0.002 in
Cold Plate Temperature: 129°R

	Hot Plate Temperatures (Part b. Test Material: 5% Ni Felt)					
	$T_1 = 178°R$		$T_2 = 216°R$		$T_3 \approx 252°R$	
	$\Delta T_1 \approx 35°R$		$\Delta T_2 = 73°R$		$\Delta T_3 = 109°R$	
Nitrogen			0.0148	$\dfrac{Btu}{hr\text{-}ft\text{-}°R}$		
Helium			0.0565	$\dfrac{Btu}{hr\text{-}ft\text{-}°R}$		
Vacuum			0.00592	$\dfrac{Btu}{hr\text{-}ft\text{-}°R}$		

Other Conditions:

Test Material: 5% Ni Felt
Material Thickness (Uncompressed): 0.35 in. nom.
Material Thickness (Compressed): 0.020 ± 0.002 in.
Cold Plate Temperature: 143°R

0900C

Mixture Ratio (O/F) = 6.0
Stage 2 Insulation Conductivity = 0.033 Btu/ft-hr°R

Hydrogen inlet
T_{out} = 639°R
P_{out} = 47.1 psia

Oxygen Inlet
T_{in} = 167°R
P_{in} = 84.3 psia
$\dot{m}$ = 2.84 lbm/sec

Stage 1

Oxygen
T = 199°R
P = 90.8 psia
Quality = 0.12

Stage 2

Hydrogen Exit
T_{in} = 260°R
P_{in} = 46.2 psia
$\dot{m}$ = 0.182 lbm/sec

Hydrogen
T = 547°R
P = 46.6 psia

Stage 3

Oxygen Exit
T_{out} = 198°R
P_{out} = 78.3 psia
Quality = 0.95
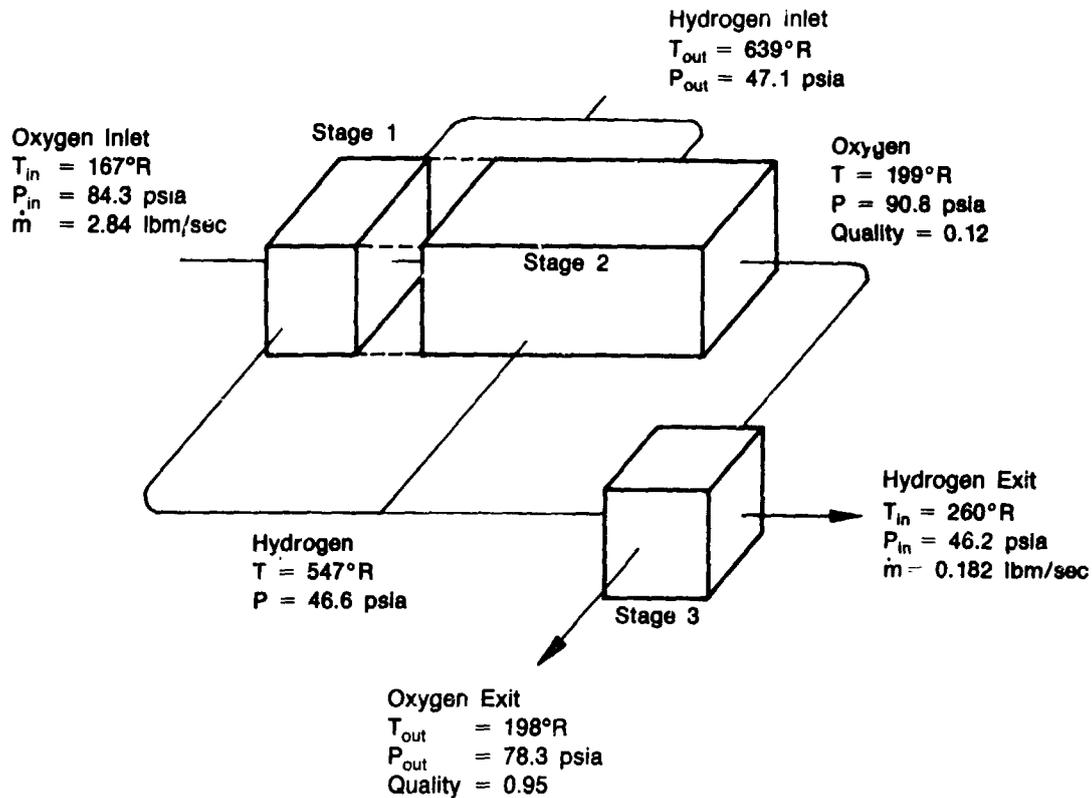
FD 278950

Figure 76.   RL10-IIB Oxidizer Heat Exchanger — Pumped Idle Performance (Reversed Hydrogen Flow)

Figure 77. RL10-IIB Oxidizer Heat Exchanger — Stage 2 (Heat Flux Map)

77

SECTION V
BREADBOARD CONTROLS DESIGNS

The four breadboard controls to be used for the low thrust demonstration program were designed and tested during earlier RL10 engine variable thrust programs. They are to be used to perform the functions of the cavitating venturi valve (CVV) turbine bypass valve (TBV), gaseous oxidizer valve (GOV), and liquid oxidizer flow control. Each is a variable area hydraulically-actuated valve capable of being scheduled to preprogrammed positions for THI, PI and FT operation. Valve position feedback is provided by a position potentiometer. The breadboard components are discussed in the following paragraphs.

The breadboard CVV, (TL-215351) design is shown in Figure 78. The primary construction materials are aluminum and stainless steel. It is a high-recovery design and has a throat pressure tap. The calibration curve, showing effective area versus pintle travel, is shown in Figure 79.

The breadboard TBV (S/N CKD-1188) shown in Figure 80 was originally designed and used as a liquid control valve for RL10 throttling engine demonstrations. It is a 90 degree contoured port sleeve valve driven by a rack and pinion with a feedback potentiometer driven by the pinion through a flexible coupling. Housing materials are aluminum and drive materials are stainless steels. The calibration curve showing effective area versus actuator shaft rotation is shown in Figure 81.

The breadboard GOV (S/N CKD-1311) is shown in Figure 82. It is a direct-drive butterfly valve with vertical shaft, and shutoff via butterfly to housing interference. Again, basic housing construction materials are aluminum and drive materials are stainless steel. The feedback potentiometer is driven by the actuator lever which is attached to both the butterfly shaft and the potentiometer. The calibration curve showing effective flow area versus actuator shaft rotation is shown in Figure 83.

FD)280452
61584
HPH
Disk 4
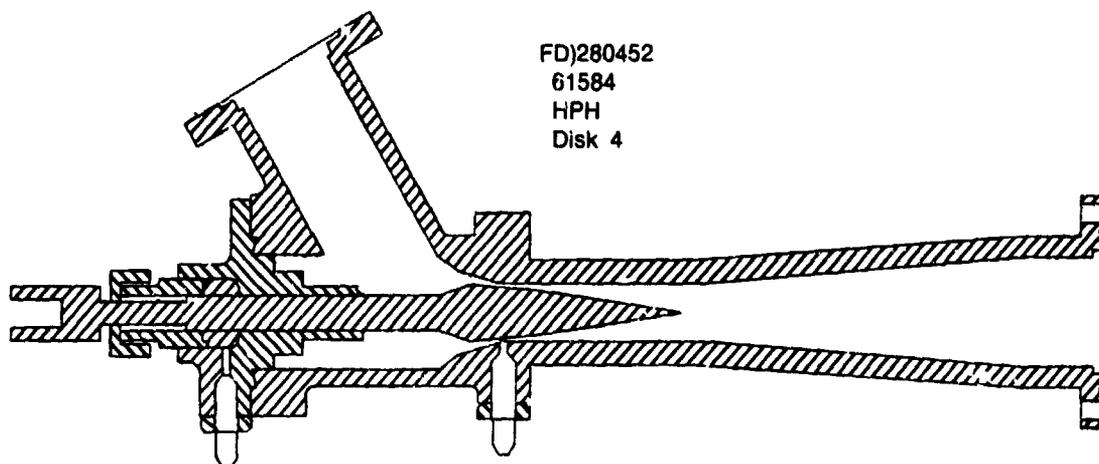
FD 280452

Figure 78.   RL10 Cavitating Venturi Valve (CVV)
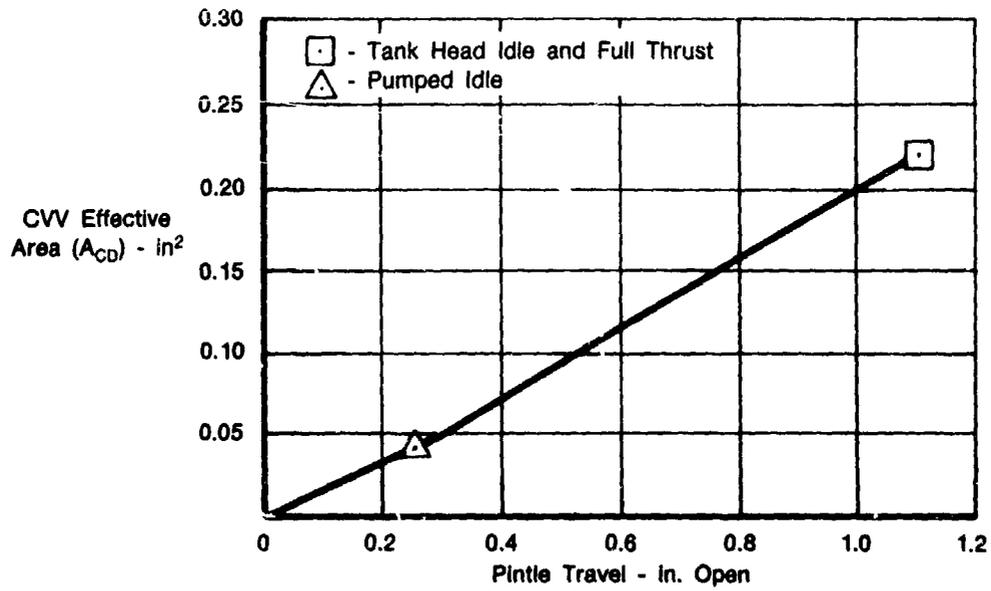
FD 280453

Figure 79. Cavitating Venturi Valve (CVV); S/N B54X-012; Operating Characteristics
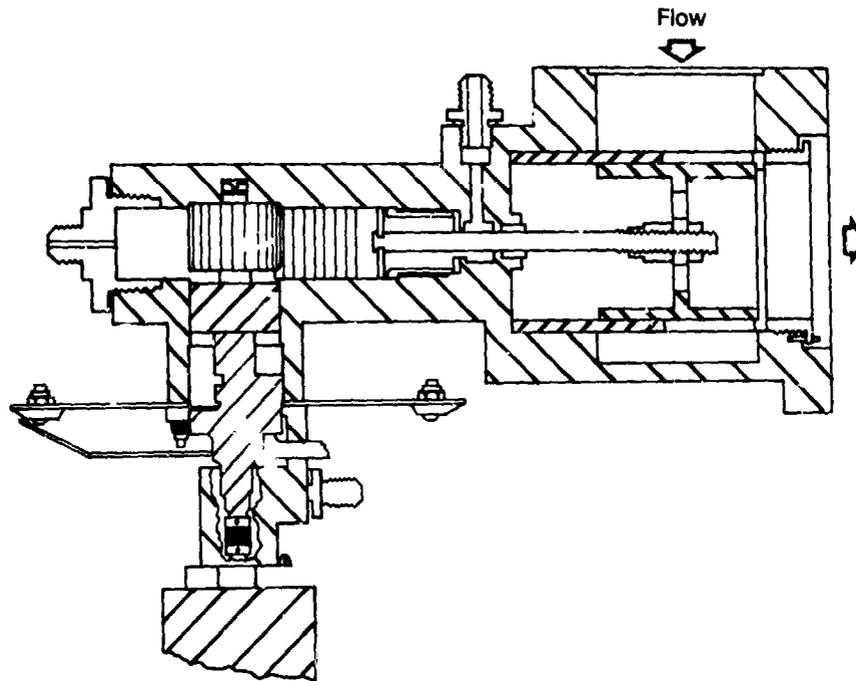
FD 280454

Figure 80. Turbine Bypass Valve (TBV) Assembly
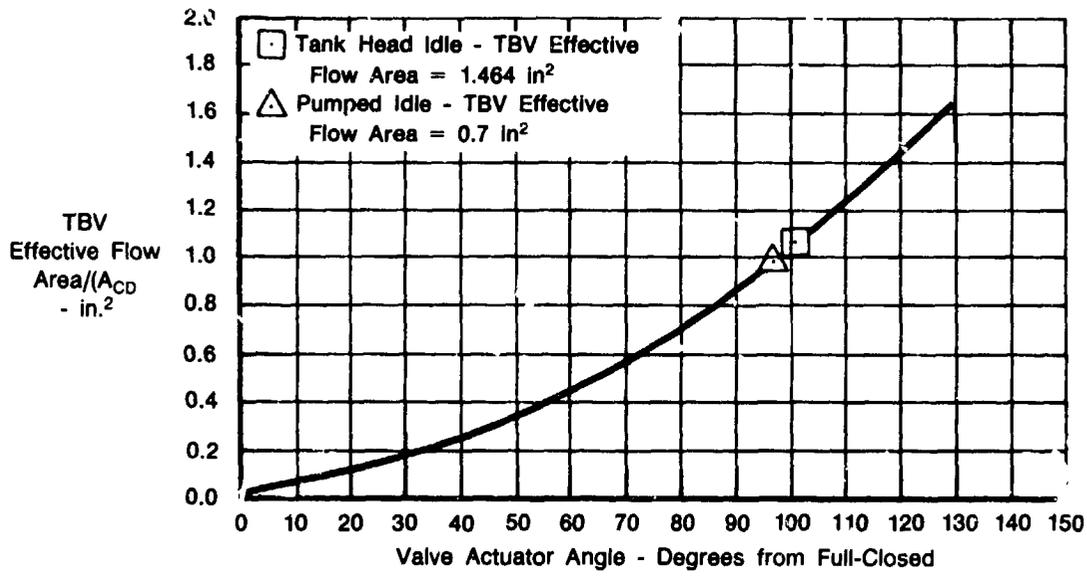
FD 280455

Figure 81.   Breadboard Turbine Bypass Valve (TBV) Operation; Tank Head Idle and
Pumped Idle
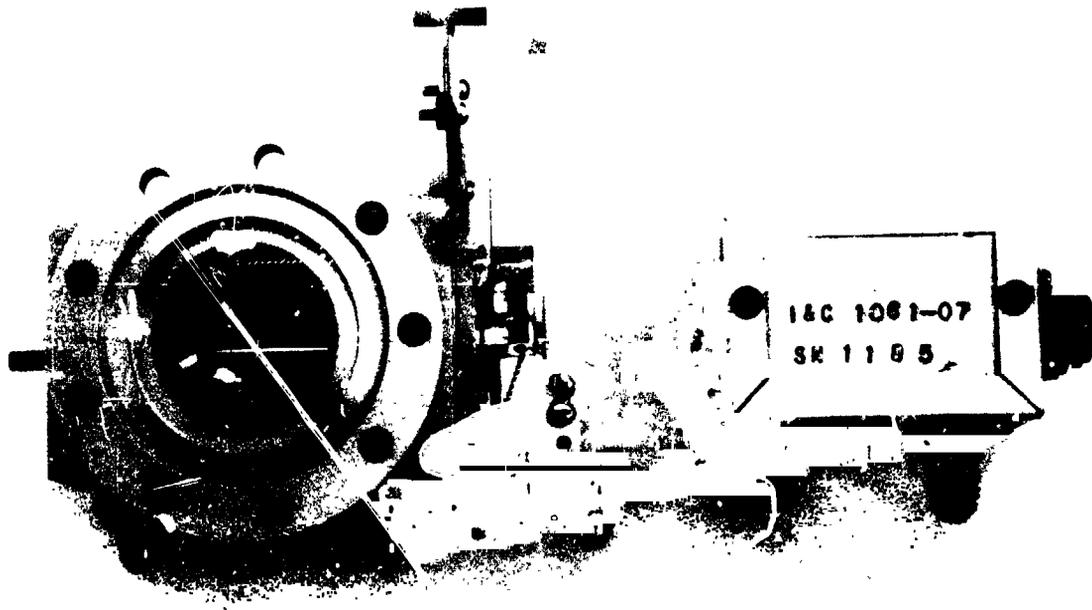
FC 14352

Figure 82. RL10 Gaseous Oxidizer Valve (GOV)
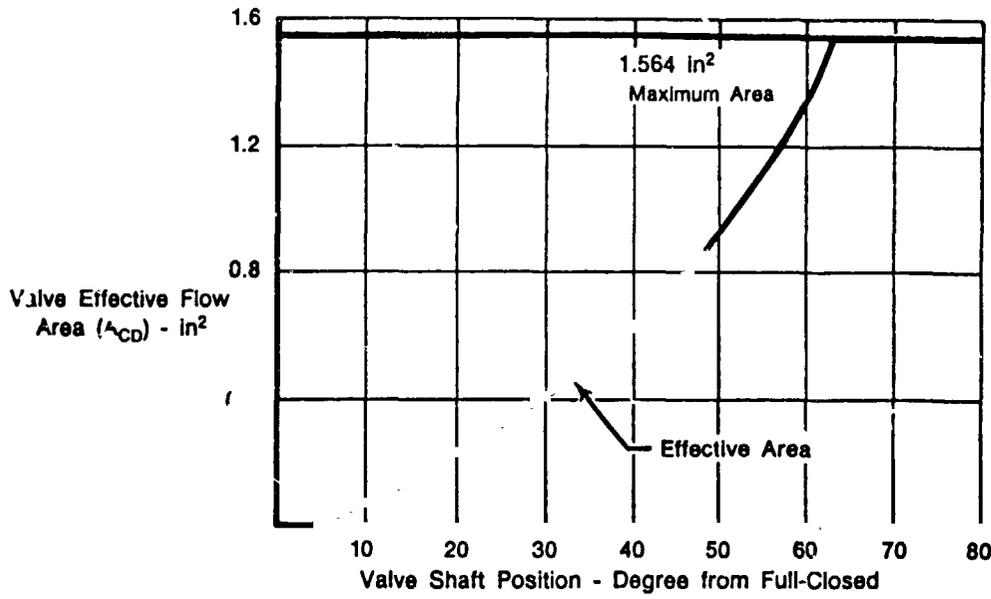
Figure 83. Gaseous Oxidizer Valve (GOV) Operation (S/N CKD-1311)

FD 280457

A fourth breadboard valve that is not specifically a part of the Low Thrust Program, but provides extra flexibility for liquid oxidizer control is the oxidizer control valve (OCV), which will be used instead of the RL10A-3-3 engine oxidizer flow control (OFC). The valve is assembled as P&W part number BKD 7935 and is shown in the exploded view in Figure 84. It is essentially a modified OFC that provides complete liquid oxidizer flow control from shutoff to full thrust flow. The basic construction is consistent with that of the RL10A-3-3 OFC, with parts modified to eliminate unneeded functions and to provide a contoured flow control and minimum-clearance shutoff pintle instead of the RL10A-3-3 propellant utilization (PU) pintle. The calibration curve showing effective flow area versus actuator shaft angle is presented in Figure 85.

Design modifications to the turbopump were confined to those necessary for incorporation of the 2.1:1 ratio drive gears (fuel pump to oxidizer pump) and the single-bearing idler gear (both of which are features that were demonstrated in earlier RL10 programs). The only turbopump design effort in this analysis and design task was to adapt the 2.1:1 ratio gear design to the RL10A-3-3A engine pump shafts and modify the oxidizer pump elbow housing to the shorter shaft center-distance required by the 2.1 gears (shown on P&W drawings L238361 and SL-238056 respectively).

The injector was modified to incorporate the torch ignition system, and the 120 cfm Bill-of-Materials fuel plate rigimesh was replaced by 240 cfm AISI 347 rigimesh to provide more face cooling flow during low thrust engine operation.

Heat exchanger mockups were built and used to modify existing throttling engine plumbing and to route new plumbing, as necessary, to install the oxygen heat exchangers and breadboard valves on the basic RL10A-3-3 engine. No designs or engineering drawings were produced for the breadboard engine. Mockup photographs at the end of the fabrication stage were used to document the configuration. The photographs of the breadboard demonstrator low thrust engine mockup are shown in the summary as Figures 1 to 4.
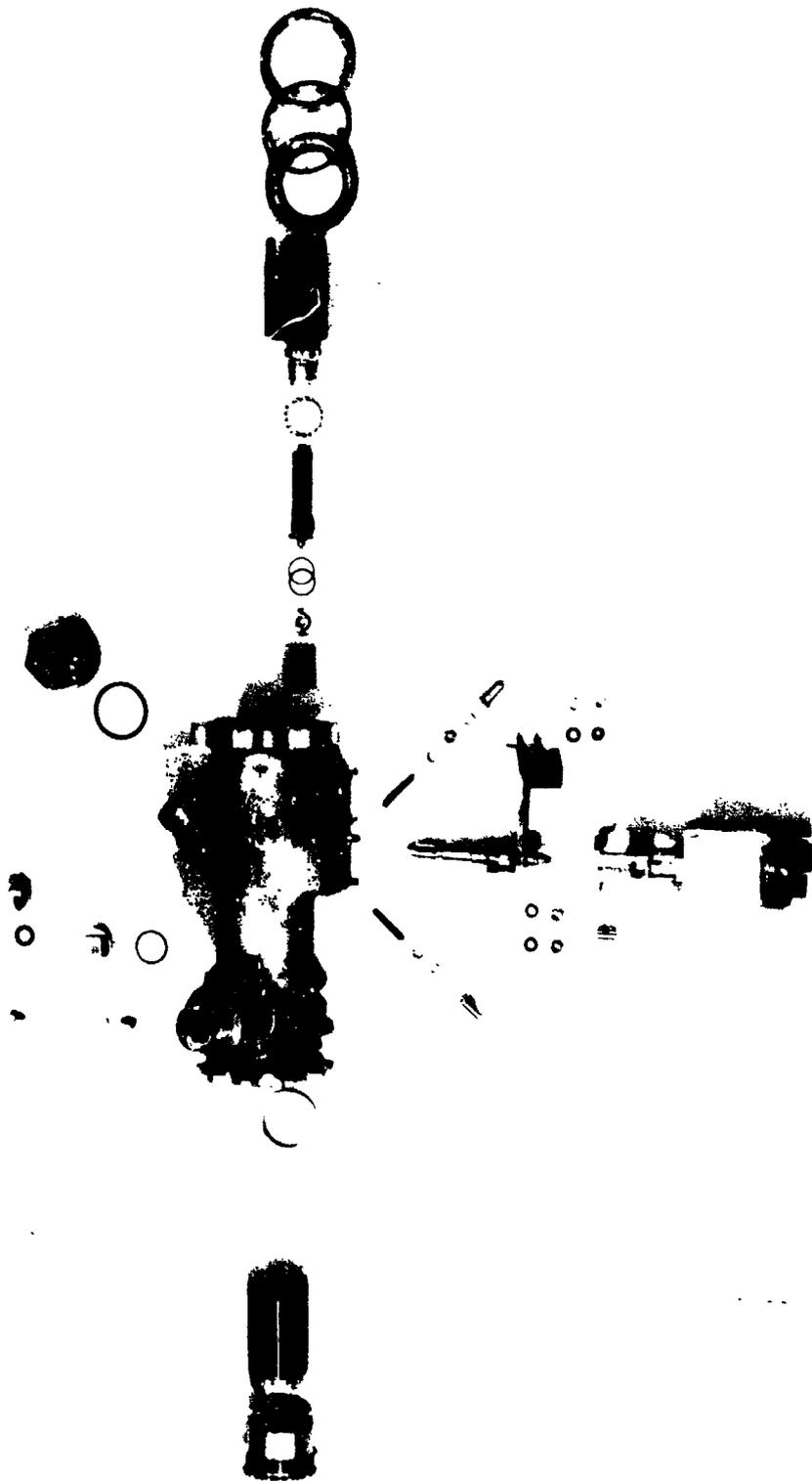
Figure 84. Oxidizer Control Valve (OCV); S/N BKD-7935
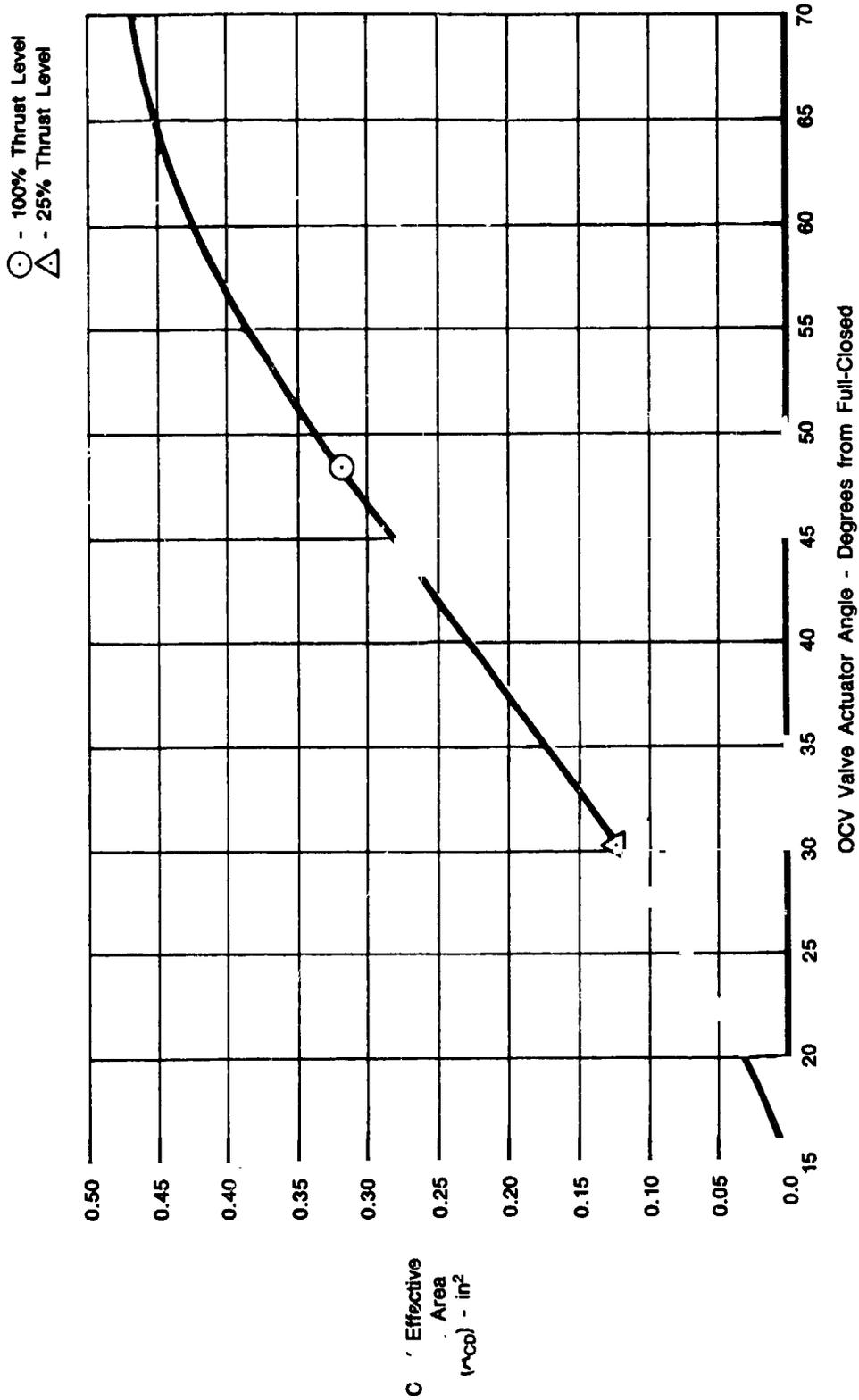
FE 62549

Figure 85. *Oxidizer Control Valve (OCV) Operation (S/N BKD)*

86

APPENDIX A
ENGINE STEADY STATE CYCLE CALCULATIONS

The computer cycle program can be balanced in three ways: it can be balanced (1) to a particular vacuum thrust and inlet mixture ratic (2) to particular oxidizer flow control and turbine bypass valve effective areas, or (3) to a particular chamber pressure and oxidizer flow control valve effective area. The first method is used to define control valve areas for use in running the other options. Since the engine operates in the pumped idle mode with fixed control areas, the second option is normally used to determine the effects of inlet pressure variations and/or changes in tank pressurization flow rates in that operating mode. The third method is used to simulate engine operation at full thrust where chamber pressure is held constant by the thrust control. This option is normally used to evaluate the effects of changing inlet conditions and other variables on engine operation while operating at full thrust.

A schematic of the RL10-IIB engine off-design cycle computer program is shown in Figure A-1 and Table A-1.

0907C

Figure A-1. *Cycle Schematic of the RL10-IIB Off-Design Computer Program*

*Table A-1. Symbol Usage in Figure A-1. RL10-IIB Cycle
Schematic Nomenclature (Continued)*

ABYP	Bypass Valve Area
ACDOCI	Input Oxidizer Control Valve Area
ACDOCV	Oxidizer Control Valve Effective Area
AFI	Fuel Injector Area
AFIJ	Fuel Injector Effective Area
AOI	Oxidizer Injector Area
AOIJ	Oxidizer Injector Effective Area
ARN	Nozzle Area Ratio
AT	Turbine Area
BPACDI	Input Turbine Bypass Valve Area
η_{c*}	Characteristic Velocity Efficiency
ηCFO	Thrust Coefficient Efficiency
CFVAC'	Ideal Thrust Coefficient
CSTAR'	Ideal Characteristic Velocity
CS	Nozzle Boundary Layer Loss and Divergence Loss
DNIMP	Dump Nozzle Impulse
EFFFP	Fuel Pump Efficiency
EFFOP	Oxidizer Pump Efficiency
ETAT	Turbine Efficiency
FHIJ	Fuel Injector Inlet Enthalpy
FNPSP	Fuel Pump Inlet Net Positive Suction Pressure
FOI	Input Thrust
FPDP	Fuel Pump Discharge Pressure
FPDT	Fuel Pump Discharge Temperature
FPIP	Fuel Pump Inlet Pressure
FPIT	Fuel Pump Inlet Temperature
FPIJ	Fuel Injector Inlet Pressure
FTIJ	Fuel Injector Inlet Temperature
FTIP	Fuel Turbine Inlet Pressure
FTIT	Fuel Turbine Inlet Temperature
FVAC	Thrust
FVACDEL	Delivered Vacuum Thrust
FVAC4	Pseudo Thrust
HPF	Fuel Pump Horsepower
HPO	Oxidizer Pump Horsepower
IVAC	Vacuum Specific Impulse at RMC
IVAC'	Ideal Impulse
IVACDEL	Delivered Vacuum Impulse
ηIO	Impulse Efficiency
JFIP	Jacket Inlet Pressure
JFTIT	Jacket Inlet Temperature
ΔKE	Nozzle Kinetic Loss
ONPSP	Oxidizer Pump Inlet Net Positive Suction Pressure
OPDH	Oxidizer Pump Discharge Enthalpy
OPDP	Oxidizer Pump Discharge Pressure
OPDT	Oxidizer Pump Discharge Temperature
OPIJ	Oxidizer Injector Inlet Pressure
OPIP	Oxidizer Pump Inlet Pressure
OPIT	Oxidizer Pump Inlet Temperature
ΔP	Main Heat Exchanger Pressure Loss
PC	Chamber Pressure
PCI	Input Chamber Pressure
P/P	Pressure Ratio
ΔPLOIJ	Oxidizer Injector Pressure Loss
RMC	Chamber Mixture Ratio
RMI	Inlet Mixture Ratio
RPM	Fuel Pump Speed
ΔT	Main Heat Exchanger Temperature Rise
VR	Isentropic Velocity Ratio
W_{bypass}	Bypass Flowrate

0907C

*Table A-1. Symbol Usage in Figure A-1. RL10-IIB Cycle
Schematic Nomenclature (Continued)*

WF	Inlet Fuel Flowrate
WFC	Chamber Fuel Flow
WOTP	Oxidizer Tank Pressurization Flowrate
WFTP	Fuel Tank Pressurization Flowrate
WLEAK	Coolant Flow to Gearbox and Dump Nozzle
WO	Oxidizer Flowrate
WPC	Chamber Propellant Flowrate
WT	Turbine Flowrate

The pump operating characteristics are simulated in the programs using head coefficient/flow coefficient and efficiency/flow coefficient relationships derived from RL10 pump test data. The characteristics used in this program for the main pumps are shown in Figures A-2 through A-8.

Turbine efficiency characteristics were obtained from RL10 turbine rig test data and are used in the simulation as functions of isentropic velocity ratios.

Main chamber and primary nozzle off-design coolant pressure loss and temperature rise characteristics are simulated in the programs with regression equations that calculate ΔP and ΔT characteristics as functions of fuel flow, chamber pressure, characteristic velocity efficiency, jacket inlet pressure, chamber mixture ratio, and combustion temperature. The equations are shown in Table A-2. They were generated by fitting test data and analytical predictions of chamber-nozzle heat transfer characteristics. Chamber-nozzle performance is calculated in the cycle programs by applying performance loss characteristics obtained from various Joint Army Navy NASA Air Force (JANNAF) performance programs to JANNAF One Dimensional Equilibrium (ODE) ideal performance predictions.
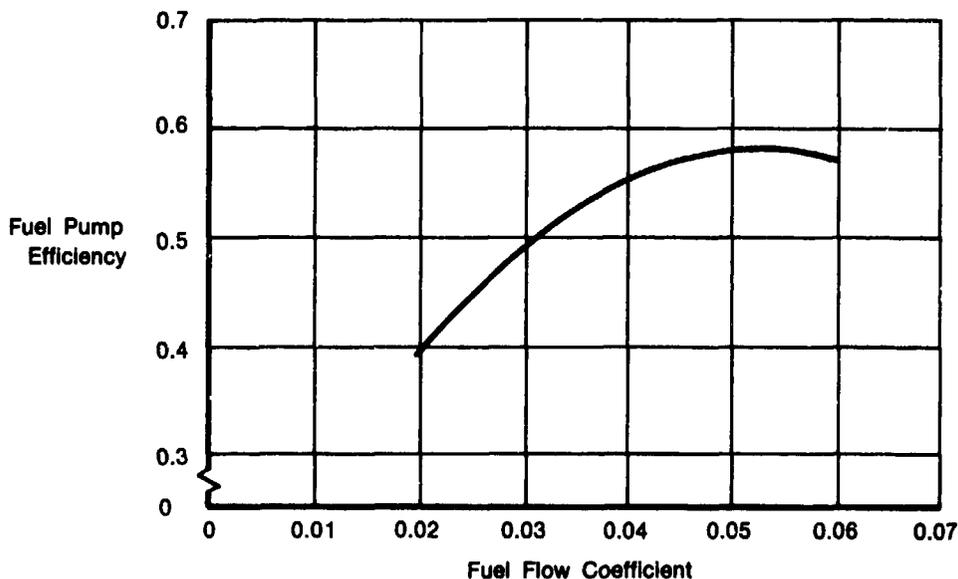
FD 280461

*Figure A-2. Fuel Pump First Stage Performance Characteristics (Fuel Pump Efficiency);
RL10-IIB Engine*

0907C
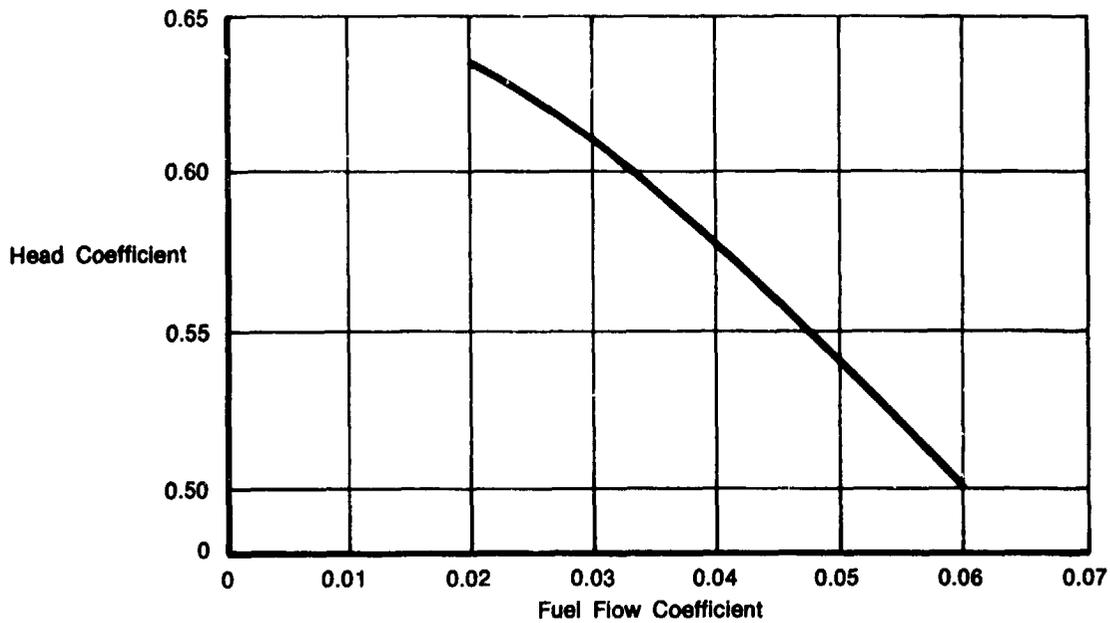
FD 260462

Figure A-3. Fuel Pump First Stage Performance Characteristics (Head Coefficient); RL10-IIB Engine
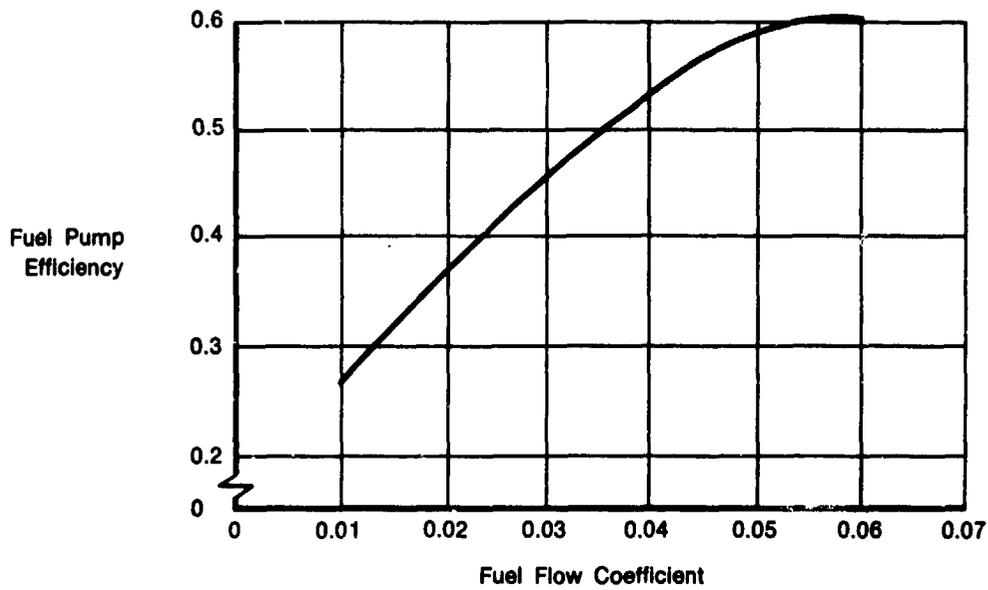
FD 260463

Figure A-4. Fuel Pump Second Stage Performance Characteristics (Fuel Pump Efficiency); RL10-IIB Engine
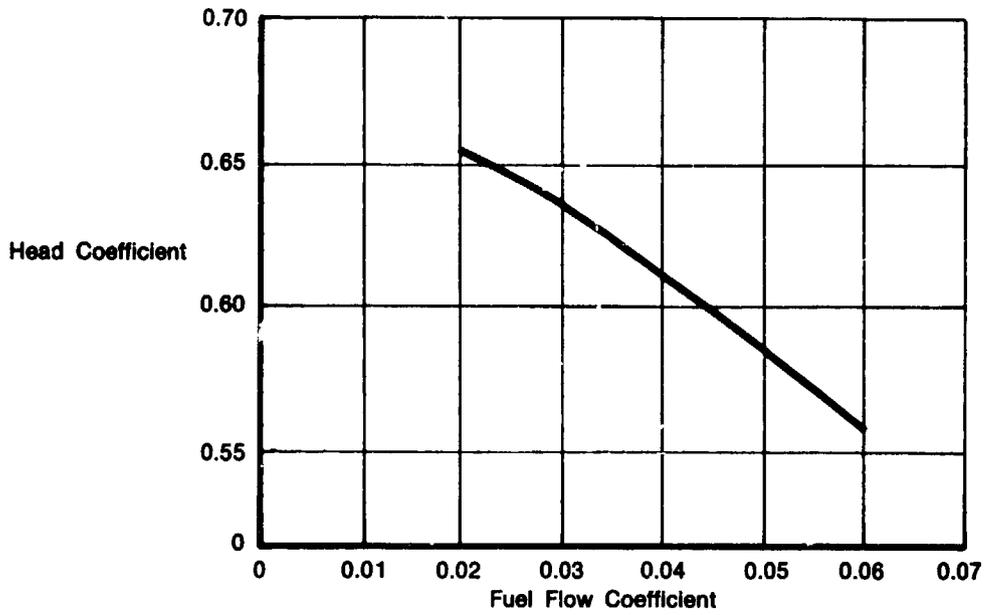
FD 280464

Figure A-5. Fuel Pump Second Stage Performance Characteristics (Head Coefficient); RL10-IIB Engine
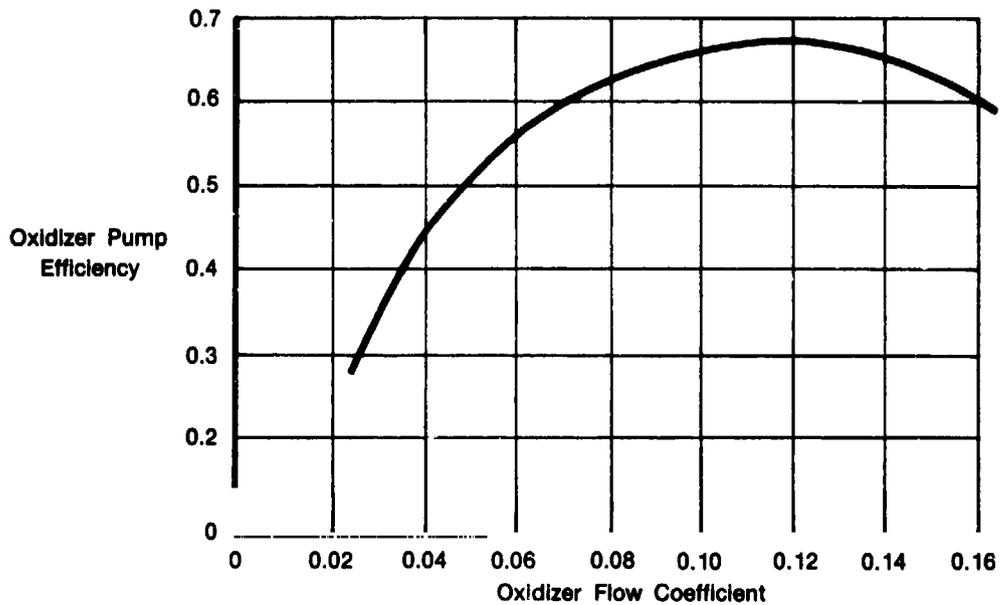
FD 280465

Figure A-6. Oxidizer Pump Performance Characteristics (Oxidizer Pump Efficiency); RL10-IIB Engine
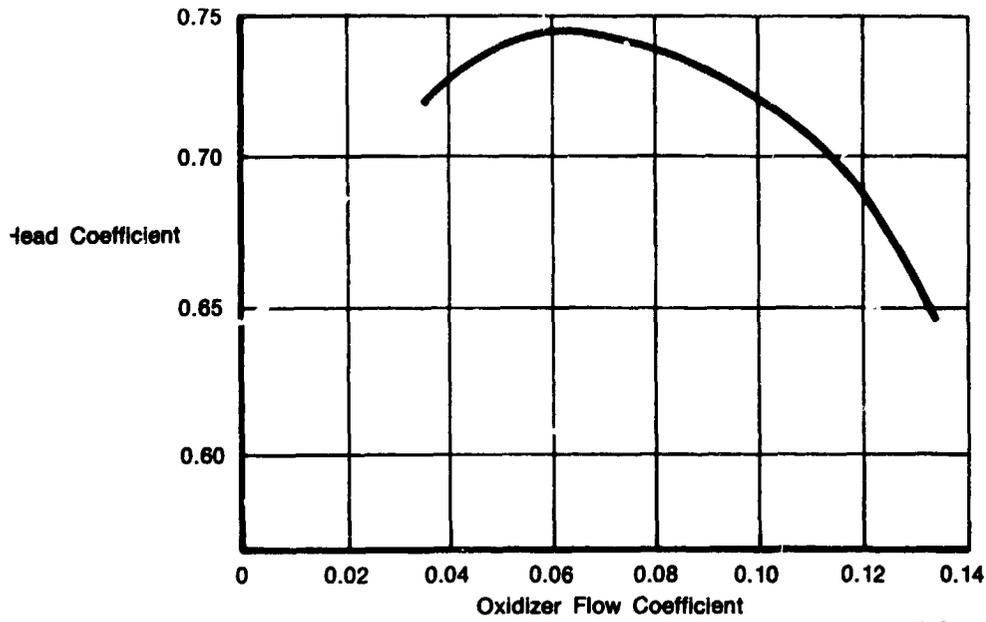
FD 280466

Figure A-7. Oxidizer Pump Performance Characteristics (Head Coefficient);
RL10-IIB Engine

	η_D	VF_D
RL10-IIB	0.711	0.392
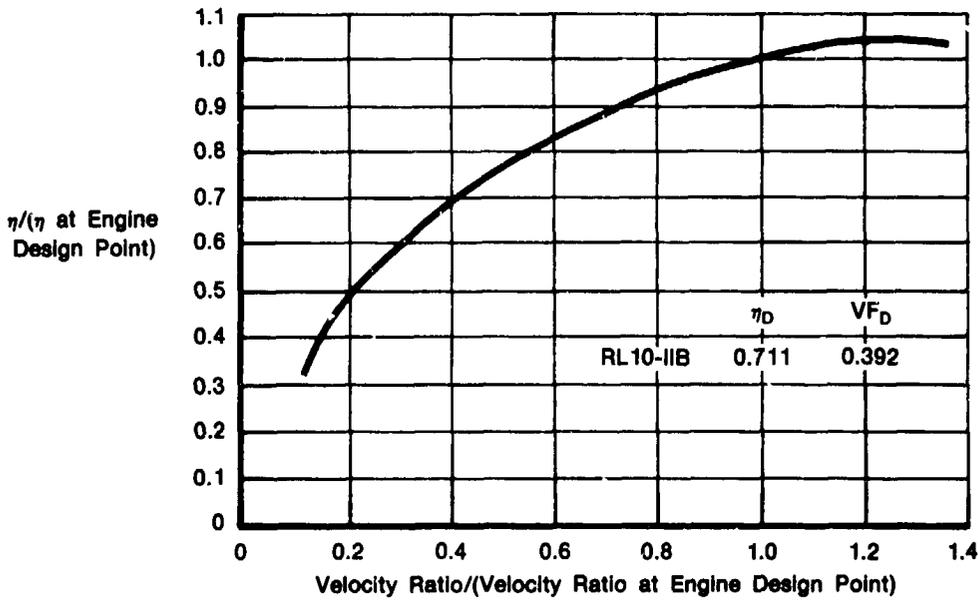
FD 280467

Figure A-8. Turbine Efficiency Characteristics — RL10-IIB Engine

Table A-2. Main Chamber and Primary Nozzle Heat Transfer Predictions

The following equations are used to predict the off-design main chamber and primary nozzle coolant temperature rise and pressure loss characteristics:

$$\Delta T = \frac{K1 \times RPC^{0.214} \times RPIN^{0.005} \times RECS^{1.951} \times RTC^{2.427}}{RRM^{1.153} \times RWF^{0.436}}$$

$$\Delta P = \left[JFIP - \left(JFIP^2 - \left(\frac{WFC}{WFCD} \right)^2 \times \left(\frac{TAVG}{TAVGD} \right) \times PAVGD \times PD \times 2 \right)^{0.5} \right] \times 1.73$$

where:

ΔT = Coolant temperature rise at off-design point

ΔP = Coolant pressure loss at off-design point

K1 = Constant to set the design point level

RPC = $\dfrac{\text{Chamber pressure}}{19.0}$

RPIN = $\dfrac{\text{Inlet Pressure of Coolant}}{70.0}$

RECS = $\dfrac{\eta_{c^*}}{0.94}$

RTC = $\dfrac{\text{Combustion Temperature}}{7147.0}$

RRM = $\dfrac{\text{Chamber Mixture Ratio}}{5.0}$

RWF = $\dfrac{\text{Coolant Flowrate}}{0.298}$

JFIP = Coolant Inlet Pressure

WFCD = Coolant Flowrate at Engine Design Point

TAVGD = Average Temperature of Coolant in Jacket at Engine Design Point

PAVGD = Average Pressure of Coolant in Jacket at Engine Design Point

ΔPD = Coolant Pressure Loss at Engine Design Point

WFC = Coolant Flowrate at Off-Design Point

TAVG = Average Temperature of Coolant in Jacket at Off-Design Point

Off-design heat transfer characteristics for the GOX heat exchanger are simulated in the programs using correlations established for similar heat exchanger configurations. These correlations are for a compact configuration. The equations used are shown in Table A-3.

Table A-3. Oxygen Heat Exchanger

Heat Transfer Predictions

The following equations are used to predict the off-design GOX heat exchanger heat transfer characteristics in the off-design cycle programs:

C_{min} = Lowest of $C_{P_O} \times W_O$ or $C_{P_F} \times W_F$

C_{max} = Highest of $C_{P_O} \times W_O$ or $C_{P_F} \times W_F$

UA = Overall Heat Transfer Coefficient × Surface Area

$XNTU = \dfrac{UA}{C_{min}}$

Effectiveness = $f\left(\dfrac{C_{min}}{C_{max}}, XNTU\right)$, from curve

Heat Flux = Effectiveness × (TFIN-TOIN) × C_{min}

Kays, W. and London, A. L., *Compact Heat Exchangers*, McGraw-Hill, New York, 1964.

0907C

APPENDIX B
DEFINITION OF ENGINE TRANSIENT CHARACTERISTICS

Two transient computer simulation programs were used to define the transient characteristics and control system requirements for the RL10-IIB engine. One of these programs was used to simulate turbopump cooldown (THI transients). The other program simulated acceleration transients to PI and FT for the engine.

Tank Head Idle simulations can be made with various propellant conditions (gas, liquid or two-phase), and various initial metal temperatures. The methods used to simulate the components in the transient simulations are similar to those used in the steady state cycle program. The major differences in the programs are the dynamics included in the transient programs and additional routines required for THI cooldown.

1. ACCELERATION TRANSIENT SIMULATION

Figure B-1 and Table B-1 present a simplified flow schematic that shows the more important calculations and convergence loops used to simulate the RL10-IIB engine operation during acceleration transients. Dynamics are among the main considerations in this program. A brief discussion of the dynamics used is included later in this Appendix.

0908C
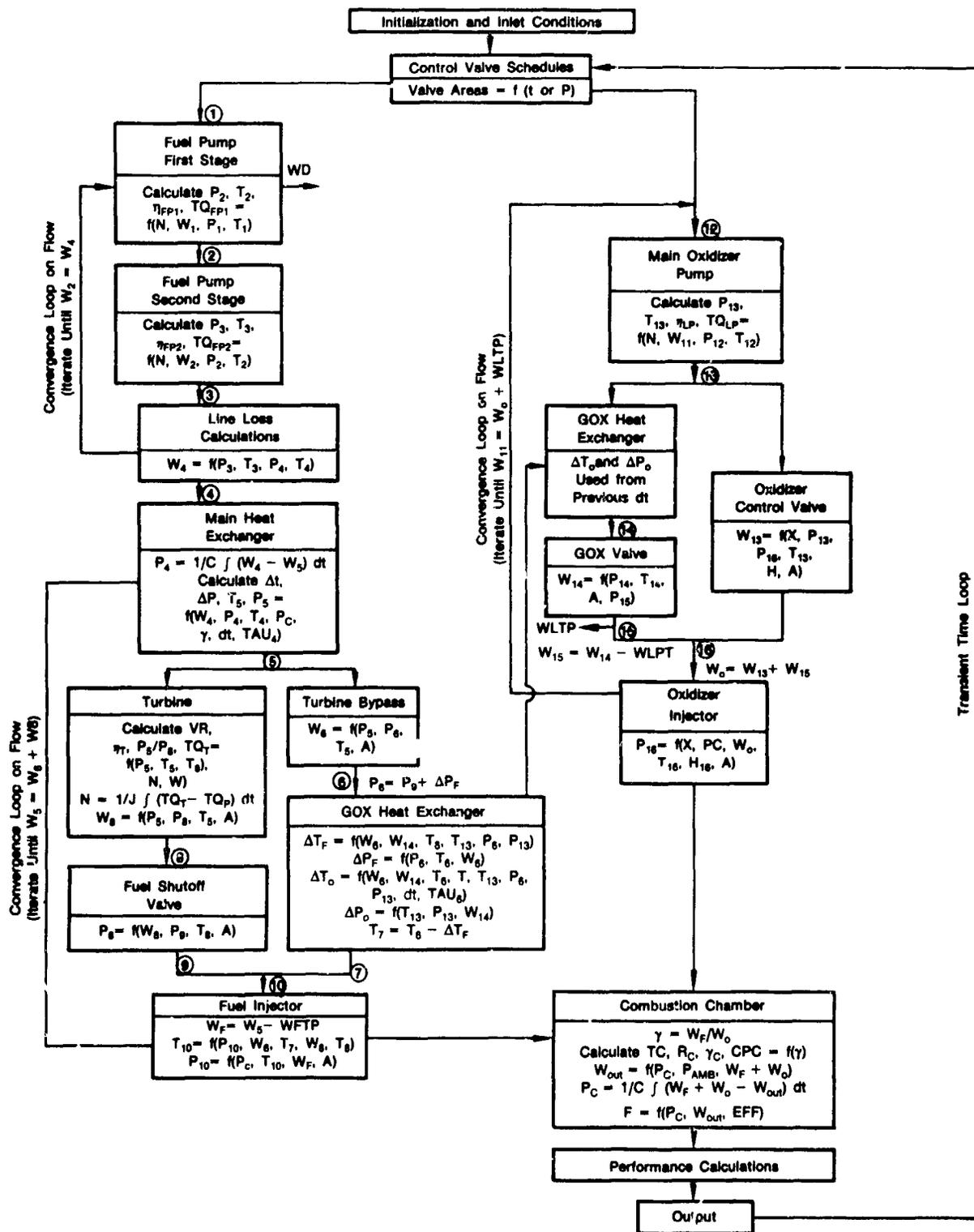
Figure B-1. Transient Simulation Flow Schematic — RL10-IIB Engine

FD 280468

Table B-1. Symbol Usage in Figures B1 and B2

A	Area — inches^2
AS	Surface Area, inches^2
C	Capacitance
C_p	Specific Heat Capacity — Btu/lb$_m$ — °R
C_L	Nozzle Boundary Layer Loss and Divergence Loss
DKE	Nozzle Kinetic Loss
dt	Time Increment, seconds
EFF	Efficiency Terms (Cs, DKE, η_c.)
FSV	Thrust — lb$_f$
HYD	Hydraulic Diameter — inches
H	Enthalpy — Btu/lb$_m$
h	Heat Transfer Coefficient — Btu/hr — ft^2 — °R
η	Efficiency (pump or turbine)
η_{Ivac}	Vacuum impulse efficiency
I_{vac}'	Ideal Vacuum Specific Impulse — sec
J	Turbopump Polar Moment of Inertia — ft-lb-sec^2
N	Turbopump Speed — RPM
P	Pressure — psia
ΔP	Pressure loss — psid
P_{amb}	Ambient Pressure — psia
Pc	Combustion chamber pressure — psia
Q	Heat transferred — Btu
R	Density — lbm/ft^3
r	Mixture ratio
Rc	Gas Constant — ft-lbs/°R-lbm
S	Entropy — Btu/lb$_m$-°R
T	Temperature — °R
t	Time — seconds
ΔT	Temperature rise — °R
TAU	Transient response time constant — second
TQ	Torque-ft-lbs
TW	Wall temperature, °R
V	Velocity — ft/sec
VR	Turbine Velocity Ratio
W	Flowrate — lbm/sec
WD	Dump coolant flowrate — lbm/sec
WFTP	Fuel tank pressurization flowrate — lbm/sec
WLTP	Oxidizer tank pressurization flowrate — lbm/sec
W_F'	Fuel flowrate calculated at second stage discharge — lbm/sec
W_o'	Oxidizer flowrate calculated through oxidizer injector — lbm/sec
X	Propellant Quality
Z	Component (Impeller, pump housing, etc.) mass — lbm
γ	Specific heat ratio

Subscript Description

1, 2,. . . 16	Station locations
BP	Boost pump
C	Combustion chamber
D	Discharge
f	Fuel (propellant)
FP_1	Fuel pump, 1st stage
FP_2	Fuel pump, 2nd stage
O	Oxidizer propellant
P	Previous value
T	Turbine
U	Upstream
	Average

2. TANK HEAD IDLE COOLDOWN SIMULATION

Figure B-2 and Table B-1 presents a flow schematic which shows how the RL10-IIB engine is simulated during a tank head idle cooldown transient. Since the effects of fluid dynamics during the transients are insignificant compared to the effects of thermal dynamics, steady state flow is assumed to exist at each time increment during the THI transients and a Newton-Raphson rapid convergence technique is used to balance the simulation at each increment. The independent variables used to balance the programs are fuel flow, pressure at the inlet of the primary nozzle heat exchanger, and chamber pressure. The dependent variables are fuel flow, primary nozzle heat exchanger exit pressure and combustion chamber inlet and outlet flows. Fuel flow, inlet pressure to the heat exchanger, and chamber pressure are varied at each time increment until: (1) the assumed fuel flow at the heat exchanger inlet equals the flow calculated through the second stage of the fuel pump, (2) the pressure calculated at the exit of the primary nozzle heat exchanger equals the pressure calculated at the inlet of the turbine bypass valve, and (3) the total flowrate entering the combustion chamber equals the flowrate calculated at the throat of the chamber.

3. METHOD FOR SIMULATING ENGINE DYNAMICS

Dynamic performance characteristics are determined by numerically integrating time-varying differential equations. This is accomplished by calculating the differentials from known variables such as pressures, flowrates, speeds, etc., multiplying the differentials by the time increment (DT) selected for the program, and adding the result to the last calculated value of the parameter being integrated. The technique of numerical integration is shown by the following example where flowrates through a known control volume are integrated to obtain the pressure within the volume.

The integral equation is defined by:

$$P = \int \Sigma\, W dt$$

where P is pressure

and ΣW is summation of flow rates crossing volume boundaries

Expressing the equation in finite difference form:

$$P_n = P_{n-1} + \Delta P$$

where P_n is pressure at time $= n$

and P_{n-1} is pressure at time $= n-1$

Using numerical integration

$$\Delta P = \Sigma\, W \cdot DT$$

where DT = integration time increment

Initialization and Inlet Conditions

Inlet Lines and Valves

Conditioned

Unconditioned

Fuel Pump First Stage

Tank Head Idle Heat Transfer Equations[1] and $P_D = f(X, P_U, W_F, T, H, A)$

Tank Head Idle Heat Transfer Equations[1]

Fuel Pump Second Stage

Tank Head Idle Heat Transfer Equations[1] and $W_f' = f(X, P_U, P_{HEX}, T, H, A)$

Oxidizer Pump

Tank Head Idle Heat Transfer Equations[1] and $P_{DI} = f(X, P_U, W_o', T, H, A)$
$W_o = f(X, P_{DI}, P_D, T, H, A)$

Convergence Loop on Flowrate (Change Oxidizer Pump Discharge Pressure Until $W_o = W_o'$)

Primary Nozzle Heat Exchanger

$\Delta T = f(P_C, \gamma, W_F)$
$T_D = f(T_U, \Delta T, T_P, dT, TAU)$
$\Delta P = f(R_{HEX}, W_F, T_U, T_D)$
$P_D = f(P_{HEX}, \Delta P)$

W_F

P_D

$P_U = P_D$ When Balanced

P_U

ΔP and ΔT Across GCX Heat Exchanger From Previous dt

GOX Valve and Oxidizer Injector

$W_o' = f(P_U, T_U, P_D, A)$

Transient Time Loop

Turbine Bypass Valve

$P_U = f(W_F, P_D, T, A)$

W_F

P_D

GOX Heat Exchanger

$\Delta T_F = f(W_F, W_o, T_F, T_o, P_F, P_o)$
$\Delta P_F = f(T_F, P_F, W_F)$
$\Delta T_o = f(W_F, W_o, T_F, T_o, P_F, P_o)$
$\Delta P_o = f(T_o, P_o, W_F)$

Convergence Loop on Temperature

W_F

P_U

Fuel Injector

$P_U = f(P_C, T_U, A, W_F)$

W_F

P_C

$\gamma = W_o/W_F$
$W_{out} = f(P_C, P_{AMB}, A, R_C, \gamma_C, T_C, \gamma)$
$FSV = f(P_C, W_{out}, \gamma, IVAC, \eta_{i\,vac}, C_s, DKE)$

Change Independent Variables Until Dependent Variables Are Balanced[2]

W_o

Notes:
(1) Standard Tank Head Idle Heat Transfer Equations:

$TW = f(Z, T_{wp}, C, h, AS, T, dc)$
$h = f(T, R, X, HYD, TW, V)$
$Q = f(h, W, T, dt)$
$V_1 = f(W, H_1, P_1, A)$
$V_2 = f(W, H_2, P_2, A)$
$H_2 = f(Q, V_1, V_2, H_1)$
$S_2, T_2, X_2 = f(P_2, H_2)$

(2) Newton Raphson Convergence Technique:

Independent Variables	Dependent Variables
W_F	W_F, W_F
P_{HEX}	P_{HEX} Outlet
P_c	$W_o + W_F, W_{out}$

FD 260469

Figure B-2. Operation of RL10-IIB Engine During Tank Head Idle Transient

This method of numerical integration is used to define the dynamic behavior of the engine. The dynamic elements that have been simulated include:

1. Acceleration of oxidizer and fuel pumps

2. Thermal dynamics of the pump (cooldown)

3. Thermal dynamics of the primary nozzle heat exchanger and the oxidizer heat exchanger (OHE)

4. Fluid dynamics of the heat exchanger and main chamber.

The integration time increment (DT) is an input variable. The DT value normally used provides a compromise between simulation accuracy and the amount of computer time required to run the simulation. The DT varies depending upon the operating mode of the simulation.

A simulation of the tank head idle mode requires much more computer time than a simulation of the turbopump acceleration to full thrust. During a cooldown, fluid dynamics are of secondary importance to thermal dynamics. This permits a large time increment (1.0 second) to be used for THI to minimize computer time. To accommodate the large DT and prevent "mathematical instabilities," steady state flow is assumed during the cooldown. Dynamic heat transfer equations are used to simulate the component cooldowns, and flowrates and pressures are calculated as functions of the exit temperatures, pressures, and densities.

At the conclusion of cooldown when the turbopumps are started, the DT is reduced to 0.001 seconds to permit the turbopump acceleration dynamics to be considered. During accelerations to pumped idle (PI) and to full thrust (FT) the turbopump and fluid dynamics become very significant.

4. METHOD FOR SIMULATING ENGINE COOLDOWN

Special calculations are required to simulate the transient thermal conditioning of the engine. These routines were developed for the RL10 engine and checked using RL10 test data generated under simulated space conditions at the NASA-LeRC Plum Brook station.

For this simulation, a quasi-steady state solution of the conventional lumped mode thermal energy transfer and storage equation is made. Conduction, heat storage, phase change, free and forced convection capability, and radiation boundary conditions are all considered. Temperature-variable solid and fluid properties are used.

The engine lines, housings, valves, etc. are transformed into equivalent rods and cylinders. The thermal model then performs a one-dimensional, quasi-steady-state heat transfer analysis of the engine system. A particular component of the engine may be subdivided into several such rod and cylinder combinations which may be linked together in different flow and conduction path patterns. A simulation of a typical engine fuel pump is shown in Figure B-3.

A typical engine cooldown calculation is shown in the following example. In this case, the engine system is made up of components (rods and cylinders) at some initial temperature, and it is subjected to known external heat loads and fluid inlet conditions. The system is evaluated over a small time increment and an energy balance is made for the first rod/cylinder combination. The change in energy stored in the cylinder is determined by calculating the heat removed from the cylinder by the convective process of the coolant flow, and subtracting the heat added to the system from external sources. The energy change of the rod is also determined by subtracting the

heat removed by the convection process of the coolant. The energy increase of the coolant then becomes the sum of the heat energies removed from both the rod and cylinder. This energy is added to the fluid in the form of enthalpy, and velocity increases are determined by continuity and energy conservation equations. The properties of the coolant leading the first component become the inlet conditions for the next component and the calculations are repeated for each component in the system. The basic equations used to calculate the thermal characteristics of the components during THI cooldown are:

1. $Q1 = h_1 A_1 (T_{W1} - T) dt$

2. $Q2 = h_2 A_2 (T_{W2} - T) dt$

3. $Q_{TOTAL} = Q1 + Q2$

4. $H_2 = H_1 + \dfrac{Q_{TOTAL}}{Wdt} + \left(\dfrac{V_1^2}{2} - \dfrac{V_2^2}{2}\right) \times 47205$

5. $\rho_1 V_1 = \rho_2 V_2$

where Q   =   heat transferred — Btu

A   = area, ft$_2$
h   = heat transfer coefficient — Btu/sec — ft^2 — °R
T   = Temperature (Average) — °R
dt   = delta time increment — sec
H   = fluid enthalpy — Btu/lbm
V   = fluid velocity — ft/sec
ρ = fluid density — lb/ft^3

and subscripts

1   = upstream condition or outer component (cylinder)
2   = downstream condition or inner component (rod)
w   = wall condition

The energy removed from each component has now created a system imbalance in the form of temperature gradients between the rods and cylinders and their adjacent components. This imbalance initiates a conduction process which alters the distribution of the remaining energy in the system and reduces the temperature gradients. The transfer of conduction energy is determined by solution per the second law of thermodynamics. The solution obtained at the end of one time increment provides the starting condition for the next time increment and the analysis is continued until the temperatures of critical components (pump housings and impellers) reach the desired steady state levels.

0908C
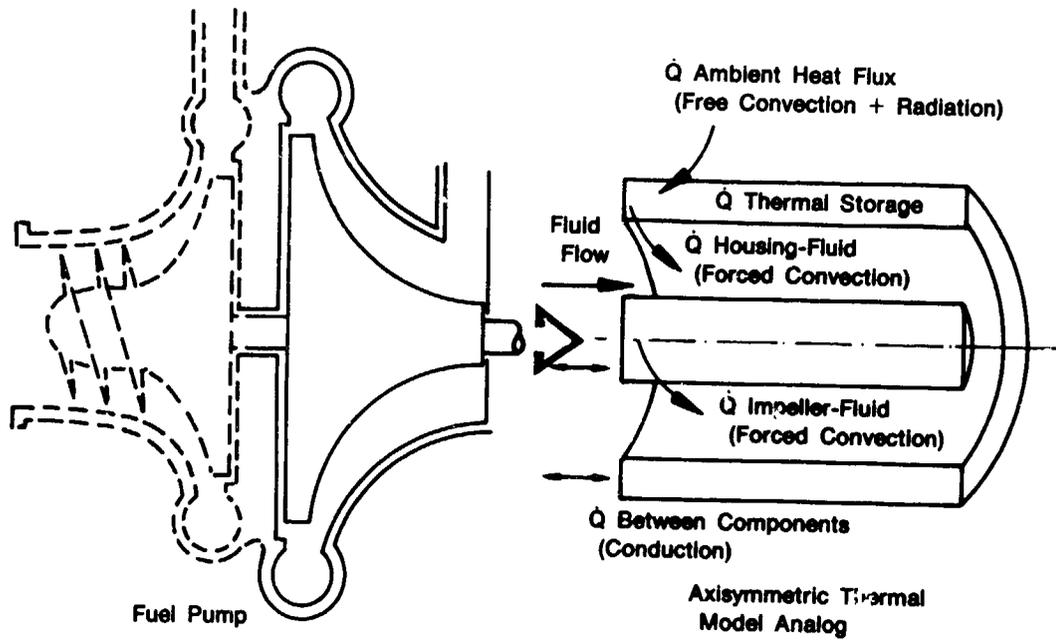
Figure B-3. Heat Transfer Model Simulates Thermal Conditions of Components and Fluids

FD 280470

APPENDIX C
PRATT & WHITNEY INTERNAL CORRESPONDENCE MEMO — HEAT TRANSFER ANALYSIS OF RL10-IIB GOX HEAT EXCHANGER

PRATT & WHITNEY AIRCRAFT GROUP
Government Products Division

INTERNAL CORRESPONDENCE

RL10 / HEAT TRANSFER
83-752-11280

To: J. Henderson
From: R. J. PECKHAM   EXT. 2938
Subject: The RL10 Derivative IIB GOX Heat Exchanger Has Been Modified Using a New Heat Exchanger Computer Deck
Date: August 27, 1983
Copy To: J. Bolch, J.D. Doernbach, T. Kmiec, C. Limerick, S. Owens

SUMMARY:

The RL10 Derivative IIB GOX heat exchanger has been revised after a review of the analysis showed performance below pumped idle design goals. The new analysis was done with a new heat exchanger computer deck which does a more detailed analysis. The major difference between the new analysis and original analysis is due to differences between the stage 3 blue print, (B/P), geometry and the geometry used in the original analysis. Once the new heat exchanger geometry was incorporated into the original model, the two analytical techniques agreed closely. Some changes to the design of the GOX heat exchanger have been made that will make the heat exchanger work properly at pumped idle. The performance of the modified GOX heat exchanger is included in this memo. The heat exchanger performance was generated by using the new heat exchanger deck because of its greater detail. Other heat exchanger variations have been examined to improve the tolerance to inlet conditions or to manufacturing problems.

RESULTS:

o Figure 1 shows the pumped idle performance of the modified RL10 Derivative IIB GOX heat exchanger.

o Figure 2 shows the detailed heat flux and oxygen quality information for the second stage of the GOX heat exchanger at pumped idle.

o Figure 3 shows the Stage 1 geometry of the GOX heat exchanger with its performance characteristics.

J. Henderson   - 2 -   August 27, 1983

o Figure 4 shows the Stage 2 geometry of the GOX
   heat exchanger with its performance characteristics.

o Figure 5 shows the Stage 3 geometry with performance
   characteristics.

o Figures 6 and 7 show the pumped idle performance of
   the reversed hydrogen flow GOX heat exchanger.

o Figures 8 and 9 show the pumped idle performance of
   the alternate GOX heat exchanger configuration.

o Figures 10 and 11 show the tank head idle performance
   for two alternate GOX heat exchanger configurations
   with two Stage 3 geometry heat exchangers.

CONCLUSIONS AND RECOMMENDATIONS:

1. The modified RL10 Derivative IIB GOX heat exchanger
   will satisfy the design requirements at pumped
   idle.

2. The second stage of the GOX heat exchanger is
   sensitive to hydrogen inlet temperature. The
   conductivity of the Stage 2 insulation should
   be able to be modified during testing for a
   hydrogen inlet temperature that is different
   than prediction.

3. Stages 1 and 2 insulation can be varied during
   testing by changing the pressure of the gas
   in contact with the insulation.

4. The sensitivity of the GOX heat exchanger to
   hydrogen inlet temperature can be reduced by
   reversing the hydrogen flow direction. The
   Stage 2 insulation conductivity must be
   reduced to 0.033 BTU/ft•hr•°R.

5. Heat leakage from the hydrogen plates to the oxygen
   plates through the headers can cause problems in
   stages 1 and 2. A 0.010 inch minimum separation
   must be provided between the axial flow plates and
   the headers.

6. If fabrication problems make it impossible to make
   stages 1 and 2, a alternate configuration which uses
   two stage 3 geometry heat exchangers can be used.
   This configuration can not be adjusted during testing
   if actual inlet condition are not the same as predicted.

J. Henderson   - 3 -   August 27, 1983

DISCUSSION:

The changes to the GOX heat exchanger due to fabrication problems that affected the heat transfer model are as follows:

1. Change Stages 1 and 2 flow path coverplates from 0.010 inches to 0.02 inches.

2. Reduced Stage 2 insulation thickness from 0.025 inches to 0.020 inches.

These modifications to the GOX heat exchanger are needed to make sure hydrogen doesn't leak through the brazed aluminum.

Several changes have been made to the GOX heat exchanger to correct heat transfer problems. Conduction of heat from the hydrogen plates to the oxygen plates through the headers will cause oxygen boiling instability in Stages 1 and 2. To correct this probelm an 0.010 inch minimum separation will be provided between the axial flowpath plate edges and the headers. Two hydrogen passages on each side of the external plates will also be plugged since these plates must be brazed to the oxygen headers.

The Stage 3 B/P geometry has a higher heat transfer convection area than called for in the original analysis. The hydrogen and oxygen passage hydraulic diameters are also smaller than what was used in the original analysis. The passage hydraulic diameter is set by what can be made during the fabrication of the plates. These differences in the Stage 3 geometry cause more heat to be transferred from the hydrogen, lowering the hydrogen temperature to Stages 1 and 2 at pumped idle. To correct this heat transfer problem, the total heat transfer area of Stage 3 must be reduced. The number of hydrogen passages per plate in Stage 3 must be reduced from 52 to 47. The number of oxygen passages per plate must be reduced from 42 to 37. The conductivity of the Stage 2 insulation must be increased from 0.294 BTU/ft·hr·°R to 0.36 BTU/ft·hr·°R because of the lower Stage 2 inlet hydrogen temperature at pumped idle.

Figures 1 through 5 show the performance of the GOX heat exchanger with modified geometry. The modified GOX heat exchanger will operate without boiling instability at pumped idle. The exit oxygen quality of Stage 2 at pumped idle is 0.071. Stage 2 has a maximum heat flux at saturated conditions below qualities of 0.05 and 2.67 BTU/ft^2·sec. The maximum allowed heat flux is 2.8 BTU/ft^2·sec at pumped idle. The performance of the modified GOX heat exchanger at tank head idle and full thrust has not changed much from the original analysis.

J. Henderson   - 4 -   August 27, 1983

The boiling stability of Stage 1 at tank head idle and Stage
2 at idle will be sensitive to insulation conductivity and
hydrogen inlet temperature. Stage 1 has the same tolerances
to insulation conductivity and hydrogen inlet temperatures
as stated in the original memo. Stage 2 has an insulation
tolerance at pumped idle of from 0.28 BTU/ft·hr·sec to 0.4
BTU/ft·hr·°R with a hydrogen inlet temperature of 300°R.
The stage 2 hydrogen inlet temperature tolerance at pumped
idle is +5°R/-10°R with an insulation conductivity of 0.36
BTU/ft·hr·°R. The hydrogen inlet temperature tolerance can
be exceeded if insulation conductivity is modified to offset
the hydrogen temperatures. The conductivity of the insu-
lation can be varied during testing by changing the gas in
contact with the insulation or by changing the pressure of
the gas. Nitrogen, helium, and hydrogen can be used with
the insulation. The RL10 engine can tolerate a boiling
instability pressure oscillation of +/-25%. The hydrogen
inlet temperature tolerances on Stage 1 stability could be
increased to +40°R/-10°R without exceeding the pressure
oscillation limits.

Some alternative GOX heat exchanger configurations that
would reduce the sensitivities of Stage 2 to hydrogen inlet
temperature and heat flux were examined. Reversing the
hydrogen flow direction through the GOX heat exhanger will
reduce the Stage 2 sensitivities. Figures 6 and 7 show the
pumped idle performance of the reversed hydrogen flow GOX
heat exchanger. The conductivity of Stage 2 must be reduced
to 0.033 BTU/ft·hr·°R. The Stage 2 exit quality and maximum
heat flux is 0.12 and 2.3 BTU/ft^2·sec Stage 2 will have a
pumped idle tolerance to hydrogen inlet temperature of from
589 R to 689 R. The insulation conductivity can vary from
0.028 BTU/ft·hr·°R to 0.038 BTU/ft·hr·°R without causing
problems. Increasing hydrogen flow to the RL10 Derivative
IIB GOX heat exchanger will also reduce the Stage 2 sensi-
tivity at pumped idle. To increase hydrogen flow at pumped
idle and O/F = 6.0 would require an oxygen injector with a
1.0 in^2 area, which will not be used during the low thrust
testing.

A GOX heat exchanger configuration that uses two Stage 3
geometry heat exchangers has also been analyzed. The first
heat exchanger is split into two stages. Stage 1 uses 26 of
the 37 oxygen passages in the plate. Stage 2 uses 11 of the
37 passages. The oxygen flow areas of Stages 1 and 2 are
3.286 in^2 and 1.39 in^2, respectively. This GOX heat
exchanger configuration requires that a portion of the
available hydrogen be taken from the pump to cool the hydro-
gen to Stage 2. During tank head idle, part of the hydrogen
will need to be bypassed around the GOX heat exchanger.
This configuration doesn't require insulation in Stages 1
and 2.

J. Henderson   - 5 -   August 27, 1933

Figures 8 and 9 show pumped idle performance for the alternate GOX heat exchanger configuration . The alternate configuration will work at pumped idle if a hydrogen mass flow of 0.018 lbm/sec. comes to the pumps to cool the Stage 2 hydrogen inlet temperature to 275°R. No hydrogen bypass flow is required at pumped idle. The Stage 2 oxygen exit quality and maximum heat flux is 0.068 and 5.4 BTU/ft²·sec. The allowable is 5.7 BTU/ft²·sec. Figures 10 and 11 show the tank head idle performance of two alternate GOX heat exchanger configurations which use two Stage 3 geometry heat exchangers. The heat exchanger shown on Figure 11 bypasses hydrogen around the entire GOX heat exchanger. The hydrogen bypass flow is 0.043 lbm/sec. The hydrogen flow from the pump is 0.0265 lbm/sec. Stage 1 has an oxygen exit quality and maximum heat flux of 0.093 and 0.46 BTU/ft²·sec, respectively. The allowable heat flux is 0.50 BTU/ft .sec. The configuration on Figure 12 bypasses 0.065 lbm/sec. of hydrogen around Stages 1 and 2. The Stage 1 exit quality and maximum heat flux is 0.089 and 0.46 BTU/ft²·sec. The allowable heat flux is 0.5 BTU/ft² .sec.

Tables 1 and 2 of the appendix show the GOX heat exchanger performance comparison between the original and new heat exchanger decks with B/P geometry. The original GOX heat exchanger model has been modified with B/P heat exchanger geometries which are different from what was used in the original analysis. The hydrogen exit temperatures calculated in the original computer model are now based on enthalpy instead of specific heat. The two analytical techniques for calculating heat exchanger performance agree closely.

R. J. Peckham
Mechanical Components & Systems
Component Design Technology

RJP:gjt
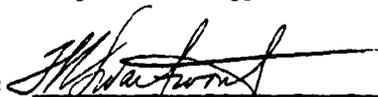
APPROVED:

T. R. Swartwout

FIGURE 1

RL10 DERIVATIVE IIB
GOX HEAT EXCHANGER GEOMETRY
WITH PUMPED IDLE PERFORMANCE

HYDROGEN EXIT
$TH_{OUT} = 221°R$
$PH_{OUT} = 46.4$ PSIA

OXYGEN
$TO = 199°R$
$PO = 81.5$ PSIA
$QUAL = 0.071$

OXYGEN INLET
$PO_{IN} = 167°R$
$PO_{IN} = 84.3$ PSIA
$M_O = 2.84 \frac{LBM}{SEC}$

STAGE 1 STAGE 2

STAGE 3

HYDROGEN INLET
$TH_{IN} = 639°R$
$PH_{IN} = 47.1$ PSIA
$M_H = 0.182 \frac{lbm}{sec}$

HYDROGEN
$TH = 300°R$
$PH = 46.6$ PSIA

OXYGEN EXIT
$TO_{OUT} = 221°R$
$PO_{OUT} = 78.0$ PSIA
$QUAL = 100\%$

FIGURE 2
RLIO DERIVATIVE II B
GOX HEAT EXCHANGER STAGE

PUMPED LE
Design Power O/F=6
T_{iH_2} = 300°R, T_{inO_2} = 213°R
T_{oH_2} = 168°R, T_{oO_2} = 199°R
$\dot{M}_H$ = 0.182 lb/s, $\dot{M}_O$ = 2.84 lb/s

O₂ OUT

H₂ OUT →

→ H₂ IN

O₂ IN ↑

| HEAT FLUX | — SUB COOLED OXYGEN HEAT FLUX BTU/FT²SEC |
| HEAT FLOW / QUAL | — SATURATED OXYGEN HEAT FLUX BTU/FT²SEC / OXYGEN QUALITY |

R/β 2/9/93

MAXIMUM ALLOWABLE HEAT FLUX
FOR SATURATED OXYGEN IS
2.8 BTU/FT²SEC
BELOW QUALITIES OF 0.05

0.91	0.94	0.97	0.99	1.00	0.98	0.95	0.90	0.86
1.08	1.09	1.12	1.13	1.12	1.09	1.04	0.98	0.92
1.27	1.28	1.28	1.29	1.26	1.20	1.14	1.06	0.98
1.48	1.47	1.46	1.45	1.39	1.32	1.23	1.14	1.08 / 0.019
1.71	1.68	1.66	1.63	1.53	1.43	1.33	1.19 / 0.004	1.27 / 0.041
1.97	1.92	1.87	1.82	1.68	1.56	1.48 / 0.005	1.26 / 0.023	1.51 / 0.069
2.27	2.19	2.11	2.03	1.84	1.72 / 0.005	1.74 / 0.026	1.49 / 0.047	1.79 / 0.101
2.61	2.49	2.38	2.16 / 0.021	2.01 / 0.001	2.01 / 0.026	2.06 / 0.050	1.77 / 0.075	2.11 / 0.139
3.00	2.83	2.67	2.38 / 0.013	2.31 / 0.096	2.39 / 0.050	2.45 / 0.079	2.10 / 0.109	2.49 / 0.185
3.45	3.22	3.01	2.67 / 0.036	2.76 / 0.075	2.84 / 0.080	2.88 / 0.115	2.47 / 0.150	2.93 / 0.193
					0.116	0.157	0.198	0.240

FIGURE

RL10 DERIVATIVE IIB
GASEOUS OXYGEN HEAT EXCHANGER
S ⁚ CORE

DIAGRAM

THERMAL SKIN
GEOMETRY BLOW-UP

GEOMETRY

	H_2 PLATE	O_2 PLATE
No. Plates	12.0	11.0
Passage Dia., In	0.05	0.03
Flow Area, In^2	1.179	1.504
H/T Area, Ft^2	4.81	
Core Weight, Lbm	7.5	
Insulation CONDUCTIVITY BTU/FT·HR·°R	0.041	

PERFORMANCE

	PUMPED IDLE	TANK HEAD IDLE	FULL THRUST
H_2 W, Lbm/Sec	0.0182	0.0106	0.006
O_2 W, Lbm/Sec	2.84	0.339	1.000
H_2 T_{in}, °R	300.0	548.3	2.738
O_2 T_{in}, °R	167.0	166.0	167.0
H_2 T_{out}, °R	286.8	482.3	247.0
O_2 T_{out}, °R	168.5	167.4	168.6
H_2 ΔP, PSI	0.14	0.93	0.0
O_2 ΔP, PSI	0.47	0.10	0.06
O_2 Exit Quality	0.0	0.075	0.0
Q, BTU/Sec	0.94	2.50	0.64
Q/A, Average BTU/ft^2·sec	0.195	0.52	0.133
Q/ MAXIMUM J/FT^2 SEC	——	0.62	——

FIGURE 4

RL10 DERIVATIVE IIB
GASEOUS OXYGEN HEAT EXCHANGER
STAGE 2 CORE

CORE GEOMETRY

O_2 IN

H_2 IN

THERMAL SKIN
GEOMETRY BLOW-UP

H_2 PLATE

O_2 PLATE
(TURNED 90°)

BRAZE 0.004" THICK
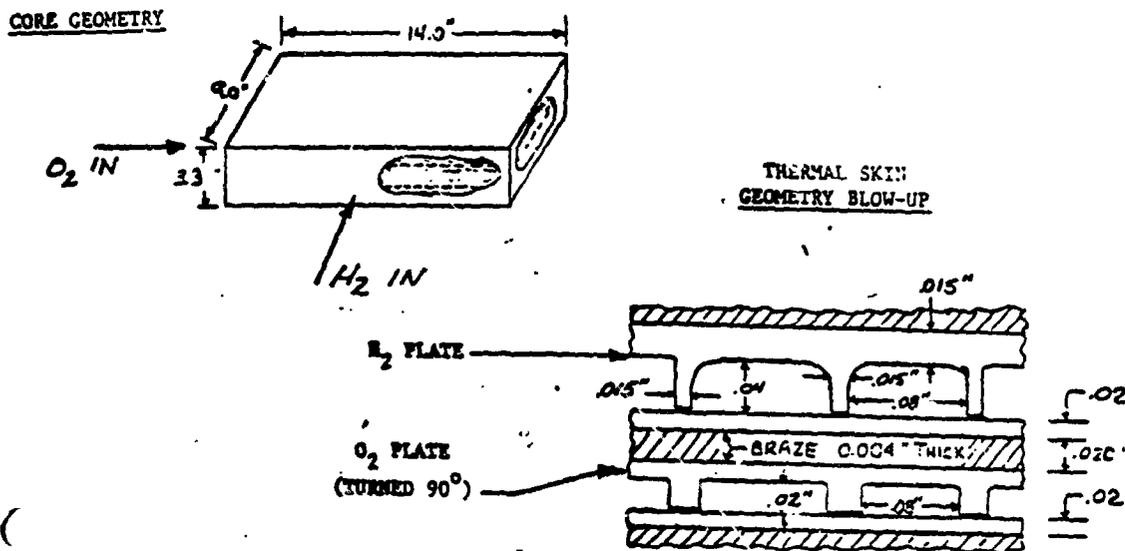
GEOMETRY

	H_2 PLATE		O_2 PLATE
No. Plates	20.0		19.0
Passage Dia., In	0.05		0.03
Flow Area, In^2	7.92		2.56
H/T Area, Ft^2		33.3	
Core Weight, Lbm		53.3	
Insulation CONDUCTIVITY BTU/FT·HR·°R		0.36	

PERFORMANCE

	PUMPED IDLE	TANK HEAD IDLE	FULL THRUST
H_2 W, Lbm/Sec	0.171	0.098	0.054
O_2 W, Lbm/Sec	2.840	0.339	1.000
H_2 T_{in}, °R	300.0	5.483	273.8
O_2 T_{in}, °R	168.5	167.4	168.6
H_2 T_{out}, °R	216.6	385.2	205.5
O_2 T_{out}, °R	199.4	496.2	201.2
H_2 ΔP, PSI	0.20	1.15	0.0
O_2 ΔP, PSI	2.29	3.72	0.1
O_2 Exit Quality	0.071	1.00	0.0
Q, BTU/Sec	53.7	57.9	15.2
Q/A, Average BTU/ft^2·sec	1.613	1.739	0.954
Q/A, MAXIMUM BTU/ft^2·sec	2.67		

FIGURE ∴

RL10 DERIVATIVE IIB
GASEOUS OXYGEN HEAT EXCHANGER
STAGE 3 CORE

DIAGRAM
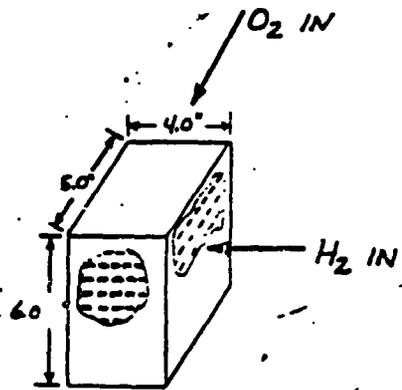
THERMAL SKIN
GEOMETRY BLOW-UP
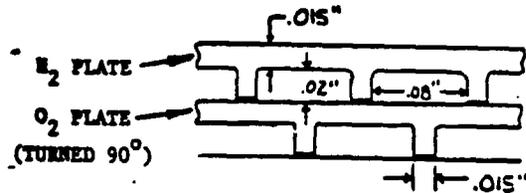
GEOMETRY

	H_2 PLATE	O_2 PLATE
No. Plates	87.0	96.0
Passage Dia., In	0.03	0.03
Flow Area, In^2	5.765	4.49
H/T Area, Ft^2	19.5	
Core Weight, Lbm	19.3	

PERFORMANCE

	PUMPED IDLE	TANK HEAD IDLE	FULL THRUST
H_2 W, Lbm/Sec	0.182	0.106	0.06
O_2 W, Lbm/Sec	2.84	0.339	1.00
H_2 T_{in}, °R	639.0	559.0	431.5
O_2 T_{in}, °R	199.4	496.2	205.5
H_2 T_{out}, °R	300.0	543.4	273.8
O_2 T_{out}, °R	221.0	545.9	263.7
H_2 ΔP, PSI	0.50	1.67	0.0
O_2 ΔP, PSI	2.80	0.63	0.03
O_2 Exit Quality	1.00	1.00	0.195
Q, BTU/Sec	226.9	3.69	36.9
Q/A, Average BTU/ft^2·sec	11.64	0.189	1.89

FIGURE 6

RL10 DERIVATIVE IIB
GOX HEAT EXCHANGER GEOMETRY
WITH PUMPED IDLE PERFORMANCE

REVERSED HYDROGEN FLOW

HYDROGEN INLET
$TH_{OUT} = 639°R$
$PH_{OUT} = 47.1$ PSIA

OXYGEN
$TO = 199°R$
$PO = 80.9 psia$
$Qual = 0.12$

OXYGEN INLET
$TIN = 167°R$
$PIN = 84.3$ PSIA
$M_O = 2.84 \frac{LBM}{SEC}$

STAGE 1   STAGE 2   STAGE 3

$Q/A_W = 2.3 \frac{BTU}{ft^2 sec}$
$Q/A_{out} = 2.8 \frac{BTU}{ft^2 sec}$

HYDROGEN
$TH = 647°R$
$PH = 46.6$ PSIA

HYDROGEN EXIT
$TH_{IN} = 200°R$
$PH_{IN} = 46.2 psia$
$M_H = 0.187 \frac{lbm}{sec}$

OXYGEN EXIT
$TO_{OUT} = 193°R$
$PO_{OUT} = 78.3$ PSIA
$Qual = 0.95$

$O/F = 6.0$
STAGE 2 INSULATION CONDUCTIVITY = 0.033 $^{BTU}/_{FT \cdot hr \cdot °R}$

FIGURE 7
RLIO DERIVATIVE II B
GOX HEAT EXCHANGER STAGE 2

CONFIGURATION:
PUMPED I.E.

REVERSED H₂ FLOW
$T_{HIN} = 639°R, T_{HOUT} = 542°R$
$T_{OIN} = 169.8°R, T_{OUT} = 199°R$
$M_H = 0.182 \frac{lb}{s}, M_O = 2.84 \frac{lb}{s}$

O₂ OUT

O₂ IN

H₂ OUT

H₂ IN

HEAT FLUX		HEAT FLUX QUAL

- SUB COOLED OXYGEN HEAT FLUX ~ BTU/FT²SEC
- SATURATED OXYGEN HEAT FLUX ~ BTU/FT²SEC OXYGEN QUALITY

MAXIMUM ALLOWABLE HEAT FLUX
FOR SATURATED OXYGEN IS
2.8 BTU/FT²SEC.
BELOW QUALITIES OF 0.05

FIGURE 5

RLIO DERIVATIVE II B
GOX HEAT EXCHANGER
ALTERNATE CONFIGURATION

PUMPED IDLE

FIGURE 9
RLIO DERIVATIVE II B
GOX HEAT EXCHANGER STAGE 2

ALTERNATE CONFIGURATION
__PUMPED IDLE__

$T_{H\,IN} = 275°R$, $T_{H\,OUT} = 240°R$
$T_{O\,IN} = 191°R$, $T_{O\,OUT} = 199°R$
$\dot{M}_{H} = 0.25 \frac{lb}{s}$, $\dot{M}_{O} = 2.84 \frac{lb}{s}$

O_2 IN

H_2 OUT

H_2 IN

O_2 OUT

... SUB COOLED OXYGEN
HEAT FLUX ~ BTU/FT²·SEC

--- SATURATED OXYGEN
HEAT FLUX ~ BTU/FT²·SEC
OXYGEN QUALITY

MAXIMUM ALLOWABLE HEAT FLUX
FOR SATURATED OXYGEN IS
5.7 BTU/FT²SEC
BELOW QUALITIES OF 0.02

RLIO DERIVATIVE ⅡB
GOX HEAT EXCHANGER
ALTERNATE CONFIGURATION

FIGURE 10

$T_o = 167.4 °R$, QUAL $= 0.093$
$P_o = 19.98$ PSIA

HYDROGEN EXIT
$T_h = 232.6 °R$
$P_h = 8.2$ PSI
$\dot{M}_h =$

HYDROGEN
$T_h = 37.9 °R$
$\dot{M}_h = 0.0265 \frac{lb_m}{s}$

STAGE 2

STAGE 1

$T_h = 215 °R$
$P_h = 8.4$ PSIA
$\dot{M}_h = 0.0625$

$T_h = 346 °R$
$P_h = 8.45$ PSIA

OXYGEN INLET
$T_o = 167 °R$
$P_o = 20$ PSIA
$\dot{M}_o = 0.339 \frac{lb_m}{s}$

$T_o = 166.6 °R$
$P_o = 19.3$ PSIA
QUAL $= 0.31$

STAGE 3

OXYGEN EXIT
$T_o = 514 °R$
$P_o = 18.7$ PSIA
$\dot{M}_o = 0.339 \frac{lb_m}{s}$
QUAL $= 100\%$

$\dot{M}_h = 0.036 \frac{lb_m}{s}$

H₂ BYPASS
$\dot{M}_h = 0.043 \frac{lb_m}{s}$

HYDROGEN INLET
$T_h = 733 °R$
$P_h = 8.6$ PSIA
$\dot{M}_h = 0.0795 \frac{lb_m}{s}$

TANK HEAD IDLE
75/25 SPLIT H_2 FLOW
$0.043 \frac{lb_m}{s}$ BYPASS FLOW

RLIO DERIVATIVE II B
GOX HEAT EXCHANGER
ALTERNATE CONFIGURATION

FIGURE 1.

H_2 BYPASS $\dot{m}_h = 0.065 \frac{\#}{s}$

$T_0 = 167°R, Qual = 0.089$
$P_0 = 19.98 psi$

HYDROGEN
EXIT
$T_h = 3904°R$
$P_h = 6.63 psia$
$\dot{M}_h = 0.106$

HYDROGEN
$T_h = 37.9°R$
$\dot{M}_h = 0.0265 \frac{\#}{s}$

STAGE 2

STAGE 1

$T_h = 238°R$
$P_h = 6.82 PSIA$
$\dot{M}_h = 0.0455 \frac{\#}{s}$

$T_h = 516°R$
$P_h = 6.86 PSIA$

OXYGEN
INLET
$T_0 = 167°R$
$P_0 = 20 PSIA$
$\dot{M}_0 = 0.339 \frac{\#}{s}$

$T_0 = 166.3°R$
$P_0 = 19.3 PSIA$
Qual = 0.36

STAGE 3

OXYGEN
EXIT
$T_0 = 588°R$
$P_0 = 18.2 PSIA$
$\dot{M}_0 = 0.339 lbm$
Qual = 1.0

$\dot{M}_h =$

HYDROGEN INLET
$T_h = 733°R$
$P_h = 8.6 PSIA$
$\dot{M}_h = 0.0795 lbm/sec$

TANK HEAD IDLE

Appendix

Comparison of Original Computer
Program With New Heat Exchanger Deck

<u>TABLE 1</u>

RL10 DERIVATIVE IIB
GOX HEAT EXCHANGER PERFORMANCE

COMPARISON OF ORIGINAL COMPUTER
PROGRAM WITH NEW HEAT EXCHANGER
DECK (WITH PRINT GEOMETRY)

OXYGEN	PUMPED IDLE		TANK HEAD IDLE		FULL THRUST	
	ORIG.	NEW	ORIG.	NEW	ORIG.	NEW
T_{IN} (°R)	167.3	167.0	166.2	166.0	167.0	167.0
T_{OUT} (°R)	209.8	212.9	528.2	544.6	263.4	263.4
P_{IN} (PSIA)	84.3	84.3	20.0	20.0	534.0	534.0
P_{OUT} (PSIA)	77.3	80.1	16.7	15.66	533.8	533.8
ΔP (PSI)	7.1	4.22	3.27	4.34	0.2	0.19
EXIT QUAL.	1.0	1.0	1.0	1.0	0.1	0.19

HYDROGEN						
T_{IN} (°R)	639.0	639.0	559.0	559.0	431.	431.5
T_{OUT} (°R)	228.8	223.4	404.4	394.1	214.	200.4
P_{IN} (PSIA)	47.1	47.1	8.6	8.6	692.	692.0
P_{OUT} (PSIA)	46.4	46.37	5.86	5.56	692.	692.0
ΔP (PSI)	0.7	0.63	2.74	3.04	0.0	0.0

TABLE 2

RL10 DERIVATIVE IIB
GOX HEAT EXCHANGER PERFORMANCE

COMPARISON OF ORIGINAL AND NEW
HEAT EXCHANGER DECKS (WITH PRINT GEOMETRY)

STAGE 1	PUMPED IDLE		TANK HEAD IDLE		FULL THRUST	
	ORIG.	NEW	ORIG.	NEW	ORIG.	NEW
MH_2 (LBM/SEC)	0.0182		0.0106		0.006	
MO_2 (LBM/SEC)	2.840		0.339		1.00	
$TH_2 IN$ (°R)	296.7	289.0	540.0	547.8	261.	258.
$TO_2 IN$ (°R)	167.3	167.	166.2	166.	167.	167.
$TH_2 OUT$ (°R)	285.6	277.3	480.2	481.9	236.	235.
$TO_2 OUT$ (°R)	168.1	167.7	168.	167.3	168.	168.
PH_2 (PSI)	0.1	0.11	1.09	0.96	0.0	0.0
PO_2 (PSI)	0.7	0.48	0.354	0.10	0.09	0.6
O_2 EXIT QUAL	0.0	0.0	0.07	0.075	0.0	0.0
Q (BTU/SEC)	0.88	0.87	2.14	2.50	0.55	0.54

STAGE 2						
MH_2 (LBM/SEC)	0.1638		0.0980		0.054	
MO_2 (LBM/SEC)	2.840		0.339		1.000	
$TH_2 IN$ (°R)	296.7	289.6	540.0	547.8	260.9	257.6
$TO_2 IN$ (°R)	168.1	167.7	168.0	167.3	168.2	168.3
$TH_2 OUT$ (°R)	222.6	217.4	396.4	386.2	211.7	196.6
$TO_2 OUT$ (°R)	199.3	199.8	429.9	487.1	195.5	198.4
PH_2 (PSI)	0.10	0.20	1.09	1.19	0.0	0.0
PO_2 (PSI)	1.50	1.44	1.72	3.59	0.08	0.1
O_2 EXIT QUAL	0.04	0.028	1.00	1.00	0.0	0.0
Q (BTU/SEC)	47.0	44.8	48.5	57.3	10.9	12.5

-2-

TABLE 2 CONTINUED

TAGE 3	PUMPED IDLE ORIG.	NEW	TANK HEAD IDLE ORIG.	NEW	FULL THRUST ORIG.	NEW
MH$_2$ (LBM/SEC)	0.182		0.109		0.06	
MO$_2$ (Lbm/SEC)	2.84		0.339		1.00	
TH$_2$IN (°R)	639.0	639.0	559.0	559.0	431.5	431.5
TO$_2$IN (°R)	199.3	199.8	429.9	487.1	195.5	198.4
TH$_2$OUT (°R)	296.7	289.6	540.0	547.8	260.9	257.6
TO$_2$OUT (°R)	209.8	212.9	528.2	544.6	263.2	263.7
PH$_2$ (PSI)	0.471	0.44	1.52	1.86	0.0	0.0
PO$_2$ (PSI)	4.2	2.3	0.82	0.65	0.02	0.02
O$_2$ EXIT QUAL	1.00	1.00	1.00	1.00	0.1	0.19
Q (BTU/SEC)	228.1	233.5 -	7.49	4.31	40.2	40.7